



STUDY REPORT
N° DRA-12-125630-04945B

05/10/2012

**Formalization of knowledge and tools in the
area of major risks
(EAT-DRA-76)**

**Vessel bursts, phenomenology and effect
modelling - Ω 15**

INERIS

maîtriser le risque |
pour un développement durable |

**EAT-DRA-76 - Formalization of knowledge and tools in
the area of major risks**

**Vessel bursts, phenomenology and effect modelling - Ω
15**

Accident Risks Division

,

INERIS-DRA-12-125630-04945A

PREAMBULE

The present report was established on the basis of information provided to INERIS, on available and objective (scientific or technical) data and regulations in force.

The liability of INERIS cannot be invoked if the information provided to them is incomplete or erroneous.

The opinions, recommendations, counsels or equivalent which would be issued by INERIS within the scope of the services with which they are entrusted, may be an aid in making decisions. Given the mission incumbent upon INERIS because of the decree creating it, INERIS does not intervene in the actual decision-making process. The liability of INERIS can therefore not be substituted for that of the decision-maker.

The addressee will use the results included in the present report entirely or otherwise objectively. Its use in the form of excerpts or executive summaries will only be made under the whole responsibility of the addressee. The same applies to any change provided thereto.

INERIS cannot be held liable for any use of the report outside the purpose of the service provided by them.

The present study report written in English is for information only. The French version shall prevail over any translation that may be made.

Table of Contents

1.	INTRODUCTION	4
1.1.	THE OMEGA REFERENTIALS	4
1.2.	AREA OF APPLICATION AND OBJECTIVES.....	4
2.	BRIEF REMINDER ABOUT THE STUDIED PHENOMENON	7
2.1.	CONCERNED VESSELS.....	7
2.2.	MAJOR CAUSES OF A VESSEL BURST	7
2.2.1.	<i>Events causing an increase in internal pressure</i>	<i>7</i>
2.2.2.	<i>Events causing a decrease in vessel strength</i>	<i>8</i>
2.3.	ENVIRONMENTAL EFFECTS	8
2.3.1.	<i>Overpressure effects</i>	<i>8</i>
2.3.2.	<i>Effects of fragment impact</i>	<i>10</i>
2.4.	SYNTHESIS OF VESSELS AND BURST CAUSES.....	12
3.	FEEDBACK	15
3.1.	VESSEL CAUGHT IN A FIRE	15
3.1.1.	<i>Port Edouard Herriot Accident (2 and 3 June 1987)</i>	<i>15</i>
3.1.2.	<i>Bordes Accident (France, 9 May 2000)</i>	<i>18</i>
3.1.3.	<i>Dagneux Accident (France, 7 May 2007)</i>	<i>20</i>
3.1.4.	<i>Other examples.....</i>	<i>22</i>
3.2.	ACCIDENTAL PRESSURIZATION	23
3.2.1.	<i>Heat exchanger burst (Indonesia, 14 April 1983)</i>	<i>23</i>
3.2.2.	<i>Other examples.....</i>	<i>23</i>
3.3.	MECHANICAL WEAKENING AND IMPACT OF A PROJECTILE.....	24
3.4.	INTERNAL EXPLOSION	24
3.4.1.	<i>Blaye Accident (France, 20 August 1997)</i>	<i>25</i>
3.4.2.	<i>Other examples.....</i>	<i>26</i>
3.5.	LESSONS FROM FEEDBACK	26
4.	RUPTURE CONDITIONS	29
4.1.	RUPTURE MODES.....	29
4.1.1.	<i>Fragile rupture</i>	<i>29</i>
4.1.2.	<i>Ductile rupture.....</i>	<i>30</i>
4.1.3.	<i>Fragile-ductile transition.....</i>	<i>30</i>
4.2.	DETERMINING RUPTURE PRESSURE.....	31
4.2.1.	<i>Rupture pressure in static load (pressurized metal equipment)</i>	<i>32</i>
4.2.2.	<i>Impact of the origin of the burst.....</i>	<i>33</i>
5.	PRESSURE WAVE PRODUCTION AND PROPAGATION	39
5.1.	DESCRIPTION OF THE PHENOMENON	39
5.2.	PRESSURE WAVE PRODUCTION AND PROPAGATION.....	40
5.3.	CONSEQUENCES MODELLING: GLOBAL METHODS	41
5.3.1.	<i>The Shock Tube-TNT method</i>	<i>41</i>
5.3.2.	<i>The PROJEX method (INERIS).....</i>	<i>46</i>
5.3.3.	<i>The Baker's method</i>	<i>49</i>
5.3.4.	<i>The UFIP method</i>	<i>53</i>
5.3.5.	<i>Accounting for the interaction of a pressure wave with an obstacle</i>	<i>56</i>
5.4.	COMPARISON OF GLOBAL METHODS.....	56
5.4.1.	<i>Without accounting for interaction with obstacles</i>	<i>56</i>

5.4.2.	<i>Accounting for interaction of the pressure wave with an obstacle</i>	58
5.4.3.	<i>Synthesis</i>	63
6.	FRAGMENT FORMATION AND PROJECTION.....	65
6.1.	FRAGMENT FORMATION	65
6.2.	FRAGMENT ACCELERATION AND PROJECTION.....	66
6.2.1.	<i>Physical representation</i>	66
6.2.2.	<i>Vessel containing pressurized gas</i>	68
6.2.3.	<i>Vessel containing a liquid</i>	68
6.3.	PREDICTION METHODS	68
6.3.1.	<i>The PROJEX method.....</i>	68
6.3.2.	<i>The Baker's method</i>	69
6.3.3.	<i>The UFIP method</i>	76
6.4.	COMPARISON OF GLOBAL METHODS.....	76
7.	CONCLUSION	79
8.	GLOSSARY	81
9.	BIBLIOGRAPHY	83
10.	LIST OF ANNEXES	85

1. INTRODUCTION

1.1. THE OMEGA REFERENTIALS

Since several years ago, the French Ministry responsible for sustainable development (currently the Ministry of Ecology, Sustainable Development and Energy) has been financing a study and research programme entitled “Formalisation of knowledge and tools in the area of major risks.” The purpose of the first part of this programme is to produce a comprehensive compendium formalising INERIS's expertise in the area of accident risks. This compendium is made up of various reports, dedicated to the following themes:

- risk analysis,
- physical phenomena involved in an accidental situation (fire, explosion, BLEVE¹, etc.),
- the control of major accident risks,
- methodological aspects in the production of regulatory services (safety studies, critical review, etc.)

These reports are part of an approach to disseminate INERIS's knowledge to public authorities, industry and the general public.

Each of these documents receives its own « Ω -x » identifier. Ultimately, these documents describing the methods for assessing and preventing accident risks will make up a compendium of INERIS's working methods in the area of accident risks.

1.2. AREA OF APPLICATION AND OBJECTIVES

This report **Ω -15** presents a synthesis of current knowledge about the phenomenon of vessel bursts, as, for example, the atmospheric or pressurized storage containing a pressurized gaseous phase at the time of rupture. The burst can be due to an increase in pressure in the vessel or to a deterioration of its physical properties.

The objectives of this document are to:

- recall the pressurization events likely to bring about a vessel rupture
- review the consequences of the rupture of vessel containing a pressurized gaseous phase,
- present a synthesis of a few available methods to describe the effects of a vessel burst, by comparing simulations to experiment results and feedback from past accidents,
- reveal the limits of these methods.

¹ Boiling Liquid Expanding Vapor Explosion

There are still few methods to predict the consequences of a vessel rupture. Our interest, in this document, is essentially to implement global and phenomenological methods.

The prediction methods presented here concern the consequences linked to the release of the gaseous phase of the vessel, pressurized at bursting time and the projection of vessel shell fragments. The effects produced by the dispersion of a toxic product following a vessel rupture are not considered in this document, but in the referential relative to atmospheric dispersion, report Ω12 - Couillet, 2002 available on INERIS's web site.

The present document does not treat the modelling of the rupture phenomenon following a hydraulic fill, nor the modelling of effects brought about by the phenomena of BLEVE or dust explosions, which are the subject of specific reports (referential relative to BLEVE phenomenon – report Ω5 - Leprette, 2002², and report Ω1 - Roux, 2000 available on INERIS's web site.

² Final update is in progress.

2. BRIEF REMINDER ABOUT THE STUDIED PHENOMENON

In this document, we are interested in modelling the phenomenon of (atmospheric or pressurized) vessel burst releasing a gaseous pressurized volume at the time of rupture.

2.1. CONCERNED VESSELS

Any vessel susceptible to contain, usually or accidentally, a pressurized gaseous phase is concerned by this document. These vessels include atmospheric storage tanks, mobile tanks and flammable liquid storage tanks, pressurized equipment, reactors and other pressurized vessels, etc.

2.2. MAJOR CAUSES OF A VESSEL BURST

The vessel burst can be due to

- an increase in internal pressure to a level superior to the vessel rupture pressure, or
- a decrease in the rupture pressure to a level inferior to the internal pressure, due to, for example, the degradation of the physical properties of the vessel shell.

Several events can be the source of these two major causes of burst, which will not be described in detail in this report. It should however be underlined that these events can have an impact on the type of vessel rupture, which, furthermore, is the subject of specific studies at INERIS.

2.2.1. Events causing an increase in internal pressure

The principle events susceptible of causing an increase in internal pressure are:

- A heating of the gaseous phase in the vessel due to an external fire,
- An accidental pressurization due to an overfill, to a dysfunction of the pressure monitoring device,
- An explosion within the vessel due to the inflammation of a flammable mixture,
- A rapid increase of internal pressure due to a runaway reaction or a mixture of incompatible products.

2.2.2. Events causing a decrease in vessel strength

The principle events likely to cause a decrease in vessel strength are:

- vessel shell fatigue,
- shell erosion or corrosion,
- a defect in the material making up the vessel shell,
- projectile impact,
- heating of the shell, for example, by a fire.

2.3. ENVIRONMENTAL EFFECTS

The consequences of a vessel burst treated in this report are, on the one hand, the emission of a pressure wave, which results from the brutal depressurization of the fluid in the vessel at the time of rupture, and, on the other hand, the projection of shell fragments.

Other phenomena, not studied here, can be caused by a vessel rupture, such as the formation of a fire ball or a secondary explosion, due to the expulsion of a flammable mixture during the burst, or additionally the atmospheric dispersion of toxic substances contained in the vessel.

2.3.1. Overpressure effects

Pressure is a force by surface unit likely to induce bending or shearing in structures, eventually compression for the human body. A pressure wave can also propel projectiles.

Effect thresholds for structures and man are proposed in annex II (relative to reference values of effect thresholds for potential dangerous phenomena likely to occur in classified installations) of the decree of 29 September 2005³.

³ French regulation : Decree of 29 September 2005 relative to the evaluation and consideration of occurrence probability, kinetics, intensity of effects and the severity of the consequences of potential accidents in studies of dangers of classified installations, Journal Officiel n°234, 7 October 2005.

2.3.1.1. Thresholds for overpressure effects on structures

The thresholds for overpressure effects on structures proposed in the decree of 29 September 2005 are the following:

- 20 hPa or mbar: threshold for significant glass damage⁴;
- 50 hPa or mbar: threshold for light structural damage,
- 140 hPa or mbar: threshold for serious structural damage,
- 200 hPa or mbar: threshold for domino effects⁵,
- 300 hPa or mbar: threshold for very serious structural damage.

These thresholds come from numerous military tests, particularly on ammunition, which served as a base for the establishment of pyrotechnical regulations^{6,7}. The thresholds and proposed values in this regulation in terms of physical damage are very consistent to what we found through experimental observation (10 to 20% margin).

According to Clancey, the rupture of hydrocarbon tanks and the destruction of foundations can occur from 200 mbar, the risk of brick or non-reinforced concrete walls collapsing from 140 mbar, and the appearance of damage on light and non load-bearing elements at around 50 mbar.

Other reference values, of the same order of magnitude, can be found in the literature, such as the apparition of significant damage on structures starting at 170 mbar (Baker, Lannoy).

Although the data allowing the establishment of these thresholds seems relatively reasonable and substantiated, it is useful to remember that it comes from the detonation of condensed explosives. It is not clear that these thresholds can be retained for the more classic situation of blasts and little information on this point is available because the analyses of blast scenarios are generally done on the basis of a "TNT equivalent."

Therefore, certain recent studies show significant damage on light metallic structures in the zone of 20-50 mbar (Reimeringer et al., 2008).

⁴ The French regulation specifies that "given the modelling dispersion for weak overpressures, for overpressure of 20mbar, an effect distance equal to twice the effect distance obtained for an overpressure of 50 mbar may be adopted."

⁵ The French regulation specifies that it is a "threshold from which domino effects should be examined. Adjustment is possible depending on the concerned materials and structures."

⁶ French regulation : Decree of 26 September 1980 establishing the rules for determining the isolation distances relative to pyrotechnical installations, abrogated by the Decree of 20 April 2007 establishing the rules relative to the evaluation of risks and accident prevention in pyrotechnical establishments.

⁷ French regulation : Circular of 8 May 1981 relative to the application of the Decree of 26 September 1980.

2.3.1.2. Thresholds for overpressure effects on man

The thresholds for overpressure effects on man proposed in the Decree of 29 September 2005 are the following:

- 20 hPa or mbar : effect threshold delimiting the zone of indirect effects on man from breaking glass (cf footnote n°4),
- 50 hPa or mbar : irreversible effect threshold delimiting the “zone of significant danger for human life”,
- 140 hPa or mbar: lethal effect threshold, delimiting the “zone of grave danger for human life”,
- 200 hPa or mbar: threshold for significant lethal effects, delimiting the “zone of very grave danger for human life”.

2.3.2. Effects of fragment impact

When a vessel bursts, a distinction is made between:

- primary “missiles” coming from the source itself—vessel fragments—they are determined by their number, mass, shape, speed and trajectory,
- and secondary “missiles” —objects in the vessel’s environment that are put into motion by the pressure wave from the burst, or eventually by other “missiles.” These missiles have a lesser effect because their momentum is weaker. Nevertheless, they must be taken into consideration in the absence of primary fragments.

A projectile is susceptible to produce two types of impact on man and structures:

- impact can cause fractures of the human body, and bring about the deformation of structures, even their collapse and destruction;
- penetration of the human body or a structural target can bring about its destruction.

The former pyrotechnical regulation⁸ established two thresholds linked to the penetration effects of small fragments (less than 1 kg), expressed in terms of the kinetic energy of the projectile:

- 20 J to the limit Z2 / Z3 (serious injuries which could be mortal) is the threshold of lethality;
- 8 J to the limit Z3 / Z4 (injuries) is the threshold of significant injuries.

For heavy projectiles (mass superior to 1 kg), it does not seem pertinent to reason in terms of kinetic energy, but rather in terms of the speed of impact. Available data (Baker, 1983; TNO, 1989) suggests retaining a threshold of 4 m/s for the appearance of irreversible injuries (skull fracture) for a projectile of a weight superior to 1 kg.

⁸ French regulation : Circular of 8 May 1981 relative to the application of the decree of 26 September 1980, abrogated by the decree of 20 April 2007.

At this time, there are no simple criteria allowing the characterization of a projectile's effect on an equipment.

The great variation of targeted equipment makes a case by case study necessary. It is easy to see that a residential house, for example, has a very different mechanical strength than industrial equipment designed to resist high pressure.

INERIS has drawn up a referential on the theme of structure resistance to the impact of accidental projectiles (Le Roux, 2010).

2.4. SYNTHESIS OF VESSELS AND BURST CAUSES

The following table collects, for the principal vessels concerned by this document, the principal causes of rupture and references to the must adapted INERIS referential.

Vessel type	Phenomenon	Principal cause	Reference document of the INERIS method
Pressurized vessel, reactor ...	Rupture due to mechanical weakening	Corrosion, impact of a projectile	Present document
	Rupture following an increase in pressure of the gaseous phase	Fire, internal explosion, runaway reaction, heating, overfill, etc.	Present document
	BLEVE (for pressurized liquefied gas) ⁹	Fire	BLEVE Referential Ω5 (Leprette, 2002, downloadable at www.ineris.fr)
Atmospheric storage of flammable liquid	Explosion of flammable vapour in an empty, poorly degassed tank	Internal explosion	Present document
	Tank Pressurization ¹⁰	Fire	Present document for the effects of pressure and fragments; but recommended model by the regulation for thermal effects ¹¹
Silo	Dust explosion	Internal explosion	Silo Referential Ω1 (Roux, 2000, downloadable at www.ineris.fr)

Table 1: Principal vessels concerned by the present document

⁹ The BLEVE phenomenon (brutal vaporization of a liquid) can occur when a vessel holding a liquid at a temperature significantly higher than its boiling point ruptures.

¹⁰ The phenomenon of tank pressurization corresponds to the rupture of an atmospheric flammable liquid storage tank following a slow rise in pressure due to an external fire.

¹¹ French regulation : Circulation note BRTICP/200r8-638/OA of 23/12/08 relative to the modelling of effects linked to the pressurization of an atmospheric flammable liquids storage tank with a fixed roof, downloadable at <http://www.ineris.fr/aida>. This document was abrogated by the circular of 10 May 2010, but the method is still recognized by the ministry, even if the circular does not mention them directly.

In certain cases, the effects caused by a vessel burst can be calculated from regulatory methods. In this manner, the circular of 10 May 2010¹² recommends:

- for the BLEVE of LPG phenomenon¹³, when the vessel has a low liquid fill rate, to predict the effects of pressure by using a model of pneumatic burst on the gaseous phase (subject of the present document),
- for the rupture phenomenon for an atmospheric storage tank following an internal explosion (inflammation of the gaseous phase of a vessel of flammable liquid leading to a rapid rise in pressure), apply the note « *Modélisation des effets de surpression dus à une explosion de bac atmosphérique* » (“Modelling the effects of overpressure due to an atmospheric tank explosion”)¹⁴,
- for the phenomenon of tank pressurization, determine the thermal effects by way of the model presented in a note from the general director of risk prevention dating from 23 December 2008 (cf footnote page 11).

¹² French regulation : Circular of 10 May 2010 summarizing the methodological rules applicable to danger studies, to the appreciation of risk reduction at the source, and to technological risk prevention plans in classified installations in application of the law of 30 July 2003, downloadable at <http://www.ineris.fr/aida>.

¹³ Liquefied Petroleum Gas

¹⁴ French regulation : Note available on the site <http://www.ineris.fr/aida> in attachment to the *Circulaire DPPR/SEI2/AL- 06- 357 du 31/01/07 relative aux études de dangers des dépôts de liquides inflammables - Compléments à l'instruction technique du 9 novembre 1989* (http://www.ineris.fr/aida/?q=consult_doc/consultation/2.250.190.28.8.2759) (Circular DPPR/SEI2/AL- 06- 357 of 31/01/07 relative to the study of dangers in flammable liquid storage facilities – Courtesy of the technical instruction of 9 November 1989). This document was abrogated by the circular of 10 May 2010, but is still used as a method recognized by the ministry, even if the circular does not mention them directly.

3. **FEEDBACK**

Using data from the database ARIA¹⁵ of the BARPI¹⁶ (period 1943-2011), (www.aria.environnement.gouv.fr) and literature (Holden, 1988), a survey of accidents linked to the theme of this document has been undertaken and broken down into four main categories:

- bursts consequential to a fire under or around a vessel,
- bursts consequential to an accidental pressurization (overfill...),
- bursts consequential to a mechanical weakening (corrosion, impact of a projectile...),
- bursts resulting from an internal explosion (dust explosion in silos, explosion in empty, poorly degassed atmospheric tanks ...).

The following is a description of several accidents and tests for which there is sufficient information for them to be of use. Still, it is difficult to use the information coming from the database because they're generally heterogeneous. For example, the nature of the contained product is not always specified, nor the size of the vessel. As for environmental effects, information about pressure effects is generally not provided. However, fragment projection distances are sometimes indicated, but the weight of the debris generally is not.

For information purposes, other accidents are presented in annex 1.

3.1. **VESSEL CAUGHT IN A FIRE**

An initial situation capable of leading to a vessel burst is the case where it is caught in a fire. In this case, under the warming effect of the fire, two simultaneous events can take place: an increase in internal pressure and a decrease in shell strength.

We will detail here three accidents of this type:

- The Port-Edouard Herriot accident which occurred in 1987, bringing about the explosion of a tank of liquid hydrocarbons caught in a fire,
- The Bordes accident which occurred in 2000, bringing about the successive explosion of bottles of gas on a transporter truck caught in a fire,
- The Dagneux accident which occurred in 2007, bringing about bursts and BLEVE of tanker trucks of LPG.

3.1.1. Port Edouard Herriot Accident (2 and 3 June 1987)

This accident allows the illustration not only of the phenomenon of vessel pressurization due to an external fire, but also the phenomenon of an atmospheric tank rupture due to an internal explosion.

¹⁵ Analyse, Recherche et Information sur les Accidents

¹⁶ Bureau d'Analyse des Risques et Pollutions Industrielles

Progression:

Around 1:15 p.m., a team moved an electric cable linking a generator to welding posts situated in diked area n°3 of the **oil storage depot** of Port Edouard Herriot. At this time, an additive aerosol jet was produced in the sector of the former pump, near tank n°14, in the same basin. After several seconds, a “flash” fire occurred. Approximately one minute later, a violent explosion occurred, which was felt several kilometres away. Tank n°14 sagged against tank n°13. In a few minutes, a **fire** propagated and **several hundred m³ tanks exploded** and **projected up to 200 m high**, freeing their contents into the basin. The internal means of intervention were destroyed. The Emergency Response Plan was activated at 2:30 p.m. Firemen cooled the tanks with water then fought the 4500 m² basin fire with foam. Around 6 p.m., with the fire regressing, tank n°6, with a 2900 m³ capacity and 1/3 full of diesel, began making sharp whistles and then burst, forming **a fireball 300 m high and 200 m wide** (Figure 1). It sagged partially outside of the basin. The intervention means were affected, the foam reserves were nearly exhausted and the fire surged. The neighbouring port was isolated by a floating barge, the sewer network was buffered and the neighbouring depot of chemical products was protected. The fire extended to the neighbouring basin and 2 tanks of petrol caught fire. The fire regressed and was controlled at 2 p.m. the 3rd of June; the ERP was lifted at 7:45 p.m.



Figure 1: Photograph of the fireball over tank n°6 (ARIA sheet of the BARPI, consultable at <http://www.aria.developpement-durable.gouv.fr>, accident n°4998)

Two hundred firemen intervened for more than 24 hours using more than 200 m³ of emulsifier. Two subcontracting employees were killed; six firemen and eight operators were injured, five seriously. The storage depot was destroyed and 1900 m³ of diesel, 1200 m³ of petrol and 600 t of additives were released. Hydrocarbons seeped into the soil and 10 000 m³ of extinction water was pumped and treated in refineries in the Southeast. The groundwater table had to be monitored until 2001. Material damages were estimated in 1987 at 130 million francs.

In 1996, judiciary experts retained the hypothesis of faulty upkeep of a barrelling pump of petroleum additive left functioning despite zero withdrawal, provoking its heating up and a breach by which the inflammable liquid may have been discharged and self-inflamed. The 21/12/00, the company was found responsible for the two deaths and required to give 1.4 million francs to the civil plaintiffs, while the storage depot director was sentenced to 15 months in prison and given a fine of 30,000 francs.

Lessons:

The disaster began in the zone of additive mixture, products that are unstable from 130-160°C, which was under construction even though other tanks were kept in service. The disaster's development was propelled by the explosion of the tanks of additives, known to be frangible, the absence of a means to close the foot valves of the tanks automatically or remotely, and the presence of alcohol compounds decreasing the effectiveness of the emulsifiers. The fireball emitted during the explosion of tank n°6, of a "welded" design and of which the roof was known to be "frangible," could be linked to a tank pressurization phenomenon¹⁷ or to a similar phenomenon, supposing that the relief valves, set to 175 mbar, could not evacuate the pressure differential due to product vaporization.

Several explosions were recorded, of which one was felt "several kilometres away." However, the effects engendered by this accident were essentially thermal (fireballs).



Figure 2 : Tank blown over by the explosion (ARIA sheet of the BARPI, consultable at <http://www.aria.developpement-durable.gouv.fr> , accident n°4998)

¹⁷ Groupe de Travail Dépôts Liquides Inflammables, June 2007, *Les boil over et autres phénomènes générant des boules de feu concernant les bacs des dépôts de liquides inflammables*, Annex 1 of Circular DPPR/SEI2/AL-07-0257 of 23/07/07 relative to the evaluation of risks and effect distances around depots of flammable liquids and flammable liquefied gas, available at <http://www.ineris.fr/aida>, abrogated by the circular of 10 May 2010 summarizing the methodological rules applicable to danger studies, to the appreciation of the risk reduction at the source approach, and technological risk prevention plans in classified installations according to the law of 30 July 2003.

3.1.2. Bordes Accident (France, 9 May 2000)

Progression:

Early in the morning of the 9th of May 2000, a truck transporting 777 bottles of gas (butane and propane of 6, 13 and 35 kg) arrived in the proximity of a company depot where it was due to deliver. The driver parked in the car park of the carwash located 20 meters from the depot and discovered, when getting out of the cab, that **one of the tyres** of the trailer was **on fire**. After trying in vain to extinguish the fire with foam, he left to alert emergency services. The **first bottles exposed to the heat of the flames exploded**; 3/4 of the load was progressively concerned. A security perimeter was put into place and the fire was controlled after a 4-hour intervention. Traffic was deviated for 5 hours and 30 minutes. There were no victims. The security perimeter was lifted the following day around 7 p.m. Prior to this, the scattered bottles were recovered. Those which had not exploded were sent to be destroyed. The carwash, the adjoining hangar, the depot's offices and several nearby houses were damaged. Bottle debris was found as far as **800 to 900 m** from the disaster location, according to witnesses. **90% of the debris was localized within a 100 m radius** around the vehicle in the accident. According to the investigation, the chronology is the following: 6:15, a tyre bursts (front left, first axle), inflammation of the tyre, effort to extinguish it; 6:18 the driver gives up / calls for help; 6:20: the bottles are reached; 6:25: first bottle explosions, firemen arrive; 7:35: last bottle explosion.

Figure 3 illustrates the resulting damage at the site.



Figure 3: Aerial photograph of the Bordes site after the accident

Lessons:

Approximately 570 bottles of gas exploded, generating fireballs and numerous fragments of different sizes. Around one hundred bottles showed breaches while another hundred were found without a shell breach with their total or partial contents. Examination of the bottle fragments showed three predominant cases:

- The bottle split into two nearly equal parts. This case is representative of a ductile rupture, just as the cases in which the bottle cracked longitudinally (Figure 4).



Figure 4: Ductile rupture

- The bottle burst in several different pieces (approximately 5); this is characteristic of fragile rupture.
- The top of the bottle is expelled, for example, the flange unit, valve and lid. This group of projectiles is consistent with the correct functioning of the safety feature of the bottle top. Indeed, the bottles were all equipped with a brass valve. When the bottle heats up, the brass valve dilates faster than the bottle flange, which is made of steel. Around 200-225°C, the flat joint softens, and then melts with the increase in temperature. Under the effect of gas pressure, the part sealing the nose of the valve swells and bursts, freeing the gas (Figure 5).



Figure 5: Projection of a bottle top

3.1.3. Dagneux Accident (France, 7 May 2007)

Progression:

The 7th of May 2007 around 8:30 p.m. (Leprette, 2005), **three inflamed LPG trucks** were reported in the industrial zone of Dagneux-Montluel (Ain). Despite the rapid intervention of emergency services, the trucks exploded, bringing about very significant material damage in a several hundred-metre radius. There were only minor injuries.

The three propane trucks were parked on a private site during the explosion. Two of them (20 m³ trucks containing respectively 0 and 2500 kg of propane) fragmented into multiple pieces that were projected into the environment (cf below). The third (15 m³, 500 kg of propane) **opened** and was projected approximately **60 m, without fragmenting**.

The **two 20 m³ tankers** exploded simultaneously approximately **40 minutes** after the fire started; it is unknown if the burst of the first is the source of the burst of the second. The explosion of the empty truck is a pneumatic burst while that of the partially full one is related to a BLEVE, and engendered the classic effects of this phenomenon. A fireball of an **approximately 80 m diameter** formed and lasted **9 seconds**.

No thermal radiation effects could be detected on the structures. However, it was visible on the vegetation (**scorched grass and bushes**) within an approximately **80 m** radius. This distance should be considered the enclosure of the weakest threshold of effect on man (3 kW/m²). The quantity of liquid was seemingly too weak to produce radiating effects at a great distance.

Some pressure effects were observed **as far as 400 m (broken glass)**, but the majority of the effects was concentrated to a radius of 200 m. Analysis of the damage in comparison with a table of typical damage allows the placement of the threshold of **50 mbar between 50 and 100 m**, and the threshold of **20 mbar between 150 and 250 m**. This result is confirmed by strength calculations of the structures made on several points (windows and single skin steel cladding).

Lessons:

Very large tank fragments were found **as far as 900 meters** away, but **75%** of the fragments were found in a **radius of 250 m**. The **favoured projection direction** was **perpendicular to the axis** of the tanks and the number of fragments was very high (in average 6 per tank), which is very uncommon when compared to available feedback on these types of phenomena (bursts and BLEVE). However, the maximum projectile distances are consistent with feedback, even if, from one accident to another, they are extremely variable.

It is theoretically possible, from the observation of lines of maximum deformation, to identify the rupture modes of a tank and to localise the probable start of the initial rupture. It seems that this rupture mode is the cause of the very pronounced directional effect observed at Dagneux. This nevertheless depends on the ability to reconstitute the tank from the fragments that were found. Unfortunately, this is not possible due to the great number of fragments, no more than it is possible to attribute the fragments to one or the other of the two tankers, for the tankers were of identical

design and had no distinguishing characteristics that would facilitate the identification of the fragments.

The regulatory distances are consistent with observed effects and modelling. However, we note that glass breakage was observed beyond the regulatory threshold distance of 20 mbar, which confirms that this value does not indicate the threshold where glass begins to break, but rather should be considered as the threshold of significant glass breakage (at least 10% of windows broken). Broken glass can indeed take place at weaker pressures (from 5 to 10 mbar¹⁸), depending on geometric and mechanical characteristics.

Finally, it was observed that the greatest effect distances in case of burst or BLEVE could come from fragment projection. These fragments can cause very significant damage. The hot and incandescent fragments are also vectors of domino effects. At Dagneux, the greatest material damage was caused by fires propagated by the projection of incandescent fragments.

¹⁸ The distance at 10 mbar is equal to at least 2 times the distance at mbar. Furthermore, at these weak pressure levels, exterior phenomenon such as wind or the reflection of pressure waves on low atmospheric layers are no longer insignificant.

3.1.4. *Other examples*

Other burst accidents or tests of vessels caught in fires are listed in the following table. In the majority of cases, only information relative to fragment projection is given in the reports.

Date	Place	Vessel description	Contents	Conditions and effects of the burst
April 1970	Refinery (Canada or USA)	Purifier of caustic gas	/	Tank rupture at the vapour phase level, projection of both extremities of the tank, one more than 17m
August 1972	Refinery (Canada or USA)	Tank with a 3.5 m diameter and 10 m length	/	/
		Tank with a 1 m diameter and 5 m length	/	Burst 10 to 15 minutes after the first burst; projection of most of the tank, which broke a pipeline, bringing about a discharge of fuel feeding the fire
28/07/1973	White Sands (New Mexico)	120 m ³ capacity tanker	Propane	Burst after 24 minutes of fire, at a pressure near the relief valve pressure setting Relatively high temperature gradient on the tank Around 10 tank fragments were projected to a maximum distance of 407 m
08/04/1979	Florida	Tanker	Ammonia	Rupturing of the tank into two sections projected 200 m (probably in an axial direction) and 75 m (probably in an angle of approximately 100° in relation to the axial direction) Rupture of a second tanker caught in a fire after obstruction of the valves, 20 minutes later, with fragment projection up to 200 m
19/11/1984	Mexico	Spheres (2400 m ³ and 1600 m ³)	Butane	Fragments projected 600m
		Cylinders (from 36 to 270 m ³)	Butane	Projection of 12 cigar-rockets; one (coming from a 36 m ³ cylinder) was found 1200 m away

10/03/1996	Italy	12 m ³ roadside tank	Propane	Fragment projected 500 m
27/07/2010	Port La Nouvelle (France)	13 m ³ roadside tank 64% full	Propane	Fragments up to 150 m Broken glass up to 700 m

Table 2: Examples of compiled data for bursts of vessels caught in fires

3.2. ACCIDENTAL PRESSURIZATION

The accidental pressurization of a tank can be due, for example, to the loss of output control or an accidental product injection into the tank.

3.2.1. *Heat exchanger burst (Indonesia, 14 April 1983)*

An LNG heat exchanger column 47 m long with a 5 m maximum diameter was purged with a hot, dry hydrocarbon gas to defrost and dehydrate it. The column's maximum service pressure was 2 bars and the relief valve was set to 4 bars. The source of the purge gas was more than 35 bars. A valve malfunction brought about the pressurization of the column. A pressure of 5 bars was recorded; 20 minutes later, the column broke. The vessel fragmented into three principle pieces; one struck a building 50 m away.

Lessons:

It should be noticed that the pressure at which the rupture was observed seems compatible with classic design rules which set service pressure at around one third of the rupture pressure of the tank.

3.2.2. *Other examples*

Other accidents corresponding to this cause and of which the principal data are given in Table 3 are described in Annex 1.

Date	Place	Vessel description	Contents	Burst effects
January 1966	Refinery (Canada or USA)	Tank	/	Projection of a piece of equipment 28 m
September 1970	Refinery (Canada or USA)	Reactor	Nitrogen (pressurization test with nitrogen at 27 bars)	Projection of a fraction of the head of the reactor 81 m

16/11/2008	Alès (France)	Hydrocarbon flexible pipe	Hydrocarbon (tube pressurized by a pump)	river pollution
13/03/2010	Gonfreville-l'orcher (France)	Water Degassing tank of a heater	Inert gases and steam	Damage to nearby equipment, diesel leak

Table 3: Examples of principle data compiled for bursts due to accidental pressurization

3.3. MECHANICAL WEAKENING AND IMPACT OF A PROJECTILE

A mechanical weakening of the shell of a pressurized tank can cause rupture. The bibliographic research relative to feedback undertaken in preparing this document allowed the identification of several accidents of this type, beyond those due to a temperature increase caused by a fire, treated in paragraph 3.1.

Date	Place	Vessel description	Contents	Burst effects
26/11/2000	Petit-Couronne (France)	LPG Pipeline	LPG	Quake of the control room, black cloud, H2S odour
17/12/2001	Huningue (France)	copper piping	R134a	R134a leak

Table 4: Examples of compiled data for bursts resulting from mechanical weakening

Bibliographic research did not allow the identification of a burst accident caused by the impact of a projectile; however, this type of burst is related to those caused by a mechanical weakening.

3.4. INTERNAL EXPLOSION

Explosion often leads to the rupture of the vessel in which it takes place. An explosion is a brutal freeing of energy; different phenomena can be at the origin of an internal explosion: combustion, a runaway chemical reaction, a brutal phase change...

Bursts of poorly degassed atmospheric hydrocarbon tanks following a vapour explosion (during cleaning or maintenance) belong to this category.

3.4.1. Blaye Accident (France, 20 August 1997)

An example of a burst of a storage vessel following an internal explosion is given by the accident that occurred at Blaye the 20/08/1997. A violent dust explosion largely destroyed a cereal storage facility.



Figure 6: Silo at Blaye after the explosion of 20/08/1997 (excerpt from the detailed sheet ARIA of the BARPI downloadable at <http://www.aria.developpement-durable.gouv.fr> , accident n°11657)

This vertical silo was made up of three rows of cells (44 in all) in circular cross sections (6.2 m in diameter and 33 m in height) made of reinforced concrete (15 cm thick). A reinforced concrete slab covered them and served as the floor for an open-air gallery. The products to be stocked were loaded through 60 cm by 60 cm orifices in this floor. The handling gallery harboured conveyor belts. It opened at each end to reinforced concrete towers 50 m in height.

It is estimated that the cells were capable of withstanding an internal pressure of the order of 1 bar. Still, the explosion completely destroyed the cells of the central part, the towers, the handling gallery and the attenuating cells of one of the two towers. Big pieces (of metrical dimension) were found at a distance of as far as 50 m and smaller pieces (of the order of 10 cm) as far as 150 m. Windows were broken as far as 500 meters from the explosion.

Lessons:

Simulations of this accident with the EFFEX code (Proust, 2000) suggest that overpressure in the cells was of the order of 3 to 4 bars, well above the standard pressure for the destruction of the cells. This is explained primarily by the extremely brutal development of the explosion, in a time period significantly less than that of the rupture and pressure discharge by the breaches. However, one must not rule out the direct effect of mechanical stress on the rupture process which can result in an increase or decrease of the destruction pressure in relation to static capacity, as we will see in paragraph 4.2.2.3.

3.4.2. Other examples

Other accidents corresponding to this cause of which the principal data are summarized in Table 5 are compiled and described in annex 1.

Date	Place	Vessel description	Contents	Burst effects
1981	United Kingdom	Dryer	Soda hydrosulphate, water present in the bottom	Propelling of more than half the tank across the plant
November 1962	Refinery (Canada or USA)	Accumulator	Water present in the bottom	93-meter projection of the main part, 220-meter projection of a 3m by 10 m piece
June 1987	Port Edouard-Herriot, France	Empty, non degassed atmospheric tank (n°14)	Hydrocarbon	

Table 5: Examples of compiled data for bursts following an internal explosion

3.5. LESSONS FROM FEEDBACK

This report does not treat risk analysis specifically; i.e. causes of bursts. However, feedback provides indications which can serve as a reminder of some measures that allow us to guard against the most dangerous scenarios.

The principal causes of vessel bursts being known (fire, internal explosion, overfill, weakening, corrosion), preventive measures may consist in limiting the risk of fire, installing valves or breathing vents allowing the limitation of vessel pressure, discharge vents, rupture disks, automatic extinction systems, equipment surveillance via auscultation or sonogram, etc.

In order to reduce the pressure effects produced by a vessel burst, one solution may be to reduce the risk at the source. Pressure effects being a function of the parameter $(P_{rupt} V)^{1/3}$, the rupture pressure P_{rupt} of the vessel and the gaseous volume V are the main factors influencing the quantification of the phenomenon, and they are all of the same importance. Still, a decrease in the rupture pressure by two, at a constant volume, in the goal of reducing the potential of danger, would only bring about a modest reduction in effect distances (20%). Similar reasoning may be made about volume.

Protective measures against pressure effects and fragments can also be envisioned. Thus, physical protective barriers such as walls or dikes are sometimes mentioned to protect again the effects of pressure from a burst. However, the effectiveness of these barriers is quite localized. Indeed, the installation of dikes allows, according to the Guide of Good Practices in Pyrotechnics edited by the SFEPA¹⁹, the local reduction of the shock wave by only 20 to 30%, but beyond a distance of the order of 4 times the height of the dike, the shock wave reforms. One could also envision weakening preferential zones on the equipment in such a way as to sufficiently wipe out the leak at the breach and benefit from directional effects, but this is a subject for future studies.

Concerning fragments, one could envision preferential rupture zones allowing the placement of a retaining system. Alternately, the installation of an enclosure wall could limit the projection angles to near vertical incidents so as to reduce projection distances. Finally, the protection of sensitive facilities is possible thanks to anti-missile screens of which the sizing is a function of the number of incidental fragments, their speed and their mass.

¹⁹ *Guide de Bonnes Pratiques en Pyrotechnie*, Version n°1-A of 13/02/2009, on sale on the internet site of the Syndicate of Explosive, Pyrotechnics and Fireworks Manufacturers (Syndicat des Fabricants d'Explosifs, de Pyrotechnie et d'Artifices) <http://www.sfepa.com>

4. RUPTURE CONDITIONS

Before calculating pressure wave propagation or fragment projection, it is necessary to know the characteristics of the vessel (pressure, temperature, container material) at the time of the burst. These are conditioned in part by the rupture mode, which depends essentially on the nature of the vessel and of the aggression.

4.1. RUPTURE MODES

During the increase of pressure in a vessel, the most fragile walls break when the rupture pressure is reached.

At the macroscopic scale, as the internal pressure increases, the material undergoes a reversible elastic deformation as long as tension stays below the critical threshold (the limit of elasticity) then, beyond that, a permanent plastic deformation can take place before destruction appears.

At the atomic scale, elastic and plastic deformations respect the matter's cohesion, the material naturally contains micro-fissures (of the order of the micron). Rupture takes place when this cohesion is destroyed. It occurs through the enlargement of the discontinuities within the material; the micro-fissures become macro-fissures reaching dimensions of the order of a millimetre, and finally fissures at the scale of mechanical structures (Mercier, 2003).

4.1.1. Fragile rupture

If the rupture takes place when the deformations are elastic (reversible), the behaviour of the material and the rupture are said to be "fragile". Glass, grey cast iron, crude steels, ceramics, concrete, most thermosetting polymers and certain high resistance alloys have a fragile behaviour.

Fragile rupture corresponds to a situation wherein fissure propagation is difficult. For example, this is the case for metallic alloys in which the strength characteristics were strongly increased. Thus, in general, fragility increases with yield strength. Fragile rupture takes place with the inter-atomic links break without global plastic deformation (Mercier, 2003).

As the rupture phenomenon is relatively localized, a significant number of small fragments can be formed following a multiplying of the bifurcations of the fissures. For the sake of simplification, fragile rupture can be considered quasi-instantaneous.

4.1.2. Ductile rupture

If the rupture takes place after a permanent plastic deformation, the behaviour of the material and the rupture are said to be "ductile". The majority of metals, alloys and certain thermoplastic polymers show this type of behaviour.

Ductile rupture is the result of the enlargement of micro-fissures and the propagation of the resulting fissure.

Ductile rupture, a generator of significant cracks, creates few fragments, but generally large ones (Mercier, 2003). The phenomenon's spread is limited by the speed of sound in the material.

4.1.3. Fragile-ductile transition

The number and shape of the shell fragments formed during a vessel burst depend on the number of cracks and thus of the rupture type. Holden proposed a classification of projectile shapes in function of the number of detached shell pieces and the number of circumferential cracks (Figure 7).

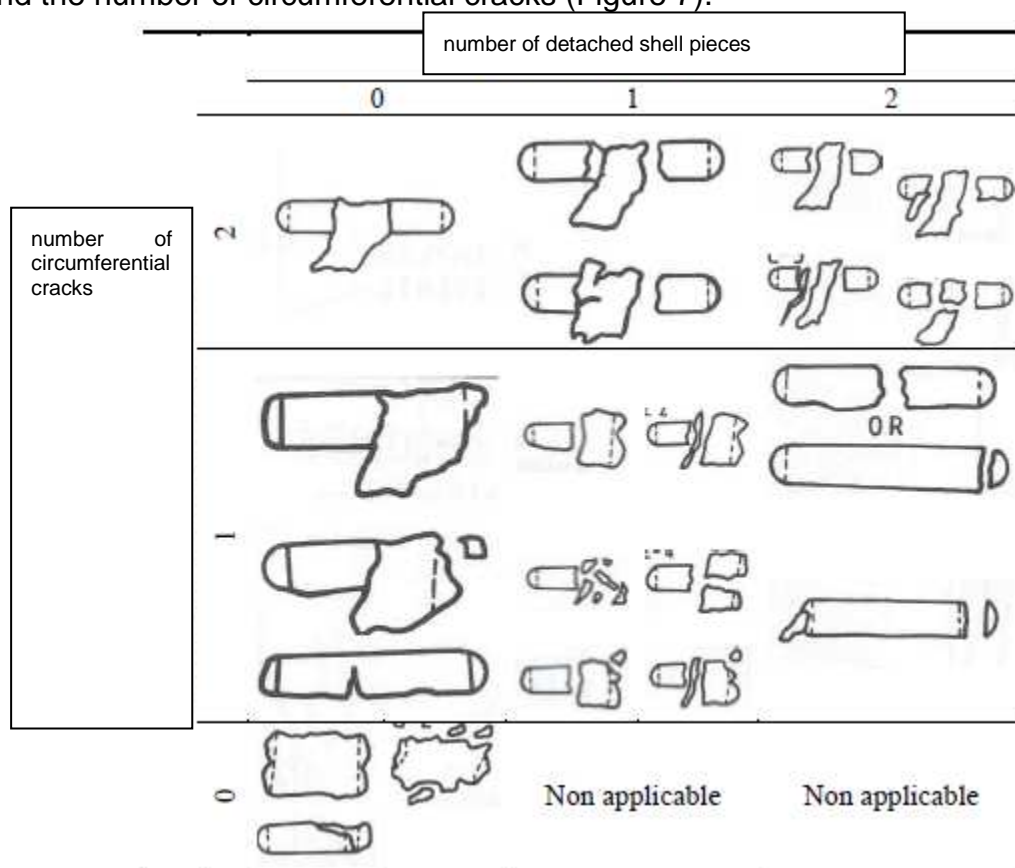
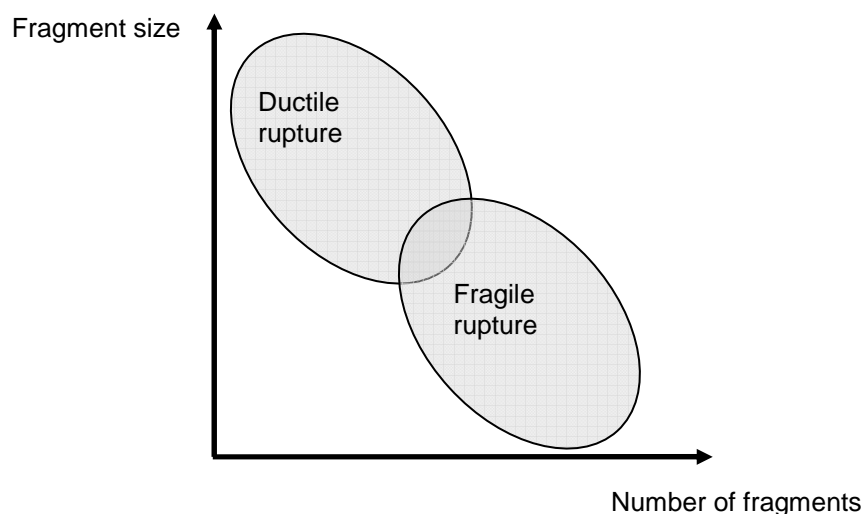


Figure 7: Classification of rupture modes (Holden, 1988)

The diagram below is a synthesis of the influence of the rupture mode in the size and number of fragments formed by a vessel burst.



Several factors influence the fragility or ductility of metals:

- *Temperature:* At a fairly low temperature, plastic deformation becomes impossible before the material ruptures. Thus, there exists a “transition” temperature below which the material becomes fragile. As the temperature increases, the transition between fragile rupture and ductile rupture takes place; there exists a temperature range where rupture is mixed.
- *Speed of deformation:* in general, ductility decreases if deformation speed increases.
- *notch effect:* the presence of a flaw or notch brings about a tension concentration which can modify the rupture mode.

4.2. DETERMINING RUPTURE PRESSURE

It is theoretically possible to determine the strength of vessel subjected to a quasi-static internal overpressure by classic calculations of structure strength.

The pressure in the vessel at the time of rupture depends on the thermodynamic conditions of the contained fluid and the vessel rupture pressure depending on its mechanical characteristics, the latter directly linked to the use for which it is designed.

Thus, atmospheric tanks designed for the storage of flammable liquids, LPG tanks, and concrete silos will have different rupture pressures.

For pressurized metal equipment, regulations and usual design rules, presented below, allow for a relatively simple estimation of the rupture pressure.

For other vessels, estimation of rupture pressure in case of static load can necessitate a calculation of structure strength.

4.2.1. Rupture pressure in static load (pressurized metal equipment)

The decree of 13 December 1999²⁰ is the transposition into French law of the European directive of 1997 (97-23-CE) relative to Pressurized Equipment. The field of application for this decree is the design, manufacture, evaluation of conformity, and sale of Pressurized Equipment. The order of 15 March 2000²¹, modified by the order of 31 January 2011, concerns maintenance of this equipment, which must be ensured by the user.

As for bursts, the regulatory constraints are in essence a function of the product $PS \cdot V$ where PS is the maximum allowable effective pressure and V the volume of the vessel under consideration. This choice seems relatively apt to the extent that this parameter represents the internal energy stored in the form of pressure.

Regulations require that the metal used in the construction of pressurized gas apparatuses be exempt of weaknesses in the temperature and pressure ranges to which this equipment is usually exposed. The design pressure is established by the manufacturer and is at least equal to the maximum operating pressure. Regulations expect that the maximum tension in the metal at the design pressure must be less than the two following values:

- $\frac{R}{3}$, where R is the conventional ultimate tensile strength of the metal,
- $\frac{R_{eT}^{0,002}}{1,6}$, where $R_{eT}^{0,002}$ is the conventional yield point, or the stress at 0,2% of strain of the metal.

Thus, it is recommended in the TNO Yellow Book²² and the UCSIP²³ guide for the development of danger studies that the relationship of 2,5 between the destruction overpressure and the effective design pressure (equal to or greater than the maximum permitted effective service pressure) be retained.

More differentiated values are proposed by the CODAP (« *CODE de construction des Appareils à Pression* » (Construction Code for Pressurized Equipment)), which depend on the type of material in use:

- 2.4 for non-alloyed steel and non austenitic alloyed steel²⁴,
- 3 for austenitic steel,
- 4 for copper or copper alloys,

²⁰ Decree n° 99-1046 of 13 December 1999 relative to pressurized equipment, published in the *Journal Officiel*, 15 December 1999, modified by the decrees of 27 July 2010, 2 November 2007, 23 December 2003 and 22 December 2003.

²¹ Order of 15 March 2000 relative to the use of pressurized equipment, published in the *Journal Officiel*, 22 April 2000.

²² *Methods for the calculation of physical effects resulting from releases of hazardous materials* (published by the Committee for the Prevention of Disasters, Second edition, 1992)

²³ Union des Chambres Syndicales de l'Industrie du Pétrole

²⁴ Austenitic steels are stainless steels of which the crystalline structure (the material's atomic arrangement) is a body-centred cubic structure.

- 2.4 for aluminium, nickel and nickel alloys,
- 3.5 for titanium

In practice, it is possible that rupture overpressure occasionally deviates significantly from this scale.

Thus, when rupture overpressure is unknown, one can retain as an acceptable order of magnitude an overpressure equal to 3 times the effective design pressure.

4.2.2. Impact of the origin of the burst

4.2.2.1. Vessel caught in a fire

The study of accidents shows that temperature has a significant influence on rupture pressure. Indeed, the mechanical characteristics of materials depend on temperature. The figure below traces the evolution in relation to temperature of the yield strength, tensile strength, elasticity modulus and linear dilation coefficient for steels. These curves were obtained from tensile tests on test pieces.

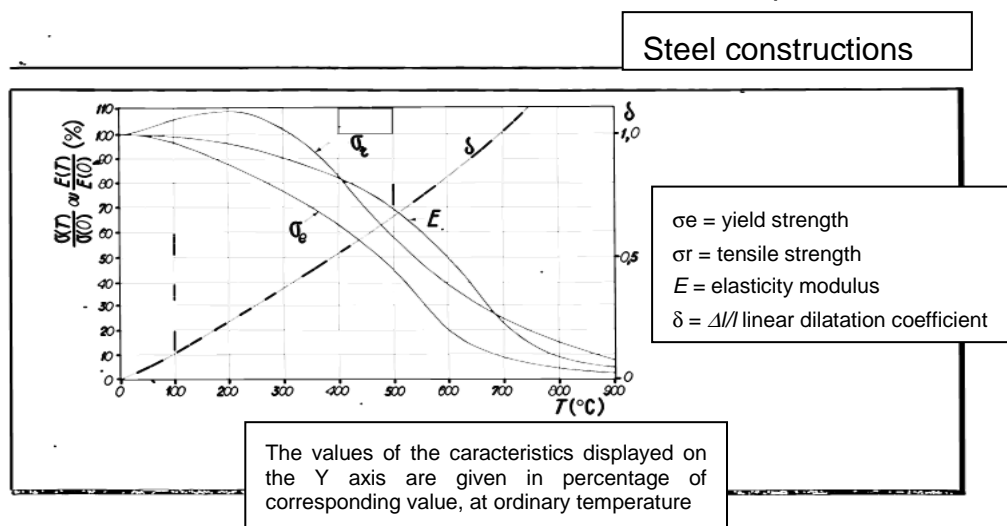


Figure 8 : Mechanical characteristics of steel in relation to temperature on a tensile test piece (Fruitet, 1979).

For example, the tensile strength of steels decreases above a temperature of several hundred degrees Celsius, to such an extent that when a vessel is caught in a fire its internal pressure increases and tensile strength decreases. Because the type of steel has a weak influence, it is possible to consider, in a first approximation, that the curves in Figure 8 are valid for all types of construction steel, as long as the ordinates are read as a relative value in relation to basic characteristics at an ordinary temperature (Fruitet, 1979).

Consider, for example, a cylindrical tank of 10 m³ completely filled with gas of which the design pressure is 1.7 bars. The diameter of the cylinder is 1.60 m and the shell thickness is 5 mm, in accordance with CODAP rules. The rupture pressure of the tank at an ordinary temperature of 25°C is considered, for the purpose of this calculation, to be equal to 6.1 bar absolute (3 times the tank's design pressure).

Imagine the cylinder is caught in a fire and that therefore the pressure of the gas inside the vessel increases linearly with temperature, following the law of perfect gasses (Figure 14).

The rupture pressure P_R of the tank is linked to the tensile strength σ_R by the classic relationship:

$$P_R = \frac{\sigma_R \times e}{R}$$

where R is the tank's radius and e the shell thickness. From this relationship and data from Figure 8, which links tensile strength to temperature, it is possible to estimate the evolution of bursting pressure in relation to temperature (Figure 9), which has the same rate as the change in tensile strength.

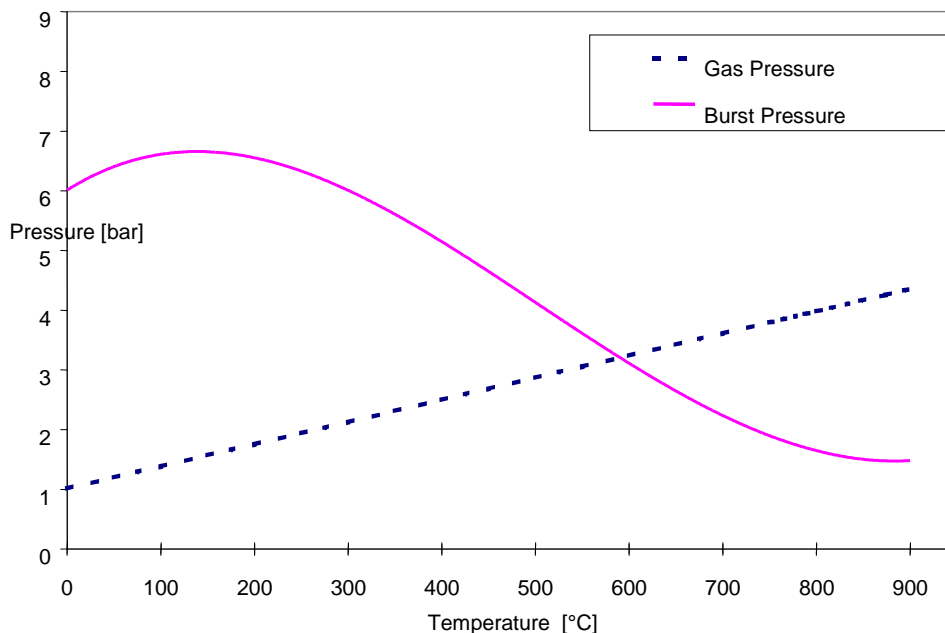


Figure 9 : Change in gas pressure and burst pressure versus temperature

Thus, the characteristic curves of burst and internal pressure cross near 550°C for an overpressure approximately half of the nominal burst overpressure.

We can thus state that a gas tank caught in a fire can burst at half of its maximum burst overpressure for a temperature around 500°C. Moreover, Figure 8 (Fruitet, 1979) shows that for steels, the tensile strength at 500°C is about half the tensile strength at ordinary temperature.

This result, rather roughly obtained in the case of the example above, is consistent with feedback that shows that a vessel caught in a fire can burst at a pressure less than its burst pressure at ambient temperature, as was observed, for example, in the test of a tanker caught in a fire (White Sands test, presented in annex 1).

4.2.2.2. Relatively slow accidental pressurization (overfill)

When the burst is due to a relatively slow accidental pressurization, as in the case of overfill, for example, the pressure in the vessel at the time of bursting may be considered equal to the burst pressure in static capacity.

4.2.2.3. Internal explosion

Baker (1983), for example, points out that equipment strength depends on the speed of mechanical load. This phenomenon is taken into account by adding the inertia terms into the matrices of deformation of the considered equipment. By in large, the system is, in its most simple configurations, a mass-spring model in which stiffness stands for the structure's elasticity and mass its inertia. Depending on the type of load, the mass's acceleration can add to (or subtract from) the external stress and increase (or decrease) the deformations, to such an extent that rupture appears for much lower (or higher) pressures than in static load (Proust, 1997).

Indeed, the structure is susceptible to behave in a different manner when pressure is no longer applied quasi-statically (typically 0.01 bar/s) but rather dynamically (load speeds of the order of 1 bar/s or more), as in internal explosions, for example. The behaviour of the structure depends on the relationship between its own frequency and that of the rise in pressure due to the explosion. For many situations, it can be considered that only the fundamental mode of the structure, i.e. its characteristic vibration frequency, is affected (Proust, 2000).

In simplifying the structure to a mass-spring system, a characteristic parameter allows a fairly simple determination of the influence of a dynamic load on the vessel's rupture. This parameter, *DLF (Dynamic Load Factor)*, represents the relation between dynamic and static loads at the origin of the material's rupture, i.e. the relation between the tensile strengths for a dynamic load and for a static load; it is an adimensional parameter.

The following figure represents the variations in strength of an inset membrane of a characteristic dimension of 0.5 m, exposed to explosion effects of various force (membrane installed on a 10 m³ chamber inside of which dust explosions were initiated).

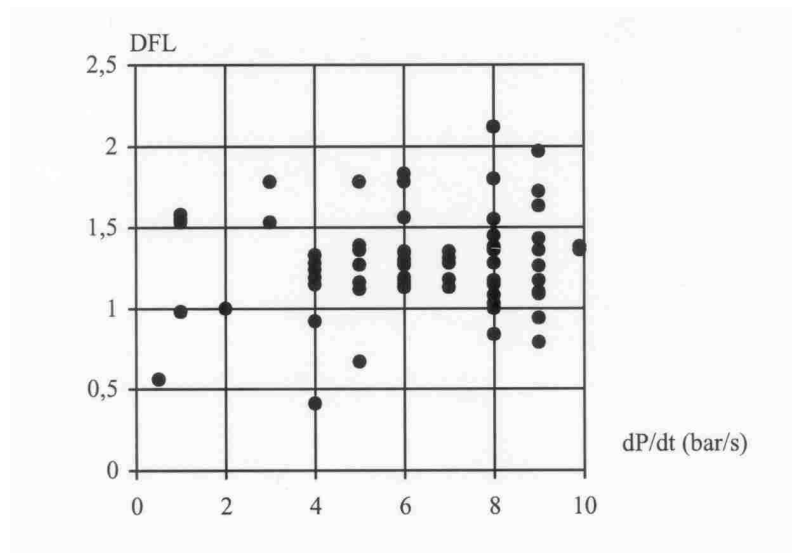


Figure 10 : Dynamic Load Factor for a thin membrane exposed to explosions of varying force (Proust, 2000)

We notice that the explosion's dynamic effect on a structure can lead to either an increase or a reduction of the considered equipment's strength compared to a static load of equivalent amplitude (Proust, 2000). In practice, it is possible to consider that the effective dynamic burst pressure is between half and double the nominal static burst pressure.

This dynamic behaviour increases risk under its two aspects. First, burst probability increases because it becomes possible as soon as overpressure nears half of nominal static burst pressure, whereas, other than for this type of dynamic load, the danger of burst is near the nominal burst pressure. Secondly, the burst effects are susceptible of being more significant for the burst can take place when the pressure has reached twice the nominal burst pressure.

Thus, when the burst is caused by an internal explosion, the container's burst pressure can be considered as roughly equal to double the static burst pressure, under the condition that this value does not exceed the maximum pressure of theoretical explosion.

4.2.2.4. Impact of fatigue

Under the action of repeated or alternating loads, a rupture can take place at a stress less than the material's static strength: this is rupture by weakening. This rupture mechanism could result from an increase in cracking during repeated loads.

The simplest fatigue test consists of submitting test pieces to cycles of periodic stress, of maximum amplitude and constant frequency, and to note the number of cycles N after which the rupture takes place. This number N is reported, in general on a logarithmic scale, in function of the maximum stress of the cycles. A point on the chart corresponds to each test piece (σ , N) and, from a batch of test pieces submitted to different maximum stresses, a curve is obtained which has the shape of that represented in Figure 11, known under the names of de Wöhler's curve and S-N curve (Stress-Number of cycles). In many cases, it is possible to trace an asymptotic line to Wöhler's, the asymptote being the limit of endurance or point of fatigue σ_D (Rabbe et al., 2000).

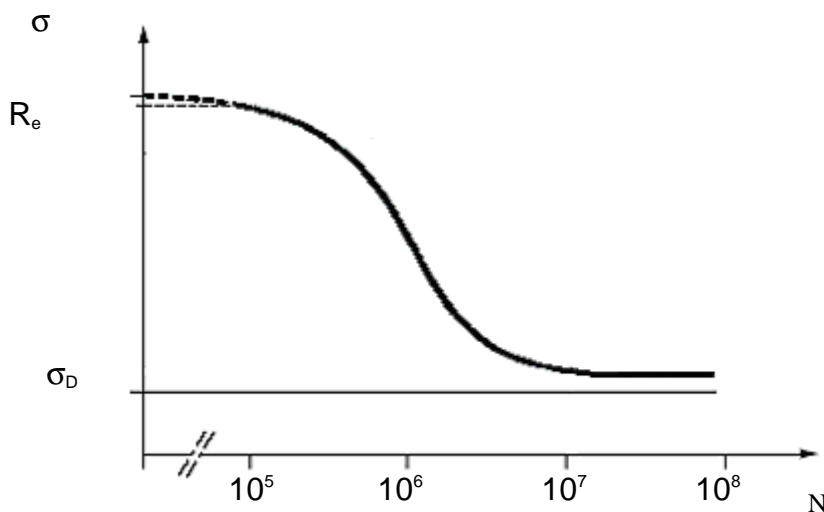


Figure 11 : Evolution of stress σ in relation to the number of cycles N (R_e is the yield point and σ_D the weakness point)

Experiments carried out on smooth test pieces (Rabbe et al., 2000) allowed the establishment of a relationship between endurance limit σ_D and tensile strength. It was found that endurance limit is roughly between one-third and two-thirds tensile strength²⁵.

If we extrapolate this relationship to cases of containers exposed to load cycles, the burst pressure of a container with a weakened shell by fatigue can be three times less than its burst pressure in case of static load.

In a prudent manner, effects are generally calculated without taking this phenomenon into account, considering static burst pressure so as to maximize the effects.

²⁵ For tensile trials on test pieces, tensile strength can also be called rupture limit or rupture load.

4.2.2.5. Impact of a projectile

When the burst is caused by a projectile, it usually takes place at the operating pressure of the vessel.

5. PRESSURE WAVE PRODUCTION AND PROPAGATION

5.1. DESCRIPTION OF THE PHENOMENON

The vessel rupture allows the release of contained pressure, the external propagation of an aerial pressure wave (displacement of an overpressure into the air). To use a simple analogy, the vessel is like a loudspeaker. The sound put out by this loudspeaker is directly proportional to the energy that one puts into it. The impression felt by an observer will be a function of, besides this energy, the distance and size of the loudspeaker. We thus understand that the amplitude of the aerial wave produced by a vessel burst must be a function of distance, vessel size and maximum internal overpressure. We will see that this amplitude depends in fact on the parameter $(P_{rupt}V)^{1/3}$, where P_{rupt} is the pressure in the tank at the time of the burst and V the volume of pressurized gas.

As a reminder, the propagation of an aerial pressure wave in the environment manifests itself by more or less sudden variations of more or less great amplitude of pressure in any point of space. At a given point, these pressure variations are notably characterized by:

- An over pressurization phase, of duration Δt_+ and maximum amplitude ΔP_+ ,
- A depressurization phase, of duration Δt_- and maximum amplitude ΔP_- .

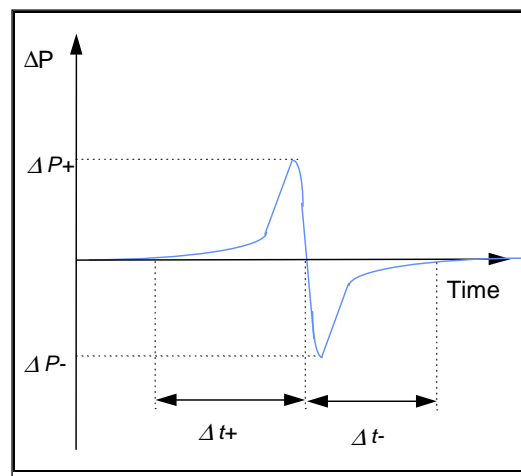


Figure 12 : Profile of a pressure wave

The rupture is accompanied by a vessel burst and the possible formation of several fragments that can be propelled under the effect of the pressure differential between the interior and the exterior.

Fragments follow a trajectory determined, besides by the initial conditions, by the effects of aerodynamic drag, eventual lift and gravity. Let us note that impulse is transferred to the fragment by fluid jets coming from the breaches and that consequently thrust force should decrease as each fragment gets farther from its departure point and deviates under the effect of earth's gravity from the axis of the jet which propels it. Fragment projection will be treated in chapter 6.

5.2. PRESSURE WAVE PRODUCTION AND PROPAGATION

To evaluate the production of a pressure wave, we imagine that the container shell disappears instantaneously at the time of rupture. We then observe a brutal acceleration of the surrounding atmosphere operated by a shock wave propagating in the atmosphere.

In these first instants, this phenomenon can be described qualitatively by means of shock tube theory (Wright, 1961). A shock tube is a long cylindrical tank divided into two compartments by a partition that is perpendicular to the tank axis. One of the compartments is filled with a highly pressurized gas, the other with a gas at a low pressure.

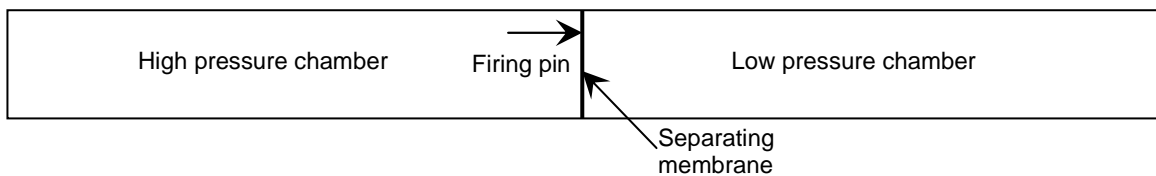


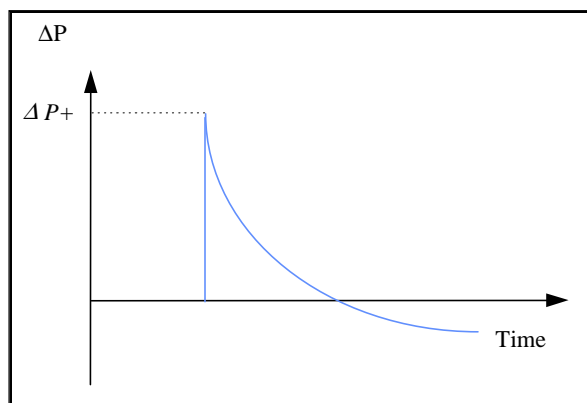
Figure 13: Shock tube

Figure 13 represents the apparatus. Grossly simplified, its functioning can be described in the following manner:

- At the moment when the striking pin bursts the separating membrane, a shock wave²⁶ of intermediary amplitude between the high pressure and the low pressure leaves from the membrane and disperses across the low pressure chamber with a speed at least equal to that of sound in the low pressure chamber.
- An expansion wave propagates across the high pressure chamber, reflects on the bottom and then follows the shock wave. After three trips of the expansion wave, the pressure has decreased to the point that the bottom of the chamber is back to atmospheric pressure (Baum, 2001).

The characteristics of the waves can be calculated by applying conservation of mass and momentum. The pressure of the shock wave is a few tenths of the pressure of the tank at the time of rupture.

²⁶ A shock wave is a wave of aerial pressure which has a brutal rise in pressure:



During a real accident, at the time of the burst, the walls (the vessel shell) do not disappear instantaneously, they thus accelerate progressively and slow the fluid initially contained in the container due to their inertia. The depressurization is thus slower, less abrupt, and the shock wave less strong. At this time, it is not easy to account for this phenomenon, thus walls are often considered without inertia to estimate the amplitude of waves (thus in excess) by means, for example, of the shock tube theory.

The expansion waves end up catching the shock wave to form a classic aerial pressure wave of which the amplitude, by virtue of the laws of fluid mechanics, must attenuate in function of the distance from the centre of the explosion.

The pressure wave produced during a burst presents thus the form of a shock wave, with an extremely rapid rise in pressure and a positive phase duration corresponding to the duration of the depressurization of the tank.

5.3. CONSEQUENCES MODELLING: GLOBAL METHODS

Methods to describe the consequences of a container burst are essentially based on principles of thermodynamics.

5.3.1. The Shock Tube-TNT method

The Shock Tube-TNT method was designed at INERIS at the beginning of the 1990's (Proust, 1991) to predict the effects of a tank burst. A description of this method was published in 1996 (Duplantier, 1996).

An approximation of the waves produced during a burst is done under the principal suppositions that:

- The gasses are perfect and ideal,
- All the pressure energy serves to produce waves,
- Near the tank, shock tube theory applies,
- Further away, the waves resemble those induced by an instantaneous release of energy, like for an explosive, and can be represented by the graph of overpressure decrease in relation to distancing in case of an explosion of a mass of TNT.

Brode (Brode, 1959) proposes a means for making the link between the zone where shock tube theory applies (near field) and the zone where TNT-type decrease is appropriate (far field). According to Brode, the parameter which allows one to differentiate the near field from the far field is the mass of gas m_r in the container before the burst. The near field is defined by the hemispheric volume of air V_0 , of mass m_0 and density ρ_0 surrounding the container such that: $m_0 = 10m_r$.

The radius of the hemisphere (measured from the tank's centre) is thus equal to:

$$R_0 = 1,7 \cdot \left(\frac{m_r}{\rho_0} \right)^{1/3} \quad (5.3.1.1)$$

Near field

Near field, the absolute pressure of the front of the shock wave p_{s0} , also called contact pressure, can be determined by the « shock tube » formula. This relationship allows the calculation of the pressure of the front of the shock wave that propagates in a tube filled with a gaseous mixture. It can be applied to the case of aerial shock waves if the flow is one-dimensional (spherical or hemispheric shock wave). This relationship is the following:

$$\frac{p_1}{p_0} = (\overline{P_{s0}} + 1) \cdot \left[1 - \frac{(\gamma_1 - 1) \left(\frac{a_0}{a_1} \right) \overline{P_{s0}}}{\left[2\gamma_0 (2\gamma_0 + (\gamma_0 + 1) \overline{P_{s0}}) \right]^{1/2}} \right]^{-2\gamma_1/(\gamma_1 - 1)} \quad (5.3.1.2)$$

where:

- p_1 is the absolute pressure in the container at the time of its rupture (Pa),
- p_0 is the ambient pressure (Pa),
- $\overline{P_{s0}}$ is the adimensional aerial overpressure after the burst: $\overline{P_{s0}} = \frac{P_{s0} - P_0}{P_0}$,
- γ_0 is the relation of specific heats of ambient air ($\gamma_0 = 1,4$),
- γ_1 is the relation of specific heats of the compressed gas,
- a_0 is the speed of sound in ambient air (of the order of 340 m/s),
- a_1 is the speed of sound in the compressed gas (m/s).

For a perfect gas:

$$\left(\frac{a_1}{a_0} \right)^2 = \frac{\gamma_1 \cdot T_1 \cdot M_0}{\gamma_0 \cdot T_0 \cdot M_1} \quad (5.3.1.3)$$

where:

- T_0 is the absolute temperature of ambient air (K),
- T_1 is the absolute temperature of the compressed gas (K),
- M_0 is the molar mass of ambient air (29,0 g/mol),
- M_1 is the molar mass of the gas in the container (g/mol).

The equation (5.3.1.2) is solved by successive iterations. Some calculated p_{s0} values are provided in the diagrams in Figure 14 and Figure 15. This pressure p_{s0} is less

than the pressure of compressed gases p_1 (or rupture pressure). This relationship cannot be used to calculate pressure effects in the far field.

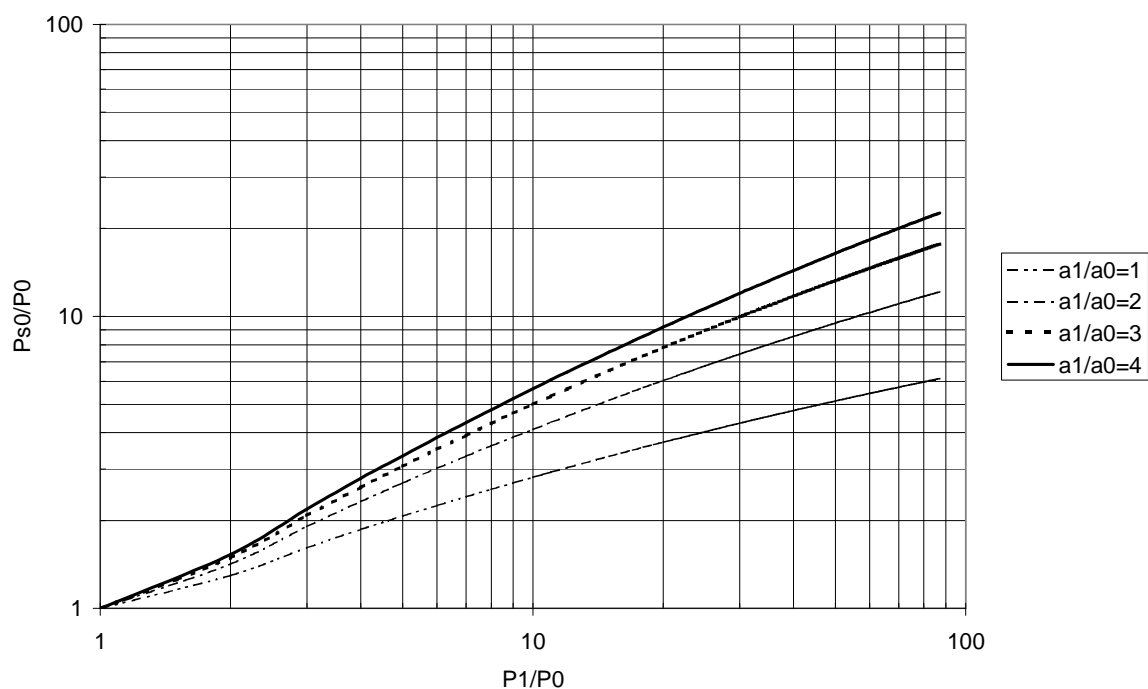


Figure 14: p_{s0}/p_0 in relation to p_1/p_0 and (a_1/a_0) for a di or tri atomic gas ($\gamma_1=1.4$)

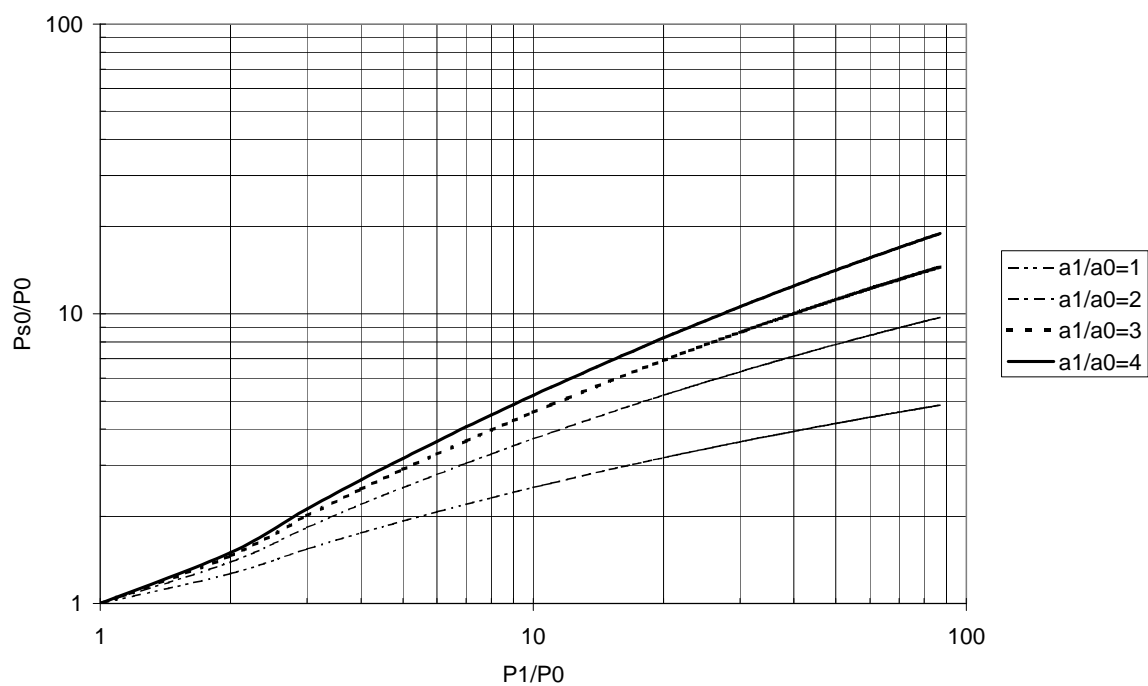


Figure 15: p_{s0}/p_0 in relation to p_1/p_0 and (a_1/a_0) for a monatomic gas ($\gamma_1=1.66$)

Far field

In the far field, i.e. for an observation distance R greater than R_0 , the blast wave's characteristics no longer depend on anything other than the source energy. The TM 5-1300 (TM 5-1300, 1990) graphs can thus be used to estimate the maximum pressure of the shock wave in a given place. These graphs were established for condensed explosives placed on the ground such as TNT. As Figure 16 shows, the change in maximum overpressure Δp ($\Delta p = p_s - p_0$, where p_s is the absolute pressure produced by the explosion at distance R) is given in relation to the reduced distance $\lambda = R/m_{TNT}^{1/3}$ (where R is the observation distance, calculated from the centre of the tank, and m_{TNT} the equivalent TNT mass of the phenomenon).

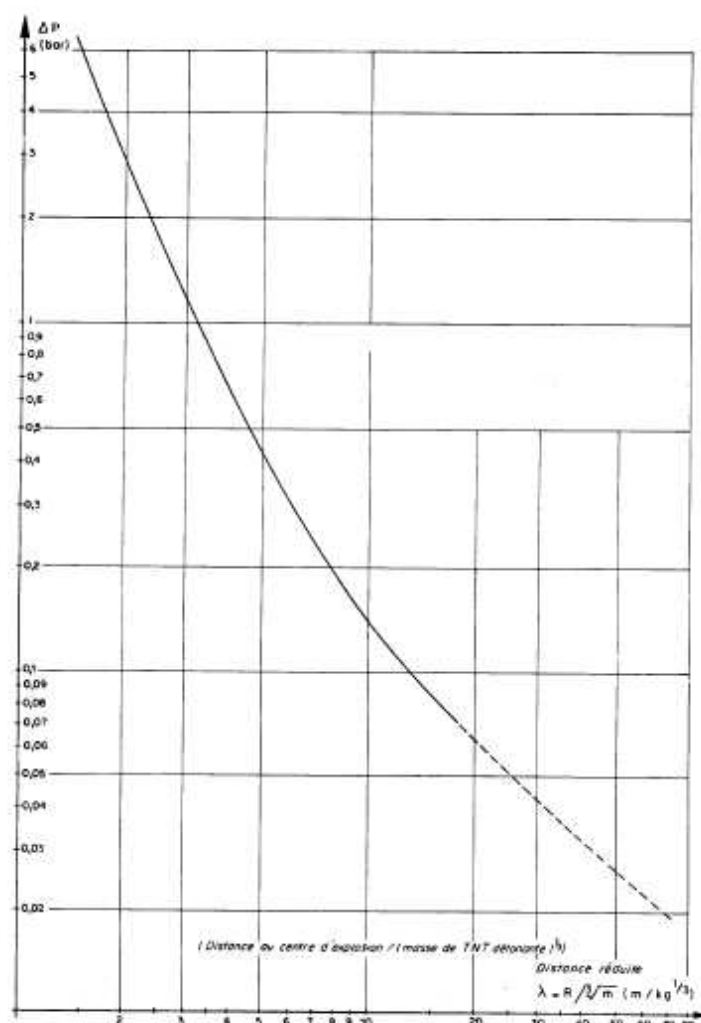


Figure 16: Overpressure produced in open field by the detonation of a load of TNT placed on the ground versus the distance to the centre of the explosion (extrapolated graph TM5-1300 taken from (Lannoy, 1984))

The equivalent TNT mass corresponds to the pressure energy available at the time of the vessel burst. The application of the first principle of thermodynamics to the moving wave allows us to show that the energy carried in the aerial wave corresponds to what is called “Brode energy”²⁷ (Proust, 1991).

$$E_{Brode} = \frac{(p_1 - p_0) \cdot V_1}{\gamma_1 - 1} \quad (5.3.1.4)$$

where V_1 represents the vessel's volume of the vapour phase (m³).

This energy represents the increase of the tank's internal energy produced by the growth of pressure. This growth can be obtained either by an increase in the temperature of the gasses (heating or combustion) or by the injection of additional gas.

There is no difference in principal between this phenomenon and the emission of an aerial wave following the brutal release of the combustion gasses of an explosive. It is thus legitimate to appropriate the graphs relative to wave propagation from the detonation of explosives, keeping in mind that the « Brode energy » of an explosive is very close to its combustion energy. A classic energetic equivalent is then defined to make the link with the graphs:

$$m_{TNT} = \left(\frac{E_{Brode}}{E_{TNT}} \right) \quad (5.3.1.5)$$

with m_{TNT} the equivalent TNT mass and E_{TNT} the specific combustion energy of TNT ($E_{TNT}=4690$ kJ/kg).

Experience shows however that the declining overpressure curve of the TM5 graph in relation to distancing is overestimating, particularly for overpressures less than 10-20 mbar.

Given that the decrease in overpressure is not known in near field, we will consider, to be prudent, that overpressure is constant and equal to the shock pressure in all of the near field.

²⁷ The formula of reversible adiabatic release (or isentropic release) is sometimes recommended:

$$E_A = \frac{p_0}{\gamma_1 - 1} \cdot \left(\frac{p_1}{p_0} - \left(\frac{p_1}{p_0} \right)^{\frac{1}{\gamma_1}} \right) \cdot V_{res} \quad (5.3.1.6)$$

It represents the energy transmitted to the environment by the slow and isentropic release of a gas. In general, it is not adapted to the case of a shock wave for this phenomenon is usually irreversible and dynamic. From a practical standpoint, it is generally remarked that the energy freed by an adiabatic reversible release is inferior to Brode's. Choosing the highest value is the conservative position.

5.3.2. The PROJEX method (INERIS)

L'INERIS has proposed replacing the Shock Tube-TNT method by the PROJEX method.

The TM5 graph has thus been replaced by the Indication 10 curve of the Multi-Energy method graph (V.d.Berg, 1985) (Figure 17) which provides more realistic results, particularly for very weak air overpressures.

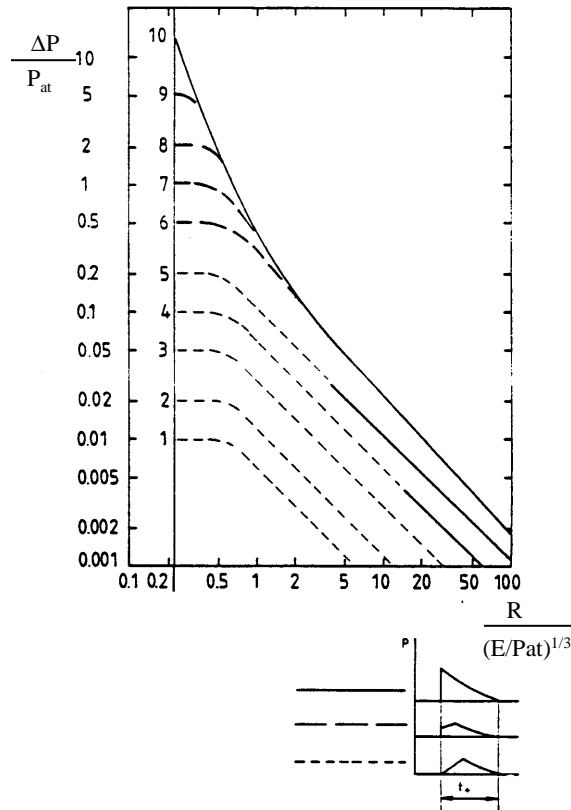


Figure 17: Graph relative to the Multi-Energy method giving overpressures produced by blasts at a constant flame speed of hemispheric explosive volumes placed on the ground (Mouilleau, Lechaudel, 1999)

The pressure effects produced by the brutal release into the atmosphere of the contents of a tank during its burst are thus assimilated to those produced during a detonation (the indicator 10 curve corresponds to the effects of a detonation).

The application of this model to cases of bursts of pressurized gas tanks was experimentally proven (Figure 18) and compared to feedback (Figure 19).

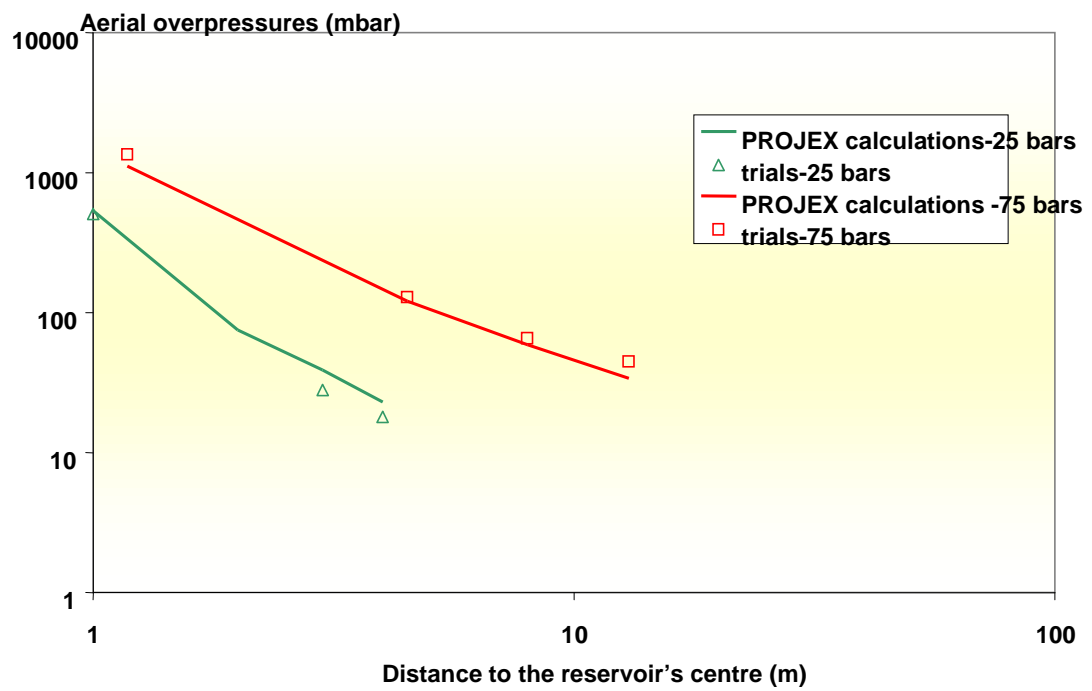


Figure 18: Comparison of overpressure levels calculated with PROJEX to those measured during gas tank bursts

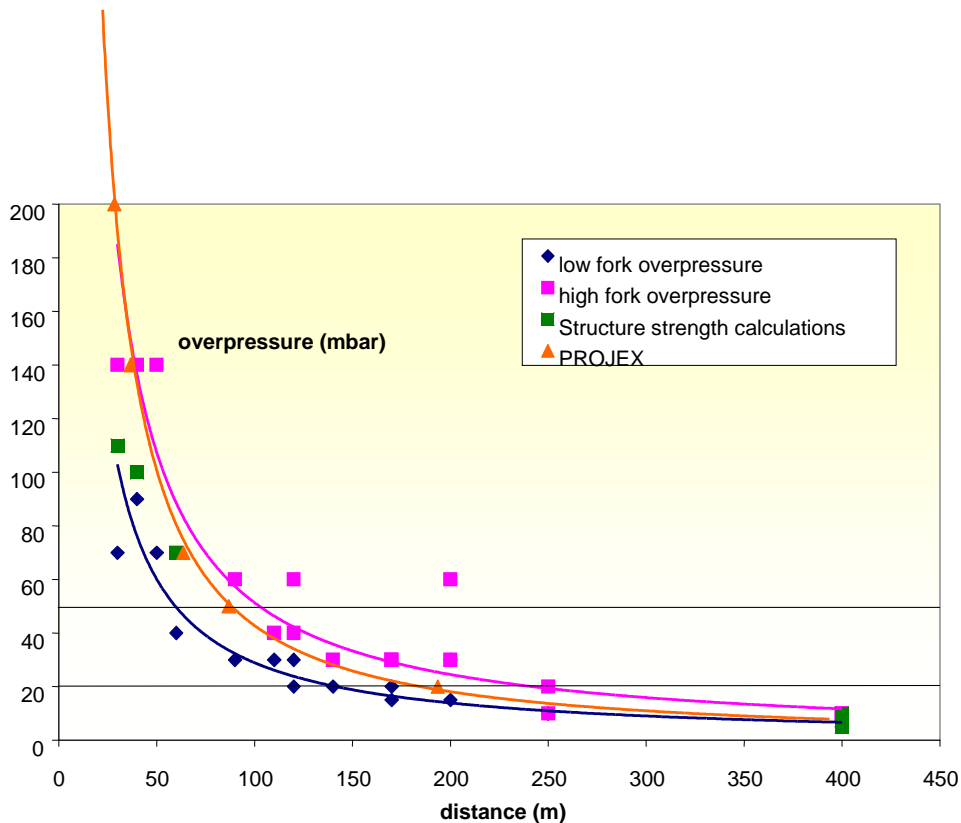


Figure 19 : Comparison of the estimation of pressure effects following the burst of a 20 m³ empty (of liquid) propane tank (Dagneux accident– 7 May 2007) with the theoretical curve calculated with PROJEX

Size of the near field:

For some situations (non isotropic discharge, very elongated container, etc.), the estimation of the size of the near field proposed by Brode is not well adapted, and can lead either to an overestimation of the size of the near field (particularly in the case of axial discharge of very elongated pressurized containers with very large volumes) or to an inconsistency (near field radius less than the radius of the tank in the case of a very elongated tank). The size of the near field would then be linked instead to the size of the opening through which the discharge occurs rather than to the volume of pressurized gas contained in the container.

Experimental data of aerial overpressure measurements during a pressurized vessel burst acquired by INERIS these last years shows that it seems fairly reasonable to extend the law of decreasing pressure waves (Multi-energy Indicator 10 curve) representative of the far field in the area of low distances until the abscissa where the calculated overpressure reaches the shock pressure, a value which cannot be surpassed.

5.3.3. The Baker's method

The method proposed by Baker is detailed in his work "*Explosion hazards and evaluation*" (1983); it allows the description of bursts of vessels containing only pressurized gas.

As in the Shock Tube-TNT and PROJEX methods, a distinction is made between the near field and the far field:

- In the near field, the method is based on the results of numeric calculations of bursts of tanks containing perfect gasses,
- For the far field, Baker bases his method on the similitude with detonation effects of condensed explosives.

The near field

In the near field, Baker comes to a graph like that shown in Figure 20.

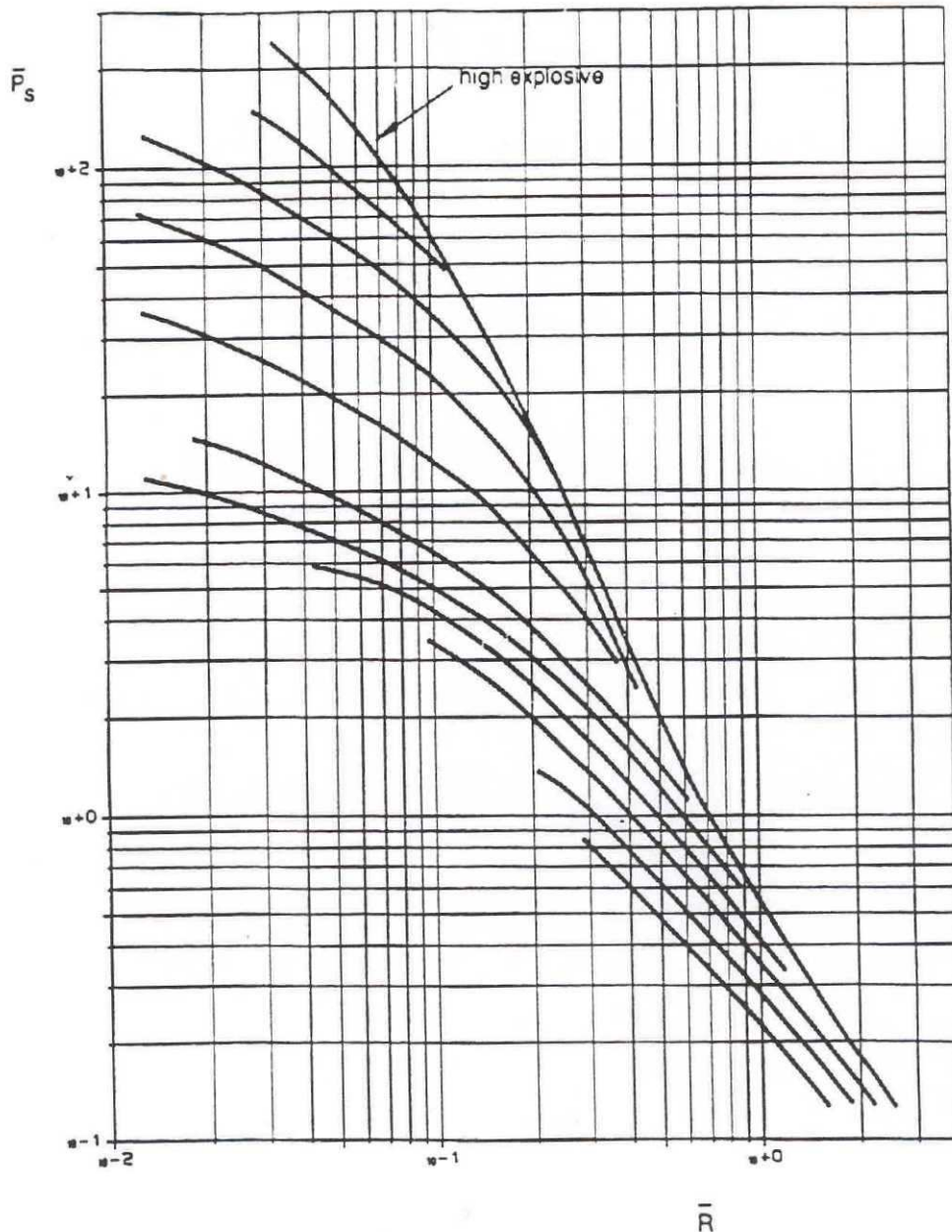


Figure 20: Adimensional overpressure versus adimensional distance (Baker, 1983)

It is a double entry graph that necessitates the calculation:

- On the one hand, the reduced distance on the abscissa:

$$\bar{R} = r_t \cdot \left(\frac{P_0}{E_{ex}} \right)^{1/3} \quad (5.3.3.1)$$

where E_{ex} is the energy of the pressure wave (in J) and r_t the real distance of the target (in m),

- On the other hand, the estimation of the shock pressure P_s on the basis of shock tube theory.

One thus finds his place on the abscissa and on the ordinate axis, which allows the selection of a declining pressure curve in the near field. To choose this curve, the parameter is calculated:

$$r_0 = \left(\frac{3V_1}{2\pi} \right)^{1/3} \quad (5.3.3.2)$$

which is the equivalent dimension of the tank of volume V_1 , assumed hemispheric, and which allows access to the original abscissa:

$$\bar{R}_0 = r_0 \cdot \left(\frac{P_0}{E_{ex}} \right)^{1/3} \quad (5.3.3.3)$$

Shock pressure at the very beginning of the release P_{s0} is equally determined by means of additional graphs (Figure 21 and Figure 22). The couple $(\bar{R}_0, \bar{P}_{s0})$ thus allows the identification of the declining overpressure curve in the near field.

The near field is defined approximately for $\bar{R} < 2$.

E_{ex} is based, as with the INERIS methods, on "Brode energy." However, Baker's graphs (**Erreur ! Source du renvoi introuvable.** and Figure 23) are made for completely spherical geometries. In reality, vessels burst on the ground, in a half-space, and to be able to use these graphs, it is necessary to multiply Brode energy by 2.

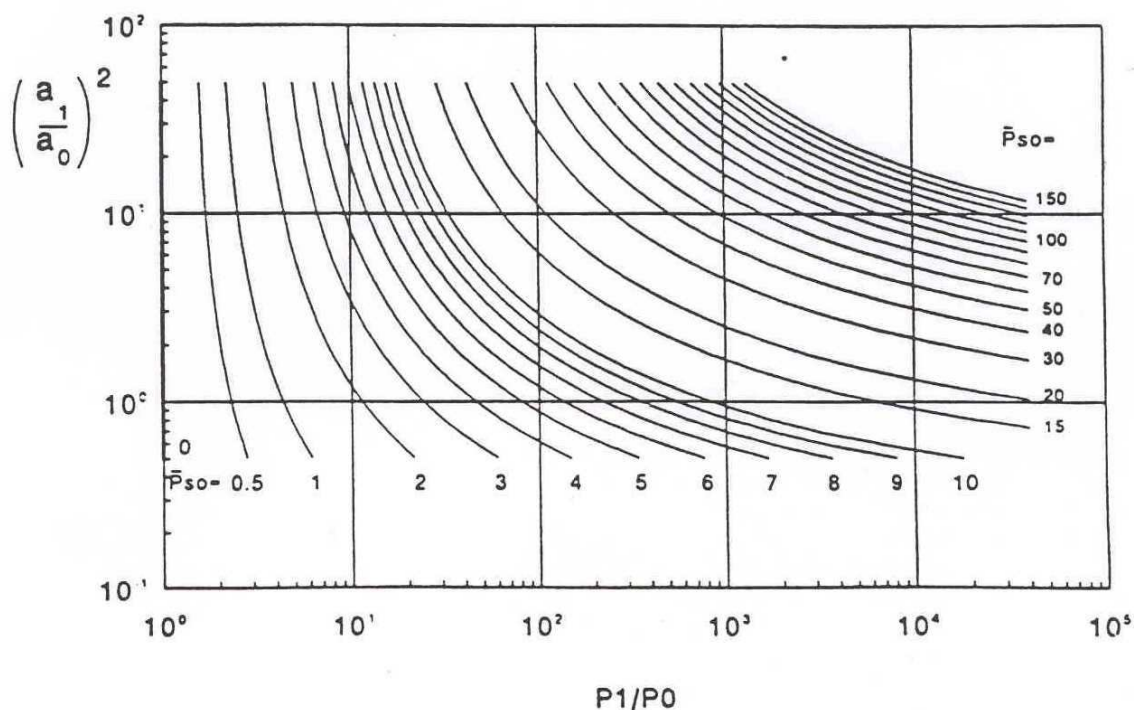


Figure 21 : Relation $(a_1/a_0)^2 = \gamma_1 T_1 M_0 / \gamma_0 T_0 M_1$ in relation to p_1/p_0 and P_{s0} (shock pressure at the time of release) for a di or tri-atomic gas ($\gamma_1=1.4$) (Baker, 1983)

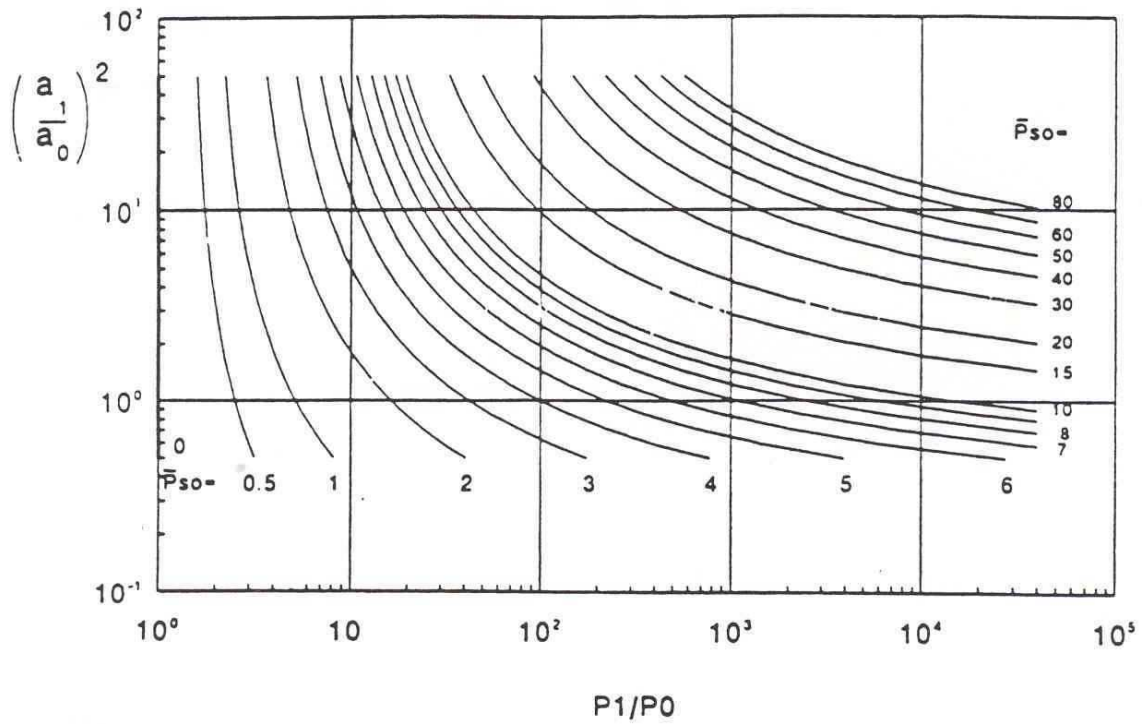


Figure 22 : Relation $(a_1/a_0)^2$ versus p_1/p_0 and P_{s0} for $\gamma_1=1.66$ (Baker, 1983)

The far field

In the far field, i.e. for $\bar{R} \gg 2$, the graph of the decline in overpressure of a condensed explosive (pentolite) is used (Figure 23).

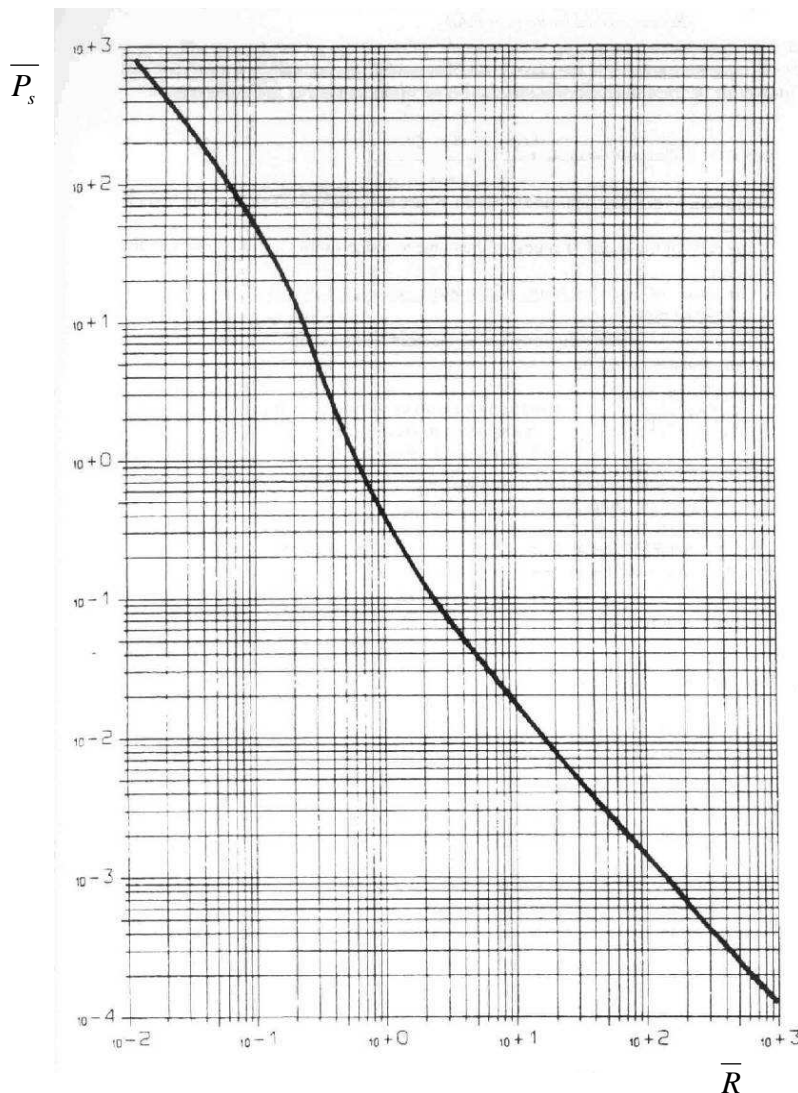


Figure 23 : Overpressure versus distance for a pentolite explosion (TNO, 1997)

Baker refined his method to take into account more precisely the geometry of the tank or its position in relation to the ground.

5.3.4. The UFIP method

The method recommended by the "Union Française des Industries Pétrolières" (French Union of the Petroleum Industries) was initially proposed by The Committee for the Prevention of Disasters in its work "Methods for the calculation of physical effects resulting from releases of hazardous materials" (1992), commonly known as the "TNO Yellow Book". It is developed in the "Guide Méthodologique UFIP pour la réalisation des Études de Dangers en raffineries, stockages et dépôts de produits liquides et liquéfiés" (UFIP Methodological Guide for Carrying Out Safety Studies in Refineries, Storage Facilities and Depots of Liquid and Liquefied Products) (UFIP, 2002). It is based on a purely energetic approach to the phenomenon.

5.3.4.1. Energy balance

The energy balance of the phenomenon is written:

$$E_i = E_r + E_{pd} + E_{fr}$$

$$\text{and } E_r = E_f + E_{sh}$$

where:

- E_r is the residual energy available for fragment ejection and the shock wave,
- E_i is the internal energy of the gas (calculated through the Brode relationship),
- E_{pd} is the plastic deformation energy of the tank,
- E_{fr} is the rupture energy of the tank,
- E_f is the available energy for fragment projection,
- E_{sh} is the energy dissipated in the shock wave.

The energy absorbed by the rupture of the enclosure ($E_{pd}+E_{fr}$) is a function of the deformation fraction of the material making up the enclosure at rupture.

The residual energy E_r is distributed between E_f and E_{sh} in the following manner:

$$E_f = FE_r$$

$$E_{sh} = (1 - F)E_r$$

where:

- $F=0.2$ for a fragile rupture,
- $F=0.6$ for a ductile rupture.

5.3.4.2. Pressure waves

The method recommended by UFIP for calculating pressure waves caused by a pressurized vessel burst uses the TNT equivalent concept as well as the TM-5 graph. For bursts of atmospheric tanks, the method recommended by UFIP is to use curve 6 from Figure 24. This method is close to the Baker method except that the graphs were apparently made for a half-space and not the complete space and include both the near field and the far field (Figure 24). The parameter of the abscissa is the reduced distance, defined by:

$$\lambda = \frac{R}{(E_{sh}/P_a)^{1/3}}$$

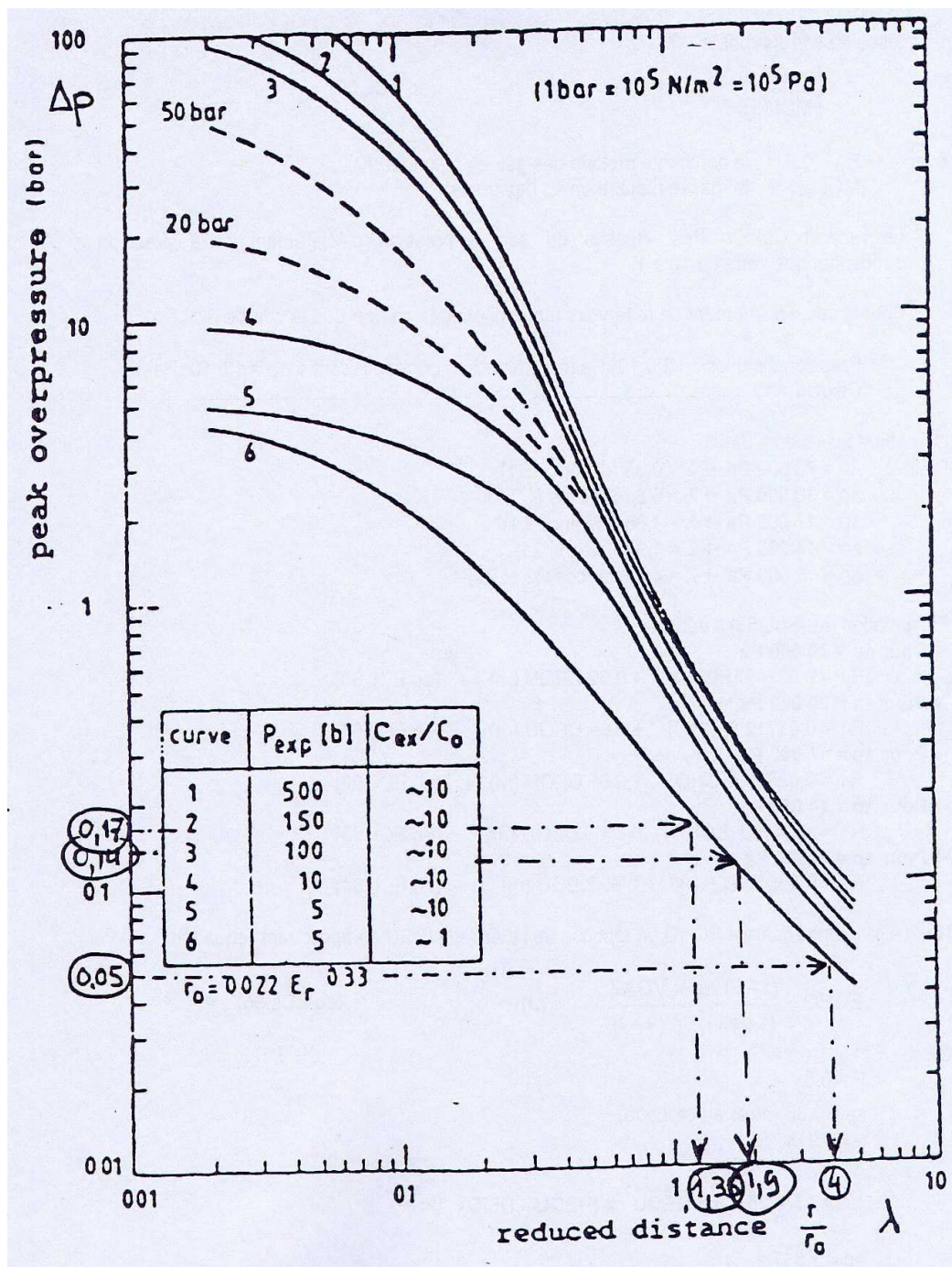


Figure 24 : Curves of TNO's model for explosion pressures ranging from 5 bars to 500 bars taking into account the parameter C_{ex}/C_0 , relation of the speeds of sound at the bursting pressure and at atmospheric pressure (according to UFIP, 2002)

5.3.5. Accounting for the interaction of a pressure wave with an obstacle

The global methods presented above assume wave propagation in an open field. Still, the phenomena of wave reflection and diffraction in the presence of obstacles can be described, in a simple and generalized manner, by means of reflection coefficients applied to incidental overpressure at the same place in the absence of obstacles (Reimeringer, 2007).

In the near field, the amplification of the overpressure due to the presence of an obstacle can be of a factor of 10 (compared to the overpressure without an obstacle).

In the far field, the orders of greatness of the increase and decrease coefficients represented in the following figure are generally accepted. These latter can be retained when using the Baker's method.

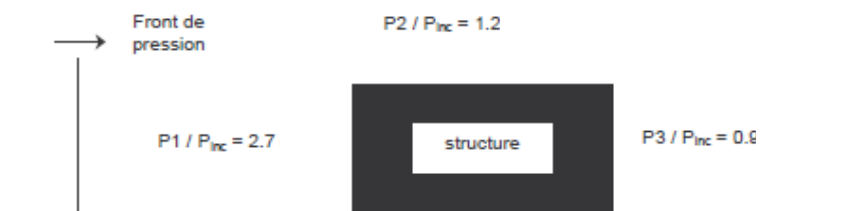


Figure 25: Coefficients of decrease and increase (P_{inc} : incidental overpressure in the absence of obstacle, $P1$: overpressure on exposed side of the obstacle parallel to the pressure front, $P2$: overpressure on the side perpendicular to the pressure front, $P3$: overpressure on the posterior side)

INERIS has developed an analytic prediction tool of pressure wave propagation, resulting from an explosion or a vessel burst, in an environment with obstacles. This tool, DIFREX (HEUDIER, 2006), allows the phenomena of reflection and diffraction of pressure waves to be described by implementing shock wave theory. The law of determination of incidental pressure programmed in DIFREX is an analytic correlation which is based on the Hopkinson model, implemented in classic decline graphs of overpressure (Baker, Multi-Energy, Indicator 10...), and thus equally implemented in PROJEX, internal tool dedicated to the phenomenon of vessel burst.

5.4. COMPARISON OF GLOBAL METHODS

5.4.1. Without accounting for interaction with obstacles

INERIS proposes in this paragraph a comparison of the methods presented above. It is important to remember that for all these methods, the rupture pressure of the container is input. The determination of this parameter is a subject of study in itself.

The points of comparison are first, the respect for physics, second, the chosen approximations as well as the associated limitations, and finally the ergonomics and implementation of the different methods, on which the risk of error depends.

We propose a comparison of results for the following example:

- Propane tank which bursts due to an internal explosion
- Molar mass of propane : 44.096 g/mol
- Contents: 10 m³ of liquid propane + 90 m³ of a gaseous propane and air mixture
- Relation of the specific heats of the burnt products: 1.314
- Temperature of the burnt products (rupture temperature): 2000°C
- Rupture pressure : 42.5 bars
- Ambient air temperature: 20°C
- Relation of the air's specific heats: 1.40
- Air density: 1.225 kg/m³
- Atmospheric pressure: 1.013 bar

In the following table, the results for distances at the thresholds of 50 mbar and 140 mbar are given.

Pressure threshold [mbar]	Distance calculated using the Shock Tube-TNT method [m]	Distance calculated using the PROJEX method [m]	Distance calculated with the Baker method [m]	Distance calculated with the UFIP method [m]
50	140	120	120	90
140	70	50	60	40

Table 6: Comparison of distances calculated with different methods at the thresholds of 50 and 140 mbar

5.4.1.1. Respect for physics, chosen approximations and associated limitations

We note a general similarity between the Shock Tube-TNT, PROJEX and Baker methods, which is in line with the proximity of the physical descriptions that are made in each method. The Shock Tube-TNT method gives slightly higher results. Indeed, the TM5 graph generally overestimates pressure levels at a given distance, therefore the two other methods are certainly more precise. However, the results for the UFIP method are lower because it takes into account the yield F (taken as equal to 0.2, the rupture assumed to be fragile).

The Shock Tube-TNT, PROJEX and Baker methods respect the physics of the emission and the propagation of pressure waves in the environment with a differentiated phenomenology for the near field and the far field. The UFIP method distributes the available energy for pressurization of the container until its rupture (Brode energy) between the air pressure wave and the projection of fragments. We do not see a physical reason for this, knowing that fragment projection is not a question of energy, or in any case cannot be linked to Brode energy, unlike pressure effects. Taking into account this yield can lead to a significant underestimation of the energy taken into account when calculating the pressure field.

These estimations all assume that the confinement walls disappear instantaneously, which allows the use of the analogy with explosives detonation. In reality, the cracks do not form instantaneously; the environment is solicited less brutally than in the case of the explosion of an explosive. Thus, in reality, the solicitation speed of the environment is slower, and the pressure effect should consequently be weaker. From this point of view, the PROJEX method is certainly easier to change for it makes reference to the MULTI-ENERGY method which predicts intrinsically a relationship between the distant pressure effects and the energy release speed; developments are thus possible.

5.4.1.2. Ergonomics

Graphic methods are manual and occasionally leave too much room for interpretation. Thus, for example, the choice of the evolutionary curve for pressure in relation to distance from Figure 24 can be difficult for intermediary pressure ranges and relations of the speed of sound between 1 and 5, which is the majority of situations.

5.4.2. Accounting for interaction of the pressure wave with an obstacle

As indicated in § 5.3.5, among the compared global methods, only the Baker's method and the DIFREX tool (Heudier, 2006) allow accounting for the interaction of a pressure wave with obstacles.

The Baker's method can be applied by implementing the coefficients of reflection and diffraction presented in § 5.3.5 .

These methods were applied so as to calculate the pressure field generated by a vessel burst. The results thus obtained were then compared to the results of an experimental simulation of the same geometry and of the same scale, presented in the following paragraph, which implements the phenomena of wave reflection and diffraction due to the presence of obstacles.

5.4.2.1. Experimental simulation

The test situation is a vessel burst (tank n°0) in an encumbered environment. The geometry of the experiment is described in Figure 26, it corresponds to the reproduction on a reduced scale of an existing industrial installation. Tank n°0 loses its two bottoms but keeps its cylindrical shell. The resulting pressure wave

propagates toward a group of parallelepipedic tanks placed on the ground. Pressure was measured on the lateral sides and the tops of these tanks (Figure 27).

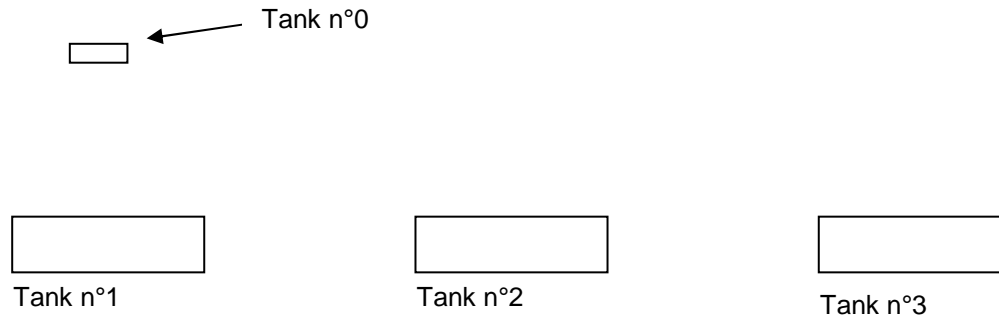


Figure 26: Descriptive schema of the considered geometry (true dimensions measured in tens of meters)

Sensors were positioned on tanks n°1, 2 and 3 as seen in the schema below:

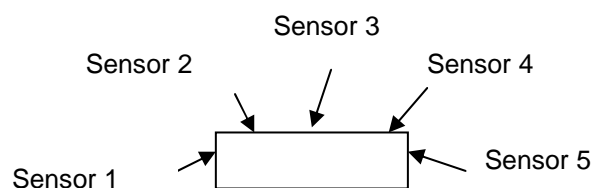


Figure 27: Placement of sensors on tanks n°1, 2 and 3

There are situations which leave only a small margin of incertitude or at least for which the margin of error must be known and controlled. It is then interesting to take advantage of the well-established laws of similitude of shock waves (Baker, 1983) to undertake experiments on reduced-scale models.

These laws indicate that the levels of incidental overpressure ΔP_i are a function only of the relation E/X^3 where X is the distance to the centre of the explosion. Therefore, if " D " represents the dimension of the real installation (for example, D can be the width of an oven, i.e. 15-16 m) and " d " the corresponding dimension on the model, then the overpressure levels measured at any point on the model will be similar to those reached in the actual installation if the pressure energy E_d delivered by the explosion source is such that:

$$E_d = E_D \cdot \left(\frac{d}{D}\right)^3$$

Thus for the real situation of Figure 26, we have used this law to represent, in the model, each tank by a plastic bin, 75 cm wide and 35 cm high. These three bins are aligned on a level floor and placed 70 cm apart. The explosion source is placed in a

cylinder 100 mm in diameter, 300 mm in length, representing tank n°0, suspended about 70 cm plumb to the bin representing tank n°1 (Figure 28). The pressure source in the cylinder is simulated by the detonation of a small explosive load, just enough to instantaneously produce in this cylinder the required pressure.

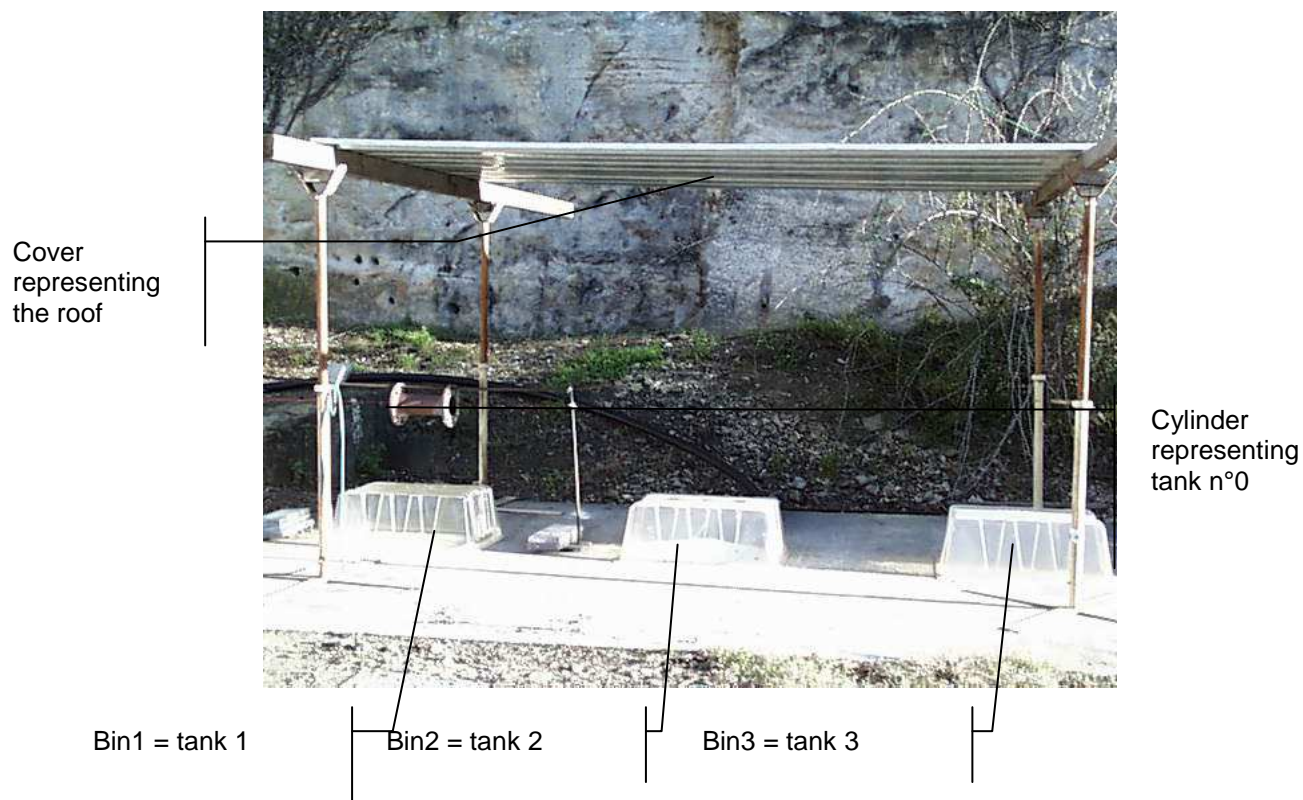


Figure 28: Experimental installation

The overpressure levels reached on the roof and the lateral sides of each of the three bins were measured. Interpretation in the context of industrial application is quite simple because the measured values are those which should have taken place in reality. Only the wave impulsion must be calculated to take into account the energy that is actually available. The level of precision is estimated to be of the order of 10%; the results are perfectly consistent.

5.4.2.2. Comparison with predictions

A comparison of the experimental results with calculations (on the same scale as that of the experimental simulation) is proposed in Figure 29, Figure 30 and Figure 31.

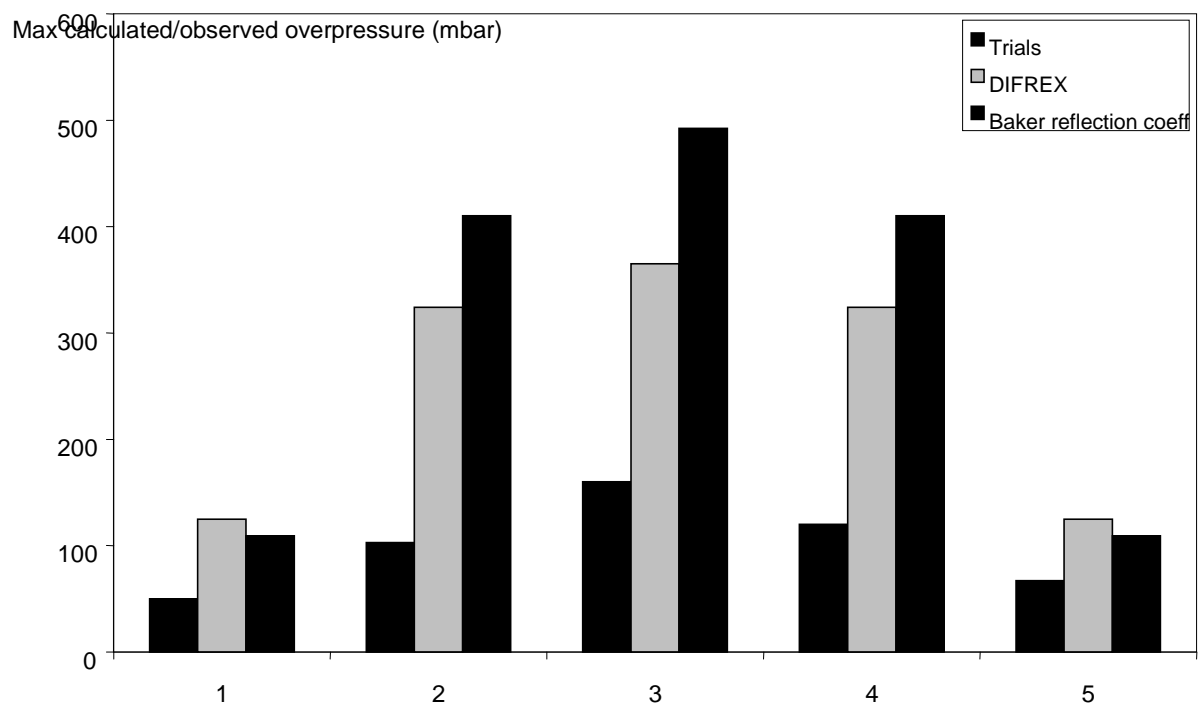


Figure 29: Comparison of maximum calculated and observed overpressure levels on bin n°1

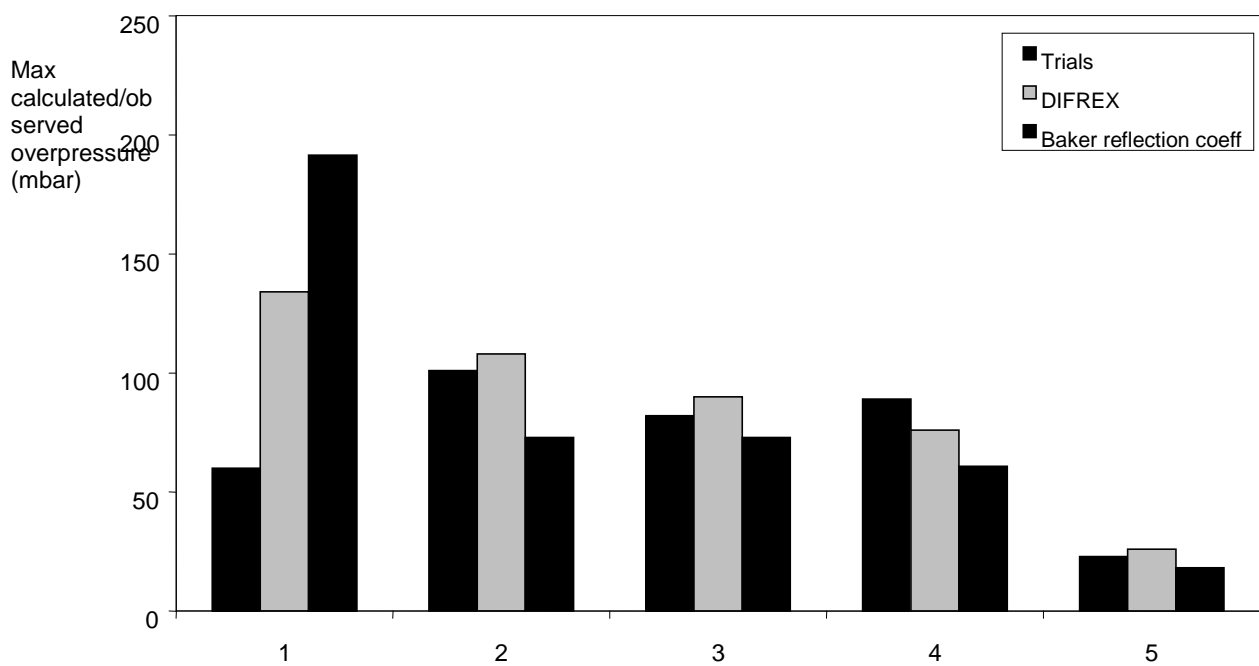


Figure 30: Comparison of maximum calculated and observed overpressure levels on bin n°2

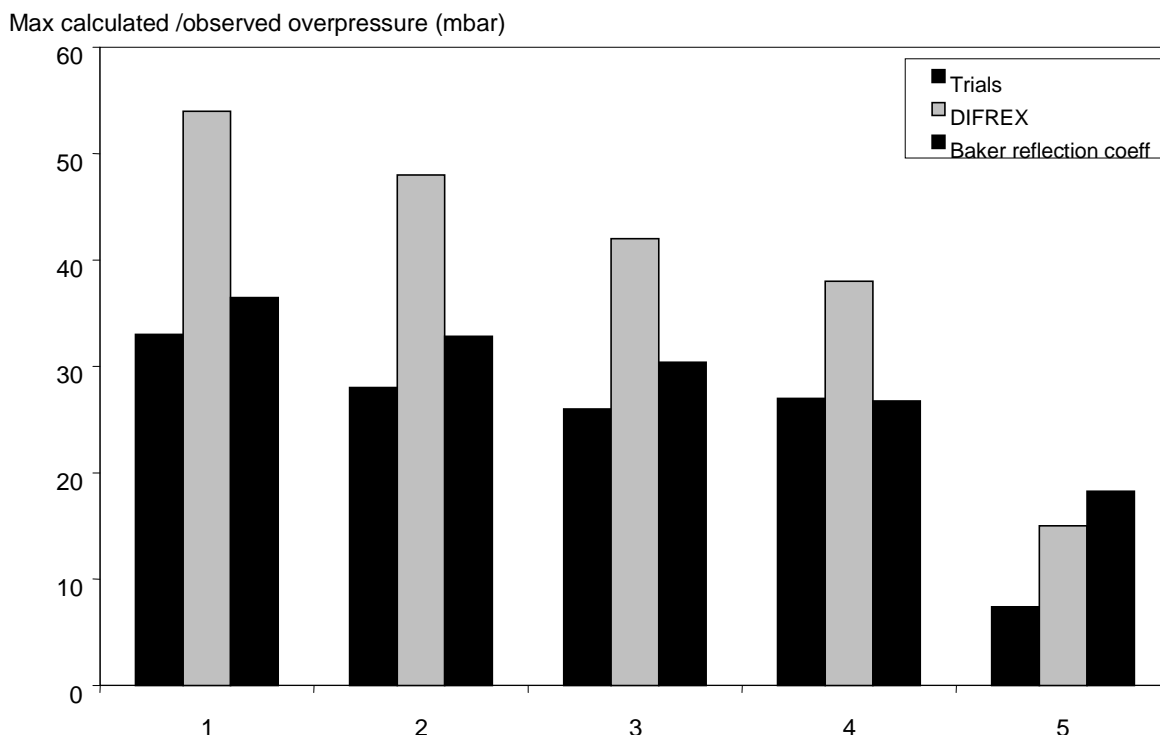


Figure 31: Comparison of maximum calculated and observed overpressure levels on bin n°3

The global methods presented in this chapter (Baker, UFIP, Shock Tube-TNT, PROJEX) were developed to calculate the effects in far field in the context of the control of urbanization, and can thus significantly overestimate in near field.

This comparative approach of experimentation and the two methods (Baker, DIFREX) is a first work of methodological validation. We note that in general trends are well respected by these methods, particularly when it comes to taking into account reflections.

5.4.3. Synthesis

Global methods, which describe physical phenomenon directly with more or less approximation, have as their primary advantage their facility of use. In the specialized area of vessel bursts, they can be deemed as covering the physics well. They do not however account for the progressive rupture of the container, or the geometric details which can reinforce or, to the contrary, reduce the pressure field.

6. FRAGMENT FORMATION AND PROJECTION

6.1. FRAGMENT FORMATION

Different techniques of sizing structures (ex : EUROCODES) allow the estimation of the destruction overpressure of a wall when the overpressure is applied in a slow manner, typically when the load speed is less than 0.01 bar/s and when the material's temperature is uniform. In a dynamic load capacity, as long as the characteristic load duration stays comparable (or greater) in order of size to that of the deformation of the considered structure, the fragments susceptible of being formed should have identical dimensions to those formed during rupture from a static load. In the opposite situation, the vibration capacities are likely to become more complex and the fragment size can no longer be easily predicted (Proust, 2000).

Figure 32 illustrates an extreme example of deformation of a cylindric tank containing a compressed gas initiated by an axial crack. It should be underlined that each of the geometries in this figure could be a final geometry. These different geometries represent thus geometries of potential missiles.

The initial crack propagates along the axis toward each extremity of the tank where the crack bifurcates. Then, the circumferential cracks turn in opposite directions around each of the extremities. A large flap forms when the crack progresses around the ends. The sides of the flaps, which were initially the exterior surfaces of the tank, converge one toward the other. The circumferential cracks propagate and eventually meet, bringing about the detachment of one or both ends of the tank.

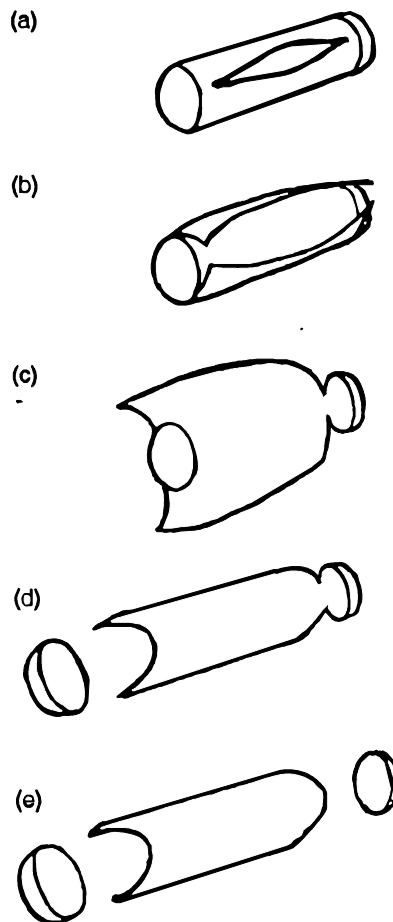


Figure 32: The successive deformations of the tank (Baum, 2001)

When thermal gradients resulting from a fire are superposed, the stress distribution can be unequal and it seems more difficult to predict the number and shape of fragments produced during the burst. Calculation in uniform static can only provide the size.

6.2. FRAGMENT ACCELERATION AND PROJECTION

6.2.1. Physical representation

The speed and distance covered by a shell fragment are primarily a function of its initial speed, mass and geometry.

From theories of mechanics, initial fragment speed can be shown to depend essentially on impulse I ($I = \int \Delta p(t) dt$ where $\Delta p(t)$ is the excess pressure in the vessel) transmitted during the depressurization of the vessel after bursting. $\Delta p(t)$ is a decreasing function to such an extent that impulse is a finite size. The greater it is, the greater the initial speed of the given fragment. After the propelling phase, the fragment is exposed to drag and gravity, and more rarely to lift effects. Indeed, lift can intervene if the extrados (upper surface of the fragment) and intrados (lower surface of fragment) profiles are dissymmetrical.

The trajectory can be deduced from ballistic equations (Figure 33), when the projection angle α , the departure height H_0 and the initial speed V_i are known.

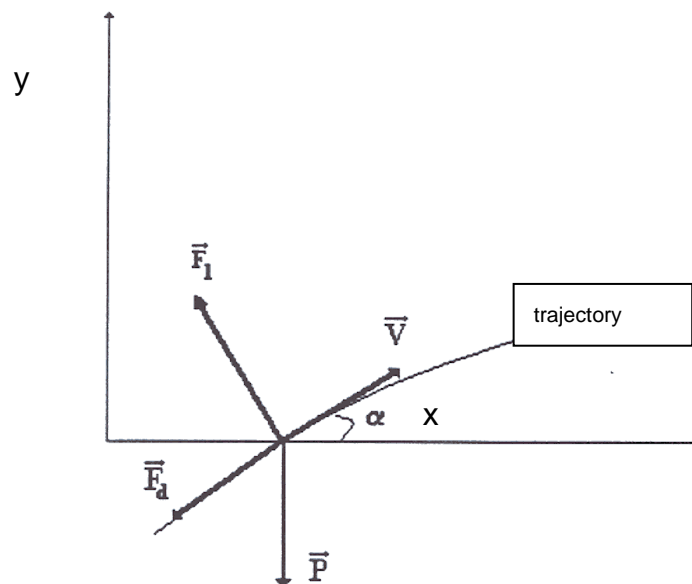
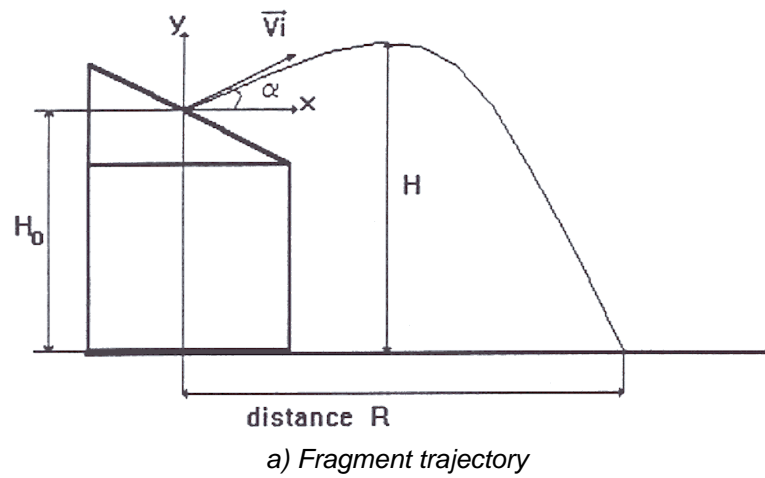


Figure 33: Fragment trajectory and assessment of external forces exercising on the fragment

Obviously, fragments cannot have an initial speed greater than that of the gaseous material that propel them. This parameter can be taken from shock tube theory. It corresponds to the maximum speed of a fragment with zero mass.

6.2.2. Vessel containing pressurized gas

Baum studied the formation and acceleration of fragments resulting from an axial rupture of a cylindrical tank of pressurized gas (Baum, 2001). He developed a simple model allowing the prediction of the speed reached by a non restrained vessel when its rupture was initiated by an axial crack. The speed predicted by this model was then compared to the results of an experimental study. The description of tests conducted by Baum as well as a comparison with theoretic results are detailed in annex 2.

When the high pressure gas initially contained in the vessel is expelled through a developing breach, the vessel is propelled with a force equal to the reaction of the gas ejection.

Baum observed that the gas ejection process is entirely complete when the deformation of the vessel has acquired the shape in Figure 32b. Thus, acceleration can be considered as terminated while the vessel is still in one piece.

6.2.3. Vessel containing a liquid

Baum (1999) studied the circumferential rupture of a cylinder containing an overheated liquid. Depending on the position of the circumferential rupture, the main fragment can be made up of one of the extremities of the vessel and a large part of the cylinder. In this case, it undergoes acceleration similar to that of a rocket when the fluid is ejected.

The sudden depressurization due to the tank rupture initiates the brutal vaporization of the liquid. The vapor bubbles cause a rapid increase in the volume of fluid. This "flash" process maintains the vessel's internal pressure at a value near to the saturation pressure of the liquid.

Taking into account the supplementary step of vaporization, the expansion and ejection of the vapor-liquid mixture are longer and greater impulsion is transferred to the fragments compared to the preceding situation (6.2.2).

6.3. PREDICTION METHODS

6.3.1. The PROJEX method

The PROJEX method also has a ballistic module to determine fragment trajectory. Basically, the *Missile* module of INERIS's *Effex* software (Proust, 2000) was integrated by adding the effects of air compressibility for great projection speeds. This module allows the calculation of:

- The fragment trajectory deduced from the assessment of external forces operating on the fragment,
- The characteristics of the impact point on the ground such as: distance, speed and trajectory angle of the fragment in relation to the ground.

The body's rotation movements are not considered in modeling of the phenomenon.

The representative equations used are entirely standard:

$$M_f \cdot \frac{d[V_f(t)]}{dt} = -M_f \cdot g \cdot z + \frac{1}{2} \cdot C_x \cdot S_f \cdot \rho_0 \cdot \|U - V_f\| \cdot (U - V_f)$$

where:

- U and V_f , speed vectors of the flow from the breach and the fragment on a fixed point,
- z , the upward direction unit vector,
- M_f and S_f , mass and surface of the fragment (surface projected in the plane perpendicular to flow),
- C_x , the drag coefficient of the fragment, usually of the order of 1 for a thin covering (Duplantier, 1996),
- ρ_0 , the atmospheric density

Comparison of numeric calculations and some experimental results (Figure 19) has shown that this calculation method allows the estimation of impact point characteristics with a satisfactory precision.

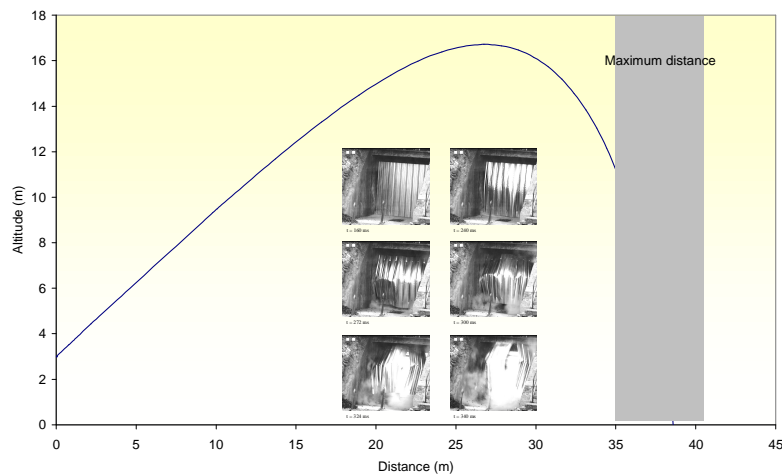


Figure 34: Comparison of calculated and measured projection distances

Besides the fragment's characteristics, an essential piece of data is the initial speed. In PROJEX, it is deduced from the calculation of the pressure impulse transmitted by the gas jet released through the breach. Impulse is a function of the maximum overpressure and discharge time of the tank. In the case of a pressurized gas, this time results from the propagation of sound waves. In the case of a vaporizing liquid, this time results from the propagation of a « vaporization wave ».

6.3.2. The Baker's method

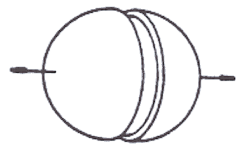
Baker proposes a method that allows us to know fragment trajectories in relation to tank pressure. The entry parameters are the number of fragments and their drag coefficient (C_x).

At first, the initial fragment speed is estimated; it depends on the tank and the manner by which it depressurizes. Then, the trajectory, which depends only on this initial speed, is determined.

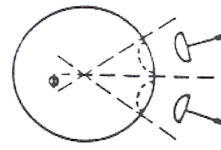
6.3.2.1. Estimation of the initial fragment speed

Baker made a synthesis of experimental findings and numerical methods anterior to 1983. This analysis concerns tests performed in the following conditions:

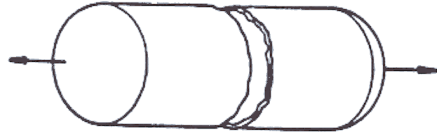
- The containers are either spherical or cylindrical,
- The container thickness is constant,
- The relation between length and diameter (L/D) of the cylindrical containers is equal to 10,
- The container is filled with a perfect gas,
- The container burst is caused by the injection of a highly pressurized gas (hydrogen, air, argon, helium, carbon dioxide),
- The obtained fragments (2, 10, 100) are of identical size. The different burst configurations are shown in Figure 35.



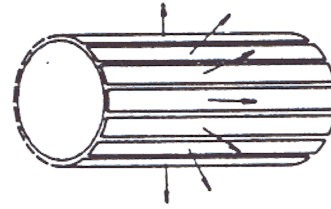
a) Burst of a sphere into 2 equal fragments



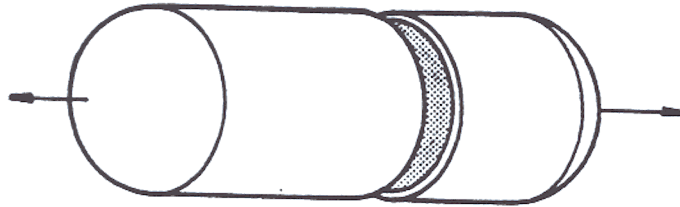
b) Burst of a sphere into several equal fragments



c) Burst of a cylinder into 2 equal fragments



d) Burst of a cylinder into several equal fragments



e) Burst of a cylinder into 2 unequal fragments

Figure 35: Splitting of spheres and cylinders into several fragments (Baker, 1983)

The results of this analysis allowed Baker (1983) to develop a diagram reproduced in Figure 36. This diagram allows the determination of the initial adimensional speed of a fragment when the the adimensional pressure of the enclosure \bar{P} just before the burst (valid for $\bar{P} < 0,2$) is known, defined by the following relationship:

$$\bar{P} = \frac{(p_1 - p_0) \cdot V}{m \cdot a_1^2} \text{ where :}$$

- p_1 is the pressure in the container at the time of rupture (Pa),
- p_0 , ambient pressure (Pa),
- a_1 , the speed of sound in the compressed gas (m/s),
- m , the total mass of the container.

The speed of sound a_1 in the compressed gas is equal to:

$$a_1^2 = \frac{T \cdot \gamma \cdot R}{M} \text{ where:}$$

- R , the constant of perfect gases (8,32 J/Kmol),

- T , the absolute temperature of the gas just before the burst (K),
- M , the molar mass of the gas (kg/mol),
- γ , the relation of specific heats.

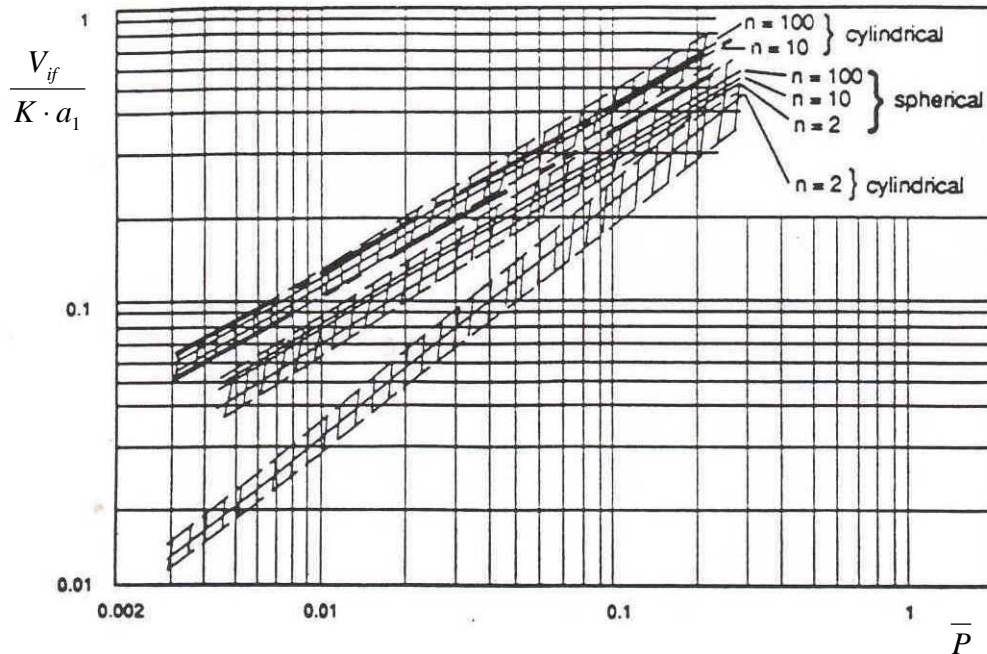


Figure 36 : Fragment speed in relation to pressure and the number of fragments (Baker, 1983)
– the dotted lines represent the uncertainty range

These curves, which represent the relation between the initial speed of fragment V_{if} and the speed of sound in the gas a_1 in relation to the adimensional overpressure \bar{P} , are drawn in relation to the number of expected fragments. It is thus necessary to know the number of fragments to use them. When the fragments are of identical form and mass, the coefficient K is equal to 1. Figure 37 allows the determination of this coefficient K in the case of a cylinder (with $L_v/d_v=10$) burst into two unequal fragments.

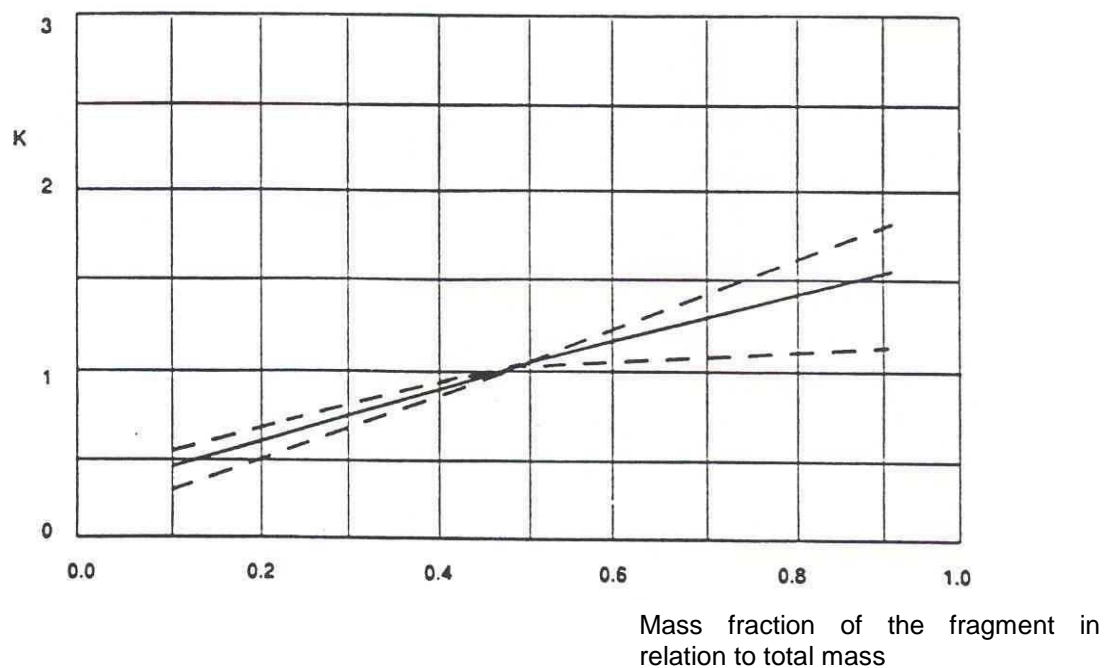


Figure 37: Adjustment coefficient K for a cylinder (with $L_v/d_v=10$) burst into two fragments of unequal size (Baker, 1983) – the dotted lines represent the uncertainty range

6.3.2.2. The projection distance of the fragments

The projection distance results from numerical simulations of classic ballistic equations. Baker (1983) represented the results in Figure 38 for a zero departure altitude. In this diagram, change in adimensional distance \bar{R} is represented in relation to adimensional speed \bar{V}_i for different relations of bearing on drag $C_L A_L / C_D A_D$.

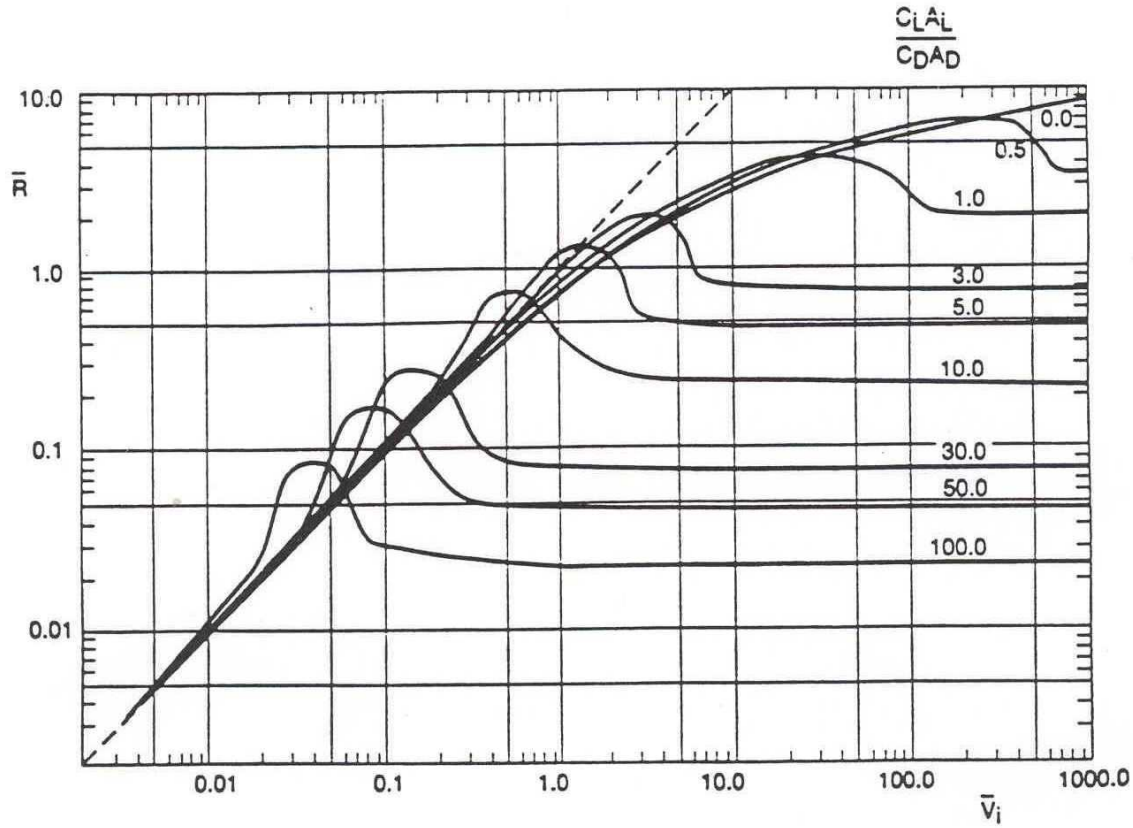


Figure 38: Maximum distance R in relation to initial speed and the relation of the fragment's drag and lift coefficients (Baker, 1983)

$$\overline{R} = \frac{\rho_a C_D A_D R}{M_f}$$

$$\overline{V_i} = \frac{\rho_a C_D A_D v_i^2}{M_f g}$$

where:

- A_D is the fragment surface in the plane perpendicular to the trajectory (m^2),
- A_L , the fragment surface in the plane parallel to the trajectory (m^2),
- C_D , the drag coefficient,
- C_L , the lift coefficient,
- g , the acceleration of gravity (m/s^2),
- M_f , the fragment mass (kg),
- R , the distance between the ejection point and the landing point on the ground (m),
- ρ_a , the density of ambient air (kg/m^3)
- v_i , the initial speed of the fragment.

The drag coefficient for differently shaped projectiles is given in tables (Table 7, from Baker, 1983). In general, the lift coefficient is assumed to be zero.





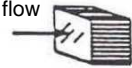
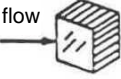
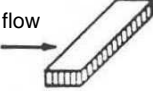
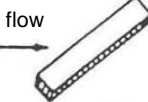

Projectile Shape	Descriptive diagram	C_D
Oblong cylinder (diameter \ll length) perpendicularly to the flow direction		1.20
Sphere		0.47
Cylinder with one end at a right angle to the flow direction		0.82
Disc with one side at a right angle to the flow direction		1.17
Cube with one side at a right angle to the flow direction		1.05
Cube with one edge at a right angle to the flow direction		0.80
Oblong parallelepiped with one side at a right angle to the flow direction		2.05
Oblong parallelepiped with one edge at a right angle to the flow direction		1.55
Thin slab with one side at a right angle to the flow direction		1.98

Table 7: Drag coefficient for differently shaped projectiles (Baker, 1983)

6.3.3. The UFIP method

The UFIP method considers the fraction of available energy E_f dissipated under the form of kinetic energy. Consequently, the initial speed of the fragment is equal to:

$$u_0^f = \left(\frac{2 \cdot E_f}{m_r} \right)^{1/2} \text{ where } m_r \text{ is the tank mass.}$$

The fragment's trajectory is then calculated from standard ballistic equations taking into account the force of gravity and the forces of fluid dynamics, drag and bearing. A simplified semi-empiric solution is proposed.

6.4. COMPARISON OF GLOBAL METHODS

From a physical point of view, the methods presented above take well account of the phenomena. A comparison on the basis of experiments (Baum, 2001: annex 2) is proposed in Figure 39 from conditions provided in the table below.

Baum's tests consisted in studying the projection of a cylindrical tank containing a pressurized gas with an initial axial crack.

	Diameter [m]	Length [m]	Mass of the missile [kg]	Rupture pressure [bar]
Tank 1	0.102	0.305	9.54	52.7
Tank 2	0.102	0.305	6.32	61.7
Tank 3	0.102	0.305	6.32	23.8
Tank 4	0.102	0.305	9.22	27.2
Tank 5	0.102	0.305	9.1	72.8
Tank 6	0.305	1.09	62.35	61
Tank 7	0.305	1.22	82.5	76.9

Table 8: Characteristics of different tanks used in Baum's experiments

For the cases considered here, the primary missile can be assimilated with the entire tank, the release of the gas is radial and the burst temperature is taken as equal to 20°C.

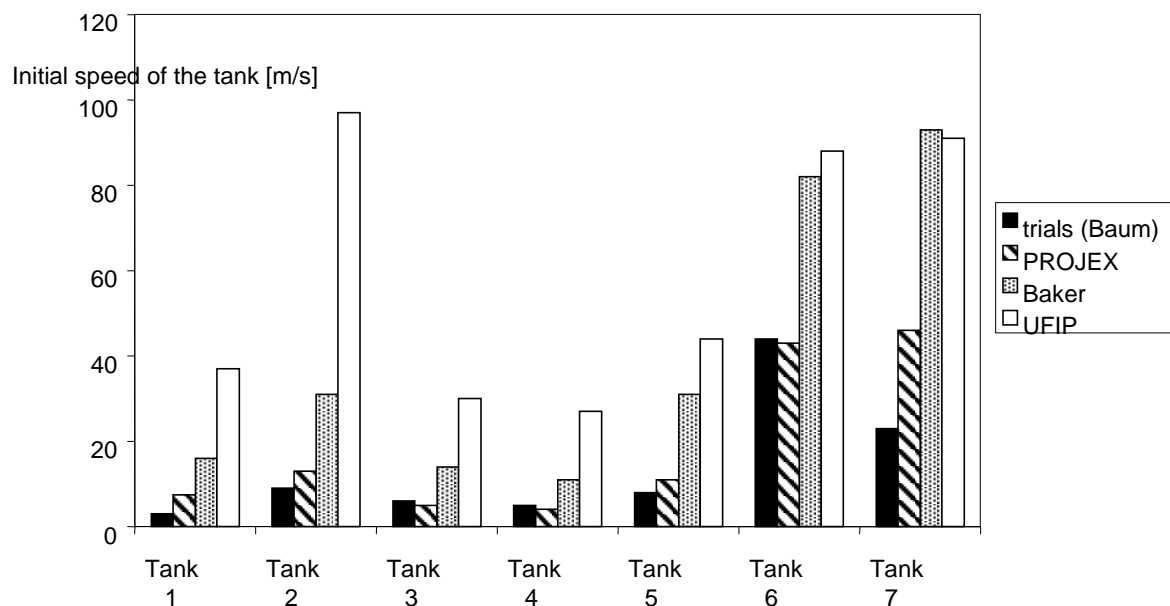


Figure 39: Comparison of the ejection speeds of an entire tank calculated with different global methods and those measured during Baum's trials

A priori Baker's method seems relatively realistic, because it is based on experiments. We see however that the results sometimes differ significantly from the experiment even if the estimations remain conservative. The results of the UFIP method are still more conservative, but we doubt its reasoning in terms of energy, when fragment projection is an effect of impulse (Proust, 2000). Finally, the PROJEX method seems the closest.

7. CONCLUSION

Feedback shows that a vessel burst can be the consequence of shell's fatigue, excessive corrosion, an internal explosion or a slower and accidental pressure increase due to heating, overfill, etc.

The environmental effects of a vessel burst considered in this report are first, the release of a pressure wave, and second, the projection of fragments. The pressure wave results from the brutal release of the gas contained in the vessel or from vapor if the vessel contains an overheated liquid.

This report presents four global methods for effects prediction: the Baker's and UFIP's methods and the Shock Tube-TNT, PROJEX and DIFREX methods developed by INERIS.

Among the global prediction methods of effects following a vessel burst presented in this report, the Baker, Shock Tube -TNT and PROJEX methods respect the physics of the emission and the propagation of pressure waves with a differentiated phenomenology between the near field and the far field. This divide between the near field and the far field depends on the quantity of gas present in the vessel at the time of the burst, but also its geometry. In the near field, the overpressure produced by the burst is determined by means of the shock tube theory. In the far field, the overpressure is assumed to follow, for these three methods, the graphs of a violent explosion.

A comparison with experiments showed that the estimations of initial fragment speed of the Baker's and UFIP's methods were conservative while those of the PROJEX method were quite near to the experiments results.

The PROJEX method allows the determination of the consequences of a vessel burst:

- The vessel's rupture pressure is an input and the rupture mode is assumed to be known and instantaneous.
- In the near field, the pressure is equal to the shock pressure generally determined from shock tube theory.
- In the far field, the overpressure decreases according to the Indicator 10 curve of the multi-energy method.
- Fragment projection is determined by means of classic ballistics equations in which initial speed is deduced from the discharge conditions of the vessel. The effects of atmospheric compressibility are taken into account.

In many situations this method provides conservative estimates, and some improvements could be made in subsequent versions. In particular, the cracking speed during rupture, fragment mass and tank geometry have an influence on wave formation and directional effects. These aspects should be the object of specific study. Other points should also be considered, such as the presence of a biphasic environment rather than a pure gas. Finally, it is not evident, and feedback confirms this, that the law of assumed decrease is strictly observed in reality, especially at a great distance from the burst and at weak pressures, due to, for example, effects of atmospheric heterogeneity.

The Baker's and DIFREX methods also allow the prediction of the interaction of pressure waves with obstacles, thanks to the implementation of reflection and diffraction coefficients. INERIS developed a specific global method (DIFREX) to predict pressure wave propagation in an area encumbered with obstacles. The interaction of pressure waves with obstacles is a subject that best be mastered for the sizing of protection barriers against pressure effects, such as walls or dikes, often recommended. Thus, the BARPPRO²⁸ research program, underwritten by ANR and dedicated to the sizing of physical protection barriers against the effects of an explosion, should allow us to improve our knowledge of the propagation of pressure waves around obstacles and the effectiveness of such protection barriers.

²⁸ ANR (Agence Nationale de la Recherche) project of the CSOSG 2010 (Concepts, Systèmes et Outils pour la Sécurité Globale) program: *Dimensionnement des BARrières Physiques de PROtection contre la propagation d'ondes de souffle consécutives à une explosion*. INERIS, as member of the BARPPRO consortium, is responsible for performing medium scale deflagration and detonation tests, designed to better understand the phenomena of interaction between pressure waves and wall or dyke like obstacles. The project, which began in February 2011, will be completed in February 2014.

8. GLOSSARY

BARPI	:	Bureau d'Analyse des Risques et des Pollutions Industrielles
BLEVE	:	Boiling Liquid Expanding Vapor Explosion
CFD	:	Computational Fluid Dynamics
LPG	:	Liquefied petroleum gas
TNO	:	The Netherlands Organisation of applied Scientific Research
TNT	:	Trinitrotoluene

9. **BIBLIOGRAPHY**

- 1- BAKER, COX, WESTIN, KULESZ, STREHLOW, 1983, *Explosion hazards and evaluation*, edition Elsevier.
- 2- BAUM, 1999, *Failure of a horizontal pressure vessel containing a high temperature liquid: the velocity of end-cap and rocket missiles*, Elsevier, Journal of Loss Prevention in the Process Industries 12, pp.137-145.
- 3- BAUM, 2001, *The velocity of large missiles resulting from axial rupture of gas pressurized cylindrical vessels*, Elsevier, Journal of Loss Prevention in the Process Industries 14, pp. 199-203.
- 4- BRODE, 1959, *Blast wave from a spherical charge*, The physics of fluid, volume 2.
- 5- CLANCEY, 1972, 6th Int. Meeting of Forensic Sciences, Edinburgh.
- 6- COUILLET, 2002, Méthodes pour l'évaluation et la prévention des risques accidentels, *Dispersion atmosphérique (Mécanismes et outils de calcul) Ω-12*, reference INERIS-DRA-2002-25427, available at www.ineris.fr
- 7- DUPLANTIER, 1996, *Les phénomènes d'explosion résultant de la combustion de gaz de vapeurs et de brouillards dans des appareils clos*, INERIS Scientific and technical report, ref. RST 04.
- 8- FRUITET, 1979, *Sécurité contre l'incendie dans la construction métallique*, Techniques de l'Ingénieur.
- 9- HEUDIER L., PROUST Ch., COUILLET J-Ch., 2006, *La propagation des ondes de pression en milieu encombré*, paru dans Préventique Sécurité n°88, July-August 2006.
- 10- HOLDEN, 1988, *Assessment of missile hazards: Review of incident experience relevant to major hazard plant*, United Kingdom Atomic Energy Authority.
- 11- LANNOY, 1984, *Analyse des explosions air-hydrocarbure en milieu libre*, Électricité de France - Bulletin de la direction des études et recherches n°4
- 12- LE-ROUX B., 2010, Formalisation du savoir et des outils dans le domaine des risques majeurs, *La résistance des structures aux projectiles accidentels Ω-23*, reference INERIS-DRA-10-111777-12037B, available at www.ineris.fr
- 13- LEPRETTE, 2002, Formalisation du savoir et des outils dans le domaine des risques majeur, *Le BLEVE, Phénoménologie et modélisation des effets thermiques, Ω-5*, ref. 25427, available at www.ineris.fr
- 14- MASSON, 1998, *Explosion d'un silo de céréales*, INERIS summary report, www.ineris.fr, ref. 21FP30.
- 15- MERCIER, 2003, *Etude de l'influence du couplage fluide/structure sur la fragmentation de capacités métalliques sous pression*, BCRD FRACA Intermediary first year report, ref. 45013.

- 16- MERCIER, PERRETTE, DAUDONNET, CHAINEAUX, 2003, *Physics of steam explosion*, 4th ISFEH (International Seminar on Fire and Explosion Hazards) - Londonderry - 8/12 September 2003.
- 17- MOUILLEAU, LECHAUDEL, 1999, *Guide des méthodes d'évaluation des effets d'une explosion de gaz à l'air libre*, www.ineris.fr, ref. 20433.
- 18- PROUST, 1991, *Distances d'isolement autour des stockages de liquides inflammables - Explosion de la phase gazeuse*, Internal technical document, Ref. 782996, INERIS.
- 19- PROUST, 1997, *Le mécanisme des explosions de poussières*, Lecture given at the seminar INERIS-EUROFORUM March 1997 in Paris.
- 20- PROUST, 2000, *Prévoir les effets des explosions de poussières sur l'environnement, EFFEX, un outil de simulation*, www.ineris.fr, ref. 22751.
- 21- RABBE, LIEURADE, GALTIER, 2000, *Essais de fatigue*, Techniques de l'Ingénieur.
- 22- REIMERINGER M., MERCIER F., RICHOMME S., 2007, Formalisation du savoir et des outils dans le domaine des risques majeurs, *La résistance des structures aux actions accidentelles*, Ω referential reference INERIS-DRA-REST-2007-46055-77288, downloadable at www.ineris.fr
- 23- REIMERINGER M. MERCIER F., ANTOINE F., 2008, *Cahier applicatif du complément technique de la vulnérabilité du bâti aux effets de surpression. Version 1*, reference DRA-08-99461-15249A, downloadable at www.ineris.fr
- 24- ROUX P., 2000, *Guide pour la conception et l'exploitation de silos de stockage de produits agro-alimentaires vis-à-vis des risques d'explosion et d'incendie*, INERIS Ω 1report
- 25- TM 5-1300, 1990, *Structures to resist the effects of accidental explosions*, Departments of the Army, the Navy, and the Air Force, TM 5-1300, NAVFAC, P-397, AFR 88-22, Washington, DC, November 1990.
- 26- T.N.O., 1989, *Methods for the Determination of Possible Damage to People and Objects resulting from Hazardous Materials (Green Book)*, Report of the committee for the prevention of Disasters.
- 27- T.N.O., 1997, *Methods for the Calculation of the Physical Effects of the Escape of Dangerous Material (Yellow Book)*, Report of the committee for the prevention of Disasters.
- 28- UFIP, 2002, *Guide Méthodologique UFIP pour la réalisation des Études de Dangers en raffineries, stockages et dépôts de produits liquides et liquéfiés*, Union Française des Industries Pétrolières.
- 29- WRIGHT J. K., 1961, *Shock Tubes*, John Wiley and sons, London.

10. LIST OF ANNEXES

Reference	Precise Designation	Nb pages
Annex 1	Examples of accidents having caused storage vessel bursts	14 pages
Annex 2	Baum's Experiment	7 pages

Annex 1:

Examples of accidents having caused storage vessel bursts

EXAMPLES OF ACCIDENTS HAVING CAUSED STORAGE VESSEL BURSTS

1. BURSTS OF VESSELS CAUGHT IN FIRES

Rupture test of a tank caught in a fire (White Sands Missile Range, New Mexico, USA, 1973)

28 July 1973 at the White Sands Missile Range, New Mexico, USA, a rupture test was performed on a 120 m³ propane tanker.

The tanker, specially designed for the test, was constructed identically to those used to transport ammonium, LPG, vinyl chloride, etc., except for the presence of measurement devices. It was subjected to a fire; the rise in temperature brought about an increase in the internal pressure of the tank.

An average heat flow of 105 kW/m² was measured on the wet surface of the tanker. The security relief valve lifted after 2.2 minutes when a pressure of 19 bars was reached. It carried out three cycles before staying open.

The internal pressure had reached 24 bars after 24.5 min when the reservoir burst. The internal pressure and temperature reached at the time of the burst were less than those to release safety devices.

127 fragments of the tanker and measuring devices were found and their positions catalogued. Among these fragments, 63 came from the tanker and between 9 and 11 came from the tank itself, the distances and directions of these latter were catalogued. The greatest distance covered by a fragment was 407 m.

Given that the tanker was placed in 8-metre deep pit, the fragments which fell outside of this pit covered ground distances lesser than those which would have been observed if the test had taken place at ground level. However, it is difficult to imagine corrections allowing us to compensate for the presence of the pit given that the distance covered by a fragment depends on two parameters (its speed and ejection angle) and that information about relative source heights and landing points are not available for most accidents.

Thermocouples indicate a considerable temperature gradient along the roof of the tanker at the rupture level. At the starting point of the crack, on one of the extremities of the tank, a temperature of 640°C was measured, while at the other extremity it was only 450°C. The hot point corresponds to the likely starting point of the fracture.

The temperature and rupture pressure as well as the time period correspond to the characteristic tensile strength of the material.

Use:

The tanker exploded at a pressure less than the activating pressure of the safety devices. This can be explained by the rise in temperature of the material which brings about a decrease in the level of tensile strength accepted by the tank.

The number of fragments from the actual tank is fairly low (9, 10 or 11).

The temperature gradient on the tank at the time of rupture is quite significant; this shows us that the temperature distribution when a tank is caught in a fire can be quite unequal.

Burst of a caustic gas purifier in a refinery (Canada or USA, 04/70)

The tank burst is due to the heat of a fire caused by the ignition of a leak by a heater. The tank burst following the weakening of the shell at the level of the vapour phase. The two extremities of the tank flew off; one was projected more than 17m before hitting the wall of a house.

Note:

This accident illustrates the fact that when a tank containing liquid is caught in a fire, its shell weakens faster at the level of the vapour phase. Indeed, this part of the shell heats up quicker for the thermal exchanges are performed less well with the gaseous phase.

Burst of tanks caught in a fire in a refinery (Canada or USA, 08/72)

A butane leak caught fire near the heaters, situated at approximately 30 m. The fire then engulfed the distillation column and two pressurized tanks situated nearby.

A tank with a 3.5 m diameter and 10 m long burst; then, 10 to 15 minutes later, the second tank (1 m by 5 m) also burst. The greater part of this tank was ejected; it hit a pipe, which it burst, thus bringing about a fuel discharge to feed the fire. A vertical tower, weakened by the heat, fell across two primary pipes.

Burst of an ammonia tanker (Crestview, Florida 8/04/79)

A train derailment caused a fire following the spill of various flammable liquids. The 59th car, containing ammonia, was gashed on both sides of the tank and burst three minutes after the derailment. The cause given for the crack propagation is the sudden deformation that followed the increase in internal pressure. The tank burst in two sections which were projected as far as 200 m and 75 m on both sides of the track.

Given the most probable position and orientation of the car before the burst, the fragment projected 200 m probably went in a more or less axial direction. The other fragment was projected in a 104° angle in relation to this direction.

The 56th car, which also contained ammonia, overturned, displacing its roof and damaging its valves to such an extent that evacuation was blocked. One extremity of the tank was caught in an acetone and methanol fire. After 20 minutes, the 56th car burst, ejecting its contents and projecting one fragment approximately 200 m and two other fragments lesser distances.

Production and distribution of gaseous fuels (San Juan Ixhuatepec, Mexico, 19/11/84)

The storage site was made up of four spheres of L.P.G. (80% butane, 20% propane mix) of a unitary volume of 1600 m³, two spheres of a unitary volume of 2400 m³ and 48 cylindrical horizontal tanks of various capacities. At the time of the accident, approximately 11,000 to 12,000 m³ of L.P.G. were stocked on the site.

During a tank filling, an 8-inch pipe (200-mm diameter) under 24 bar burst. When the top of the cloud reached a visible height of about two metres, 5 to 10 minutes after the leak began, it enflamed on a flare located 120 to 150 metres from the emission. The flammable cloud having most certainly penetrated into some houses, its ignition caused their destruction.

Several minutes after the cloud's ignition, two of the smaller spheres were the source of BLEVE, engendering a fire ball (of a diameter evaluated, with uncertainty, at 350 to 400 metres) as well as the ejection of one or two cylindrical tanks. The thermal effects and fragment ejection caused, by the domino effect, other BLEVE.

In the end, the four smaller spheres were destroyed. The larger spheres remained intact, although their supports were broken. Only 4 of the 48 cylinders were still in their initial position. Everyone in a 300-meter radius was killed or injured. This accident caused the death of more than 500 people. Approximately 7,000 were injured, and 39,000 people were evacuated. Emergency services mobilized 4,000 people. Fragments of the spheres were found more than 600 metres away and 12 cigar-rockets were projected to distances up to 1200 metres.

Note:

The cigar-rockets were made up of pieces of the horizontal cylinders; these fragments took off carrying liquid, which, through vaporization, created a propelling force. Consequently, these fragments were ejected further than those that were only propelled by the burst.

Port Edouard Herriot, June 1987

At 1:15 pm in a petroleum depot, an aerosol flashed. One minute later, an explosion took place that was felt several kilometres away. The fire spread and in a few minutes, several several-hundred m³ tanks exploded and were projected as high as 200 m, freeing their contents into the basin. The internal means of intervention were destroyed. The Emergency Response Plan was activated at 2:30 pm. Firemen cooled the tanks with water then fought the 4500 m² basin fire with foam. Around 6 pm, with the fire regressing, tank n°6, with a 2900 m³ capacity and 1/3 full of diesel, began making sharp whistles and then burst, forming a fireball 300 m high and 200 m wide. It sagged partially outside of the basin. The intervention means were affected, the foam reserves were nearly exhausted and the fire surged. The neighbouring port was isolated by a floating barge, the sewer network was buffered and the neighbouring depot of chemical products was protected. The fire extended to the neighbouring basin and 2 tanks of petrol caught fire. The fire regressed and was controlled at 2 p.m. the 3rd of June; the ERP was lifted at 7:45 p.m. Two hundred firemen intervened over 24 hours using more than 200 m³ of emulsifier. Two subcontracting employees were killed; six

firemen and eight operators were injured, five seriously. The storage depot was destroyed and 1900 m³ of diesel, 1200 m³ of petrol and 600 t of additives were released. Hydrocarbons seeped into the soil and 10 000 m³ of extinction water was pumped and treated in refineries in the Southeast. The groundwater table had to be monitored until 2001. Material damages were estimated in 1987 at 130 million francs. In 1996, judiciary experts retained the hypothesis of faulty upkeep of a barrelling pump of petroleum additive left functioning despite zero withdrawal, provoking its heating up and a breach by which the inflammable liquid may have been discharged and self-inflamed. The 21/12/00, the company was found responsible for the two deaths and required to give 1.4 million francs to the civil plaintiffs, while the storage depot director was sentenced to 15 months in prison and given a fine of 30,000 francs. The disaster began in the zone of additive mixture, products that are unstable from 130-160°C, which was under construction even though other tanks were kept in service. The disaster's development was propelled by the explosion of the tanks of additives, known to be frangible, the absence of a means to close the foot valves of the tanks automatically or remotely, and the presence of alcohol compounds decreasing the effectiveness of the emulsifiers. The fireball emitted during the explosion of tank n°6, of a "welded" design and of which the roof was known to be "frangible," could be linked to a tank pressurization phenomenon or to a similar phenomenon, supposing that the relief valves, set to 175 mbar, could not evacuate the pressure differential due to product vaporization.

Petroleum refining (Ulsan, South Korea, 22/07/90)

In a petroleum company, a leak in a sealing system of butane a storage tank inflamed, certainly due to a discharge of static electricity. The tank exploded due to the effects of the fire. More than 10,000 members of the local population were evacuated and the surrounding traffic was cut. A nearby tank was affected and exploded.

Rupture of a mobile tank in a boilerworks (Chateaubernard, Charente 20/08/91)

An explosion and a fire took place in a boilerworks. A tanker enflamed, the stock of propane and butane bottles exploded and dug a large crater in a hanger. The fire spread to a nearby cardboard factory. The firemen fought for two hours to put out the fire; 8 000 m² of cardboard on spools was destroyed. The perpend walls collapsed and the metal framework was deformed by the heat. Experts evaluated the internal tank pressure at 15 bars when it opened (the operating pressure was 16.4 bars and the test pressure 24.6 bars); heating of its inside surface probably reduced the tensile strength of the metal. The air-propane mixture (800 kg) enflamed and is said to have formed a fireball of 37 to 57 m; this phenomenon may have lasted slightly less than 5 seconds. The internal and external material damages were evaluated at 4 and 82 MF respectively.

Note:

This accident illustrates the fact that an increase in temperature brings about a decrease in the tensile strength of the metal making up the tank shell.

Basic chemical industry (El Tablazo, Venezuela, 26/06/94)

A heavy hydrocarbon leak took place on a transfer conduit during the fill of a tanker from a tank. The product entered in contact with a hot element of the pumping station and enflamed. The fire then spread to two tanks (propane and propylene), which exploded. The tanks might have been in the first five-year retest phase or in preparation. The fire was extinguished in one hour by the safety team with the help of firemen from the nearby city of Altagracia; eight rescuers were slightly injured during the explosion.

Wholesaler of non agricultural intermediary products (Treviso, Italy, 10/03/96)

In an LPG storage and bottling facility, a propane leak took place during the decanting of a 35 m³ mobile tank into a non-mobile tank. The alarm was sounded. As the firemen were preparing to disperse the cloud with water hoses, an explosion destroyed the offices of the facility. The upper part of the tank opened and a small fireball formed. The heat caused the explosion of a 12 m³ road tank and destroyed some fire fighting equipment. A tank fragment damaged the roof of a building and landed 500 m away. Three employees and 10 firemen were injured, one of the employees died four days later; 250 people in the vicinity were evacuated for 24 hours.

Bordes, May 2000

Early in the morning, a truck transporting 777 bottles of gas (butane and propane of 6, 13 and 35 kg) arrived in the proximity of a company depot where it was due to deliver. The driver parked in the car park of the carwash located 20 meters from the depot and discovered, while getting out of the cab, that one of the tyres of the trailer was on fire. After trying in vain to extinguish the fire with foam, he left to alert emergency services. The first bottles exposed to the heat of the flames exploded; 3/4 of the load was progressively concerned. A security perimeter was put into place and the fire was controlled after a 4-hour intervention. Traffic was deviated for 5 hours and 30 minutes. There were no victims. The security perimeter was lifted the following day around 7 p.m. Prior to this, the scattered bottles were recovered. Those which had not exploded were sent to be destroyed. The carwash, the adjoining hangar, the depot's offices and several nearby houses were damaged. Bottle debris was found as far as 800 to 900 m from the disaster location, according to witnesses. 90% of the debris was localized within a 100 m radius around the vehicle in the accident. According to the investigation, the chronology is the following: 6:15, a tyre bursts (front left, first axle), ignition of the tyre, effort to extinguish it; 6:18 the driver gives up / calls for help; 6:20: the bottles are reached; 6:25: first bottle explosions, firemen arrive; 7:35: last bottle explosion.

Dagneux, May 2007

At 8:24 pm, a passer-by observed a cab fire in one of three transport tankers of liquefied petroleum gas (LPG) parked at a park maintenance company. The fire developed rapidly, and near 9:15 pm, a first deflagration was produced, followed by one or more others. Two of the three tanks exploded (BLEVE) and the third was projected onto the roof of a neighbouring factory. The explosions and fires that followed caused significant material damage in a radius of 900 m (broken windows, roofs torn off, etc.), including the destruction of four warehouses of 1,000 m² capacities. The police put into place a safety perimeter around the industrial zone; a highway and the Lyon-Ambérieux train line were closed for several hours. A significant smoke cloud rose vertically, but evacuation of the surrounding population was not necessary. Five companies nearby were destroyed or significantly damaged, and in all, around twenty establishments in the zone were touched to various degrees, causing the temporary layoff of 35 people. A 100 kg metal piece dropped, crushing the roof of a house 700 metres away. Three firemen and two policemen were slightly injured. There was a legal investigation to determine the cause of the disaster, the possibility of criminal intent not being ruled out. Of the three tanks involved, one contained 2.5 tons of propane and another several hundred kilograms. The last one was empty but not degassed. A third-party expert was mandated to gather technical data on the accident. The preliminary results showed effect distances of 50 metres for thermal radiation and as far as 400 metres (broken windows) for overpressure. Pieces of the tank, projected as far as 900 metres, destroyed a business located 100 metres from the vehicles and burnt a hedge 250 metres away.

Port La Nouvelle, July 2010

A fire started around 11:40 pm near the front shock absorber of a propane tanker parked near the vehicle repair shop of a business specializing in gas bottle transport and bulk sales of liquid and liquefied hydrocarbons. The company, which employed 200 people, was subject to declaration under the legislation for « classified installations » for storage of bottles of LPG of less than 50 tons. A watchman for the surveillance company of the industrial zone alerted emergency services. A BLEVE was produced at 12:17 am on the tanker, which contained 4 tons of propane (64 % capacity). There were no serious injuries, but 12 firemen, victims of the blast effect, suffering from headaches and / or difficulties hearing, were identified but not hospitalized; warned by a whistling coming from a heavy goods vehicle, they took shelter before the explosion. The 90 firemen and 36 vehicles that were mobilized had controlled the accident with water and foam around 2:00 am, from two fire hydrants. The fire was extinguished at 4:30 am; four damaged tankers were secured during the day (one was emptied of LPG; three others had their gas burnt off by torches). A company driver whose hand was slightly injured by the broken windshield of the truck he was evacuating was treated on site. Emergency intervention ended at 10 pm. On the site, in addition to the destruction of the truck that was at the origin of the incident, BLEVE effects caused a fire in two metal weatherboard structures, the repair shop (destroyed) and a maintenance shop (seriously damaged), as well as the destruction of two liquid hydrocarbon tankers and the cabs of four gas tankers (3 empty but not degassed and one full to 80 % capacity). The overpressure effect damaged the administrative building (rubble stone walls displaced), caused the breaking of glass on cars and 48 trucking vehicles, and projected, sometimes outside the site, weatherboard. Outside the site, according to a mayor's account, 105 homeowners and 20 shop owners had broken windows; the blast effect also damaged silos (explosion discharge zones in the upper gallery and the central aspiration hole blasted, an isolation door between floors of a tower blocked) and the weatherboard of hangars. The extremity of the tank on the cab side and the manhole of the truck that exploded were projected outside the site to distances of 30 and 160 m respectively from the position of the BLEVE. Two secondary explosions also took place on gas bottles found in the repair shop during the fire. Four brush fires were set off outside of the facility. The prefecture published a press release. Judiciary and administrative investigations were held to determine the causes and circumstances of the accident.

2. VESSEL BURSTS DUE TO AN ACCIDENTAL PRESSURIZATION

Rupture of an LNG heat exchange column (Indonesia 14/04/83)

An LNG heat exchanger column 47 m long with a 5 m maximum diameter was purged with a hot, dry hydrocarbon gas to defrost and dehydrate it. The column's maximum service pressure was 2 bars and the relief valve was set to 4 bars.

The source of the purge gas was more than 35 bars. A relief valve malfunction brought about the pressurization of the column. A pressure of 5 bars was recorded; 20 minutes later, the column broke. The vessel fragmented into three principle pieces; one struck a building 50 m away.

Burst of an accidentally pressurized tank in a refinery (USA or Canada, 01/66)

An accidental high pressure vapour discharge in a tank caused an overpressure in it. A clean-out port was projected 28 m. The damage to nearby equipment was minor, although the tank was moved from its initial position and a pipe was destroyed.

Burst of a reactor in a refinery (Canada or USA, 09/70)

The burst of the reactor was due to a fragile fracture originating on existing cracks during a pressurization test with nitrogen at 27 bars. Part of the head of the tank was projected 81 m.

Burst of water vaporization tank of a heater (Gonfreville-l'orcher, 03/10)

At 4:15 am, a water vaporization tank of a heater burst in an atmospheric distillation unit of a refinery on "standby" since August 2009. The burst of the half-filled tank, with a 8m³ volume, located 6 meters above the ground on a rack, made a dull noise audible outside the site and material damage on the nearby equipment: the inside of the tank hit a reheating oven 6 metres high and caused a diesel leak on the shut-off valves of a loading pump. One half of the tank stayed on the rack but the other half was found at the foot of the unit in two pieces (bottom and collar). Simulations gave a burst pressure between 5 and 7 bars (glass was intact 40 m from the unit).

The water vaporization tank allows the elimination of inert gases that could be dissolved in the water of the heater before its transformation into steam. The user studied several hypotheses, that of an explosion due to an internal flash caused by the accumulation of flammable product (hydrocarbon residue, hydrogen) from condensate circuits and a heat source was ruled out. Water samples and a pressure test show the absence of hydrocarbon pollution in the water/vapour network. The possible ignition sources in the tank were at approximately 200°C, less than the temperature of auto ignition of the two suspected products (230°C for HC and 560°C for H₂). The retained hypothesis was of a gradual increase in pressure linked to the fragility of the coating of the tank, the user having found that:

- the coating of the tank was damaged at the corner iron of the stand of the insulating material, due to external corrosion caused by water accumulation on this horizontal stand,

- vapour at 12 bars entered into the condensate network, and then into the tank because of the failure of some taps (open or unattached bypass, installed upside down thus constantly dripping).

Condensates were entering into the tank faster than they were going out, a situation that was aggravated by the complete non-application of a frost protection procedure which provides for permanent suction of the tank, and the limiting of the tank outlets as a hatch between the tank and its flow device was found tightly clamped.

The user performed a testing campaign and a replacement of the taps of the vapour network. Learning from experience, he verified the configuration and reinforced the flow devices and the stands of the insulating materials.

Burst of a hydrocarbon flexible pipe (Alès, 11/08)

An 8.4 m³ leak of hydrocarbon was observed at the end of the afternoon in a manufactory of electrical material; the product had flown into the rainwater system and then into the Brueges. Iridescences are observed on at least 1 km of the rivier. A flexible pipe burst, maintained pressurized by a pump that had not been turned off since being used two days before, was at the origin of the spill. A specialized company came in the following morning to treat the pollution.

Burst of a fuel flexible pipe (Forges-les-eaux, 02/02)

During a decanting, the untimely closure of a valve near the tank caused a rise in pressure and the burst of the flexible pipe; 2 000 l of fuel spilled on the ground and was covered with sand.

3. VESSEL BURST DUE TO A MECHANICAL WEAKENING

Circuit burst due to piping corrosion (Huningue, 12/01)

A chloro-fluorinated refrigerant (R134a) leak evaluated at 1,600 kg occurred on an evaporator that had been in operation for only a few months. The discharge into the atmosphere did not have a notable impact on the surroundings. The leak resulted from abnormal corrosion of the copper piping of the evaporator and freezing of the water which caused the circuit burst. Of the seven refrigeration units, two would prove to be leaking and the source of the observed release of refrigerant.

Burst of an LPG pipe by internal corrosion (Petit-Couronne, 12/00)

In a refinery, at morning's end, an 8-inch LPG pipe burst on a brute distillation unit. The pipe was located above ground, in a rack (service P = 31 bars; thickness Nom. = 5.5 mm). Its installation dated from the beginning of operations of the site in 1992, and it collected gases, mostly butane and propane, coming from different units (petrol reforming, atmospheric distillation). According to witnesses in the control room, the unit was in normal working order and the violence of the burst made the control room shake. A black cloud was observed as well as H₂S fumes. The Internal Emergency Plan was activated. Twenty minutes later, the load was eliminated; the process gases were evacuated by torches. Nitrogen flushes were begun in the circuits involved. The piercing was located near a bend, not far from the compressor discharge.

After examination, the line presented symptoms of internal corrosion, notably in the lower generator. The piercing happened in the thermal zone affected by the welding. Thickness measurements showed localized under-thicknesses.

The site had a testing and preventive maintenance program but the particular sensitivity of the discharge outlet zone had not been noticed. Moreover, the lack of accessibility to this piping could have contributed to the fact that it had not been the subject of different measures during previous operating inspections. The user looked over his inspection plan. The inspection of IIC's requires in particular a better integration of the results of the corrosion manual in the lines inspection plan. At the same time, the user tested the lines of the rack near the one which burst (a 3-inch vapour line; a 4-inch naphtha line, a distillation backflow line, a residue line), as well as details such as the zone's pressure taps and vessels located in the zone.

4. VESSEL BURST DUE TO AN INTERNAL EXPLOSION

Vessel burst due to a rapid phase change in a refinery (USA or Canada, 11/62)

Water was present in the bottom of an accumulator probably due to a power supply failure when it was turned on. The presence of two phases caused vaporization and a sudden overpressure. The main part of the accumulator was projected 96 m and a 3 m x 10 m piece was projected 220 m.

Burst of a dryer due to a runaway reaction (United Kingdom, 1981)

In the United Kingdom, in 1981, a rotary dryer burst into two after a vapour explosion. The biggest piece was propelled across the factory and landed in the car park. The vapour explosion was attributed to a chain reaction involving the water that was abnormally present in the bottom of the dryer. Indeed, the pump usually used to empty low temperature tank water did not work that day. The dryer contained soda hydrosulphate ($\text{Na}_2\text{S}_2\text{O}_4$), which is a salt which reacts slowly, but exothermally, with water in ambient conditions. Due to the temperature increase, the reaction ran away and the residual water transformed abruptly into vapour (Mercier et al., 2003)

Burst of an alkyl aluminium flexible hose due to very rapid oxidation (Sarralbe, 03/06)

At 4:39 pm, in a polypropylene manufactory, an alkyl aluminium (diethyl aluminium chloride) transfer flexible hose burst near a storage unit of 1,400 l. Alkyl spilled onto the ground. This product, which ignites when in contact with the air, caught fire, causing a fire in the cubicle of the bunker as well as a very loud noise (explosion at contact with the water). An employee supervising the operation, alerted by the suspicious noises, sought shelter. Shocked by the acoustic wave, he was briefly hospitalized. Following procedures and equipment provided by the user, the enflamed liquid was directed by channels toward an offset retaining well allowing the site firemen to smother the fire by covering it with inert sands available near the well. The tank was rapidly isolated thanks to the automatic closure of the valves in the event of excessive heat. The incident ended 13 minutes after the flexible hose burst. However, the significant thermal flux caused the combustion of the roof made of plastic materials, producing dark smoke visible outside the factory. The quantity of alkyl released was estimated at 481 l.

Measures were taken such as changing the hoses (sized at 40 bars, leak proofed and tested without water), measuring for the absence of humidity in the hoses, and the use of metallic hoses of a more suitable size to reduce low points and useless lengths.

The day before, the hose had been attached to the installations following the usual procedure (nitrogen flush with several cycles). Impermeableness had been verified. After closing the hatches, the installation was ready to be used. The nature of the rupture indicates a significant overpressure. The presence of residual water and the very rapid oxidation kinetic of alkyl by water explains the hose burst. There are several possible sources of the water: residues from the hydraulic test performed by the supplier, pollution during transport, condensation during storage.

Burst of a vessel following a runaway reaction (Formerie, 07/05)

At 4:10 am, a violent explosion reverberated in the principal workshop (400 m²) of a factory specialized in detergent manufacturing and packaging. The explosion was followed by the start of a fire controlled by the firemen called in. The 50 m³ of extinction water was directed toward a basin (200 m³). According to the user, the accident occurred on a mixer (9 m³) for the manufacturing of peracetic acid (disinfectant, sterilizer in agro-business and in hospital environments). This product is obtained at atmospheric pressure by a cold mix of 50 acetic acid, 28% H₂O₂, and 5% various additives and 17% water. At the time of the accident, the mixer contained approximately 1.5 m³ of solution prepared the day before to be packaged in plastic kegs the next morning. Because production takes place during the day, no staff member was present at the time of the explosion. There was major material damage: a roof made of fibre cement plates collapsed, possible collapse of the framework, shredding of the stainless steel mixer from the force of the explosion.

According to the expert mandated by the user, the introduction of a contaminant (metallic?) in the mixture during sampling could have caused the decomposition of the peracetic acid and initiated the runaway reaction, unstable at ambient temperature. Since the energy released could not be dissipated, the pressure might have increased until the burst of the tank, as it was not equipped with a device limiting internal overpressures.

Reactor burst following a violent decomposition of organic residue (Huningue, 12/02)

In a chemical factory, an explosion occurred in a 4,000 L empty and clean enamel reactor, attached at the top to a ventilation device that was always in operation and at the bottom to a network of used chemical water via a flexible piping of which the valve remained open.

The damage observed was primarily material: enamel removed from the bottom of the reactor, manhole lid (77 kg) projected nearly 3 m high, partial burst of the valve in the bottom, and damage over several metres of the polypropylene conduits of the connection to the used water network. The source of the accident is the violent decomposition of organic residues that had accumulated in the dead volume in the bottom valve when they came into contact with chlorine. The chlorine formed in the used water circuit from a reaction between bleach coming from an overflow of a spray tower due to a technical failure and the acidic content of a buffer tank of another spray tower, which was emptied by an operator at the same time.

The chlorine gas thus formed in the sewer system than migrated toward the still connected reactor. A technical audit of the functioning of the spray towers was undertaken: a dysfunction of the treatment unit of acid gasses likely to lead to a chloride emission in the sewers by excess input of bleach was found.

5. USE

It is difficult to use information concerning past accidents for, in general, it is not exhaustive. Indeed, very few pneumatic bursts due to a simple rise in tank pressure have been reported, and those which have been do not always include all the information necessary to understand the phenomenon.

For example, the distances covered by the fragments are often given, but the fragment masses generally are not indicated.

In addition, the accidents reported do not always specify the nature of the burst. Particularly in the case of a tank caught in a fire, it is often difficult to know if it is a pneumatic burst or a BLEVE.

In the accident described below, it seems that different types of bursts took place:

Train derailment (USA, Laurel, Mississippi, 25/01/69) :

A train with 51 propane cars derailed in the city of Laurel. Two cars were pierced, one at the head, the other in the tank shell; a fire started immediately. Twelve other cars might also have burst violently. The first burst 6 to 20 minutes after the derailment, the last between 45 and 70 minutes after the derailment. Among these twelve train cars, 8 or 9 were subject to BLEVE's, one was burst by an extremity coming from another tank, and two were subject to mechanical impact during the derailment, which caused a fire and thus the increase of internal pressure until rupture.

Accident reports mention fires in buildings located more than 460 metres away. These fires were caused by flaming tank fragments propelled by the release of the propane they still contained.

Annex 2:
Baum's Experiment

Baum's Experiment

Baum developed a simple model (Baum, 2001) allowing the prediction of the speed of a cylindrical vessel containing pressurized gas when it underwent axial rupture. The phenomenon considered in this model is that described in paragraph 6.1.

Baum sought to predict the speed of the vessel when it was projected due to the release of the pressurized gas it contained. Baum's method is very interesting as he compared the results of an experimental study with those predicted by his model.

The experimental study

The experimental device is described in Figure 40. The tank used for the experiment had an axial defect machined onto the exterior surface of the shell in the middle of its length.

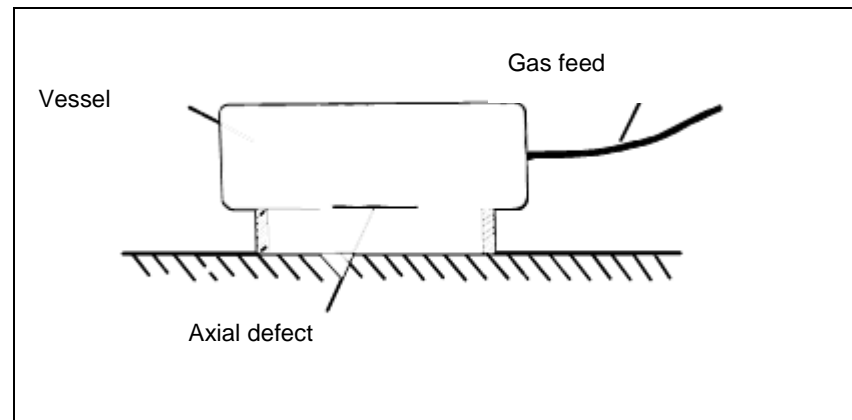


Figure 40 : Experimental device (Baum, 2001)

For each experiment, the vessel is placed horizontally on a chassis with the defect positioned on the lowest part of the vessel. The gas was supplied by a light, flexible tube, so the vessel may be considered non-retained. The vessel is pressurized with air.

The development of the breach at the lowest point of the vessel caused it to be pushed upward vertically.

Experiments were conducted on two steel vessels:

- a vessel with a 0.102 m diameter and 1.6 mm thickness,
- a vessel with a 0.305 m diameter and 6.4 mm thickness.

Of the 24 experiments conducted, the vessel remained in one piece 18 times. In three experiments, one end-cap detached; the primary missile was thus made up of the tank shell and the end-cap that had remained attached. Three experiments resulted in the detachment of both end-caps; the primary missile was thus the tank shell.

The observed speeds for the detached end-caps were generally similar to that of the primary missile. The experimental data are gathered in Table 9, which also provides, for each case, the rupture pressure and the speed of the primary missile. An experiment performed by Herzerg et al is also mentioned in this table.

Vessel Diameter [m]	Vessel length [m]	Vessel mass [kg]	Rupture pressure [bar]	Primary missile type	Primary missile speed [m/s]	Missile mass [kg]
0.102	0.305	9.54	52.7	Entire vessel	2.9	5.66
	0.305	9.6	119.6	shell +one end	10	
	0.305	6.32	61.7	Entire vessel	8.75	
	0.305	6.32	23.8	Entire vessel	5.95	
	0.305	9.1	45.1	Entire vessel	6.2	
	0.305	9.19	35.5	Entire vessel	4.76	
	0.305	6.29	35.5	Entire vessel	7.44	
	0.305	6.33	20.3	Entire vessel	5.24	
	0.305	9.22	27.2	Entire vessel	5.24	
	0.305	8.99	32.0	Entire vessel	5.58	
	0.305	6.26	37.6	Entire vessel	9.33	4.21
	0.305	6.29	38.9	Entire vessel	9.7	
	0.305	8.93	38.2	Entire vessel	6.65	
	0.305	9.22	48.6	Entire vessel	7.35	
	0.305	6.29	41.4	Entire vessel	8.84	
	0.305	8.97	55.2	Entire vessel	7.35	
	0.305	6.21	62.1	Entire vessel	10.6	
	0.305	9.10	72.8	Entire vessel	8.23	
				Entire vessel		
				shell +one end		
				Entire vessel		
0.305	1.02	57.6	76.9	End cap	39	47.5
	1.09	62.35	61	Entire vessel	43.9	57
	1.22	76	121.7	End cap	61	
	1.22	82.5	76.9	Entire vessel	23.2	62.5
	1.22	82.5	83.8	End cap	54.6	
	1.22	82.5	87.2	shell +one end	36.9	72.5
0.5 (Herzerg et al., 1981)	1.33	156	25	Entire vessel	16	

Table 9: Experimental data and results

The model for predicting the vessel speed

To predict the vessel speed, he considered the impulse *I* applied on the internal side of the side opposite to the breach. The velocity of the vessel *V* is then obtained by equalling impulse *I* to the amount of final movement of the vessel:

$V = \frac{I}{M}$ where M is the vessel mass

An approximate estimate of the impulse is obtained by considering the vessel to be a rectangular block shape with a square base with a width of two times the vessel's radius and of length E (Figure 41).

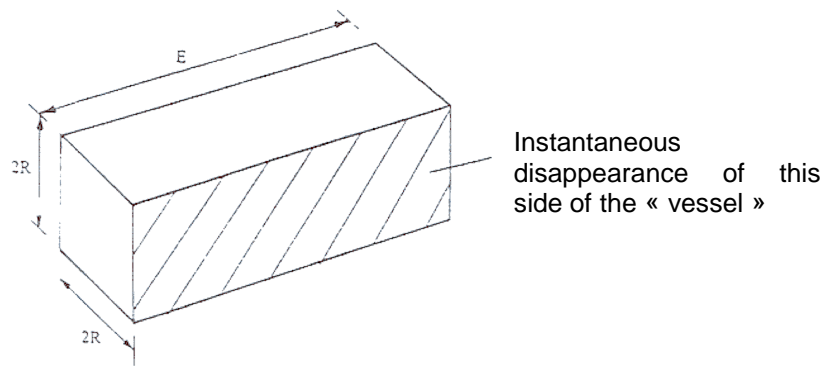


Figure 41: Schematic representation of the defective vessel

In addition, the development of the breach is simplified by the hypothesis of the instantaneous disappearance of one side of this « vessel ». This disappearance generates a level rarefaction wave in the pressurized gas; this wave propagates across the « vessel » by generating a flow across the breach.

This wave reflects off the side opposite to the breach and then returns to breach level. This process repeats until a second rarefaction wave is initiated, that is, until the first wave goes through the breach.

According to Baum, the pressure on the side opposite the breach remains at the initial value P_0 until the rarefaction wave comes, that is until time $\frac{2R}{a_0}$ where R is the

vessel radius and a_0 the speed of sound in the high pressure gas. The pressure then decreases during the reflection process. Depressurization essentially takes place between the interval of time between $\frac{2R}{a_0}$ and $\frac{6R}{a_0}$, as shown in Figure 42.

Consequently, most of the impulse was applied on the closed side of the vessel during the time passed beginning with the instantaneous appearance of the breach reached approximately $\frac{6R}{a_0}$.

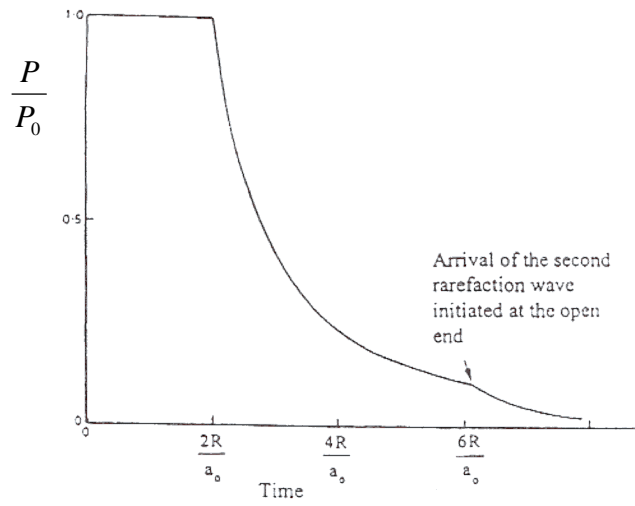


Figure 42 : Evolution of the pressure on the inner wall opposite the breach of the « vessel»

Impulse is expressed as:

$I = \int P A dt$ where P is the pressure acting on the closed side of the vessel and A the air on the closed side of the vessel, or $2RE$.

If the decrease in pressure is approached by a linear fall in pressure over the period $(\frac{2R}{a_0}, \frac{6R}{a_0})$, one obtains:

$$I \approx \frac{8 \cdot P_0 \cdot R^2 \cdot E}{a_0} \quad \text{and} \quad V = \frac{8 \cdot P_0 \cdot R^2 \cdot E}{M \cdot a_0}$$

The above approach is valid for a real event only if the development rate of the breach is such that the side of the vessel is completely open at the end of time $\frac{6R}{a_0}$ after initiation.

If an initial central defect is considered, this implies that the axial fractures propagate toward the extremities of the tank, which takes a period of time of the order of $\frac{E}{2V_p}$

with V_p the speed of axial fracture. Consequently, the model can be considered valid if: $\frac{E \cdot a_0}{12 \cdot R \cdot V_p} \leq 1$.

For steel, assuming ductile fractures, the speed of axial fracture is of the order of 200 m/s and the speed of circumferential fractures is typically two times less than the speed of axial fracture.

Thus, the separation of the extremity by fractures propagating in both directions around the extremity will take place at the end of a time period $\frac{E}{2V_p} + \frac{\pi R}{V_p/2}$ beginning with the initiation of the fracture.

Consequently, if this period is superior to $\frac{6R}{a_0}$, the separated fragments should have speeds similar to that predicted for the entire reservoir. The experiments described here belong to this category.

Comparison between the theoretical model and experimental results

Figure 43 compares the missile speeds observed with the speed of the entire vessel predicted by the theoretical model. The results of the experiment of Herzog et al. are also mentioned in this study by Baum.

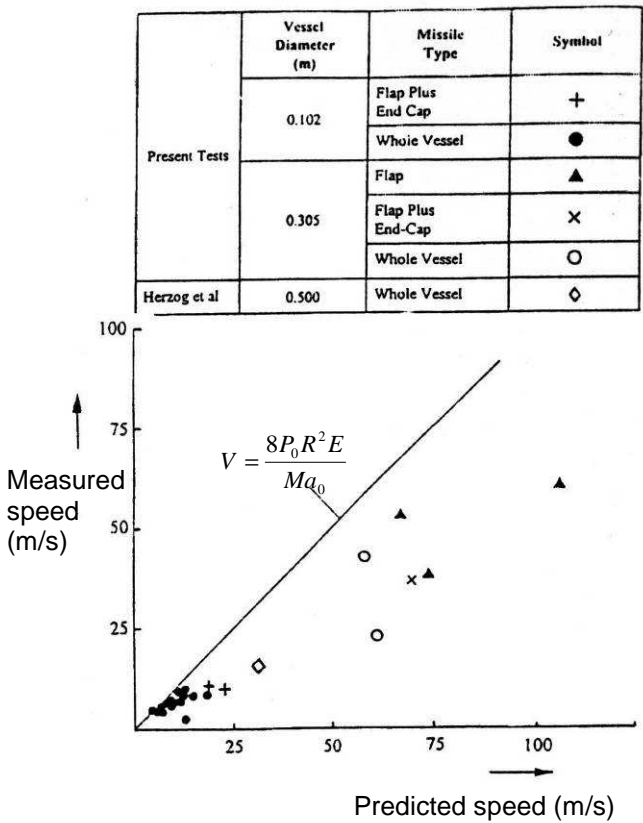


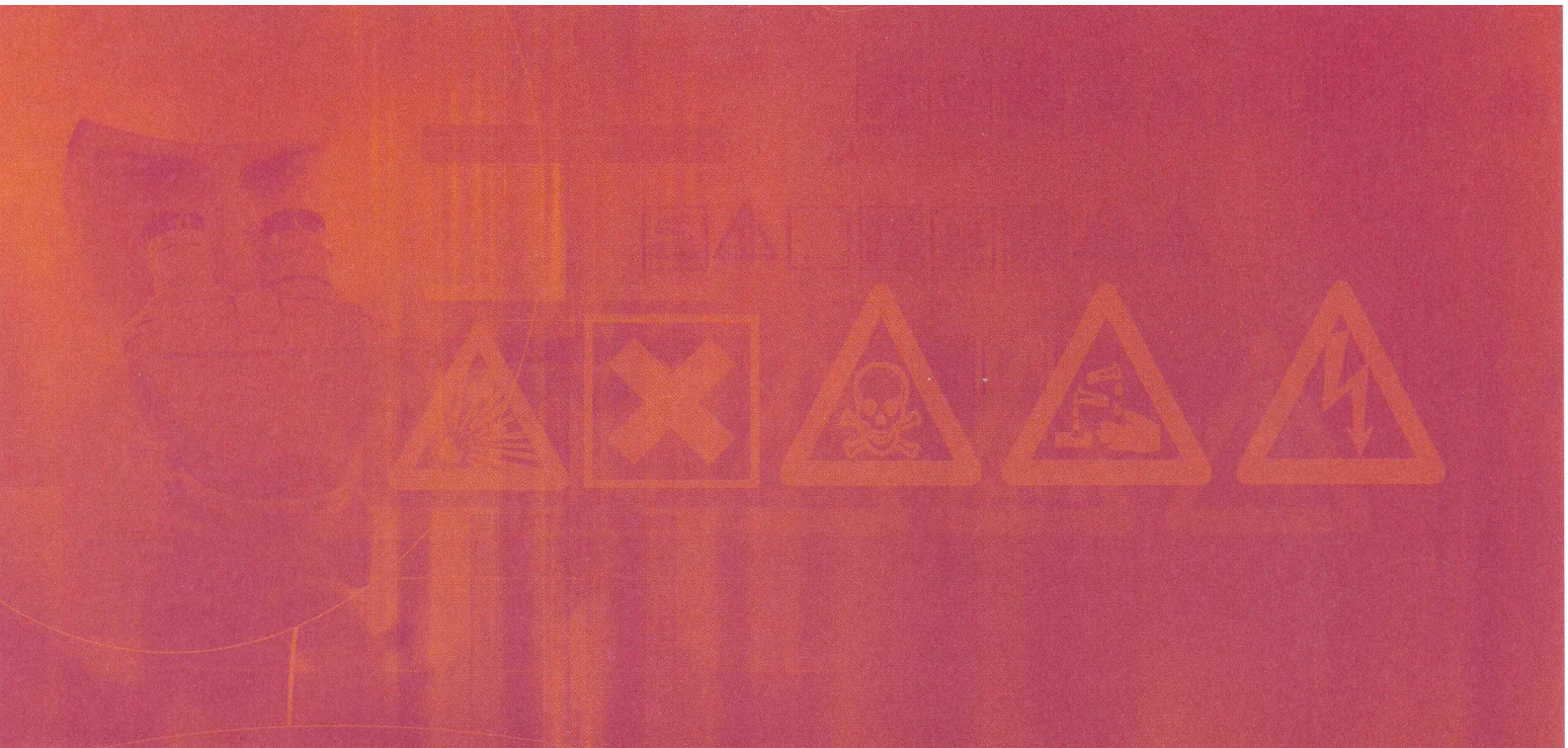
Figure 43: Comparison between the values of predicted speeds and experimental speeds

Although the data seems a bit scattered, it seems that the measured speeds for the entire vessel and large fragments are not very far from each other.

In addition, we notice that the speeds observed increase approximately linearly with the values predicted by the theoretical model and that the equation $V = \frac{8 \cdot P_0 \cdot R^2 \cdot E}{M \cdot a_0}$ provides a realistic upper limit in relation to the measured speeds.

In practice, the breach opens over a finite period of time and the depressurization rate is reduced. In these circumstances, at a given moment, the pressure acting on the inner wall opposite to the breach is greater and the air on which the unstable pressure acts is diminished.

The fact that the missile speeds observed are less than those predicted by the equation $V = \frac{8 \cdot P_0 \cdot R^2 \cdot E}{M \cdot a_0}$ shows that the existence of a finite opening time causes a reduction in the impulse applied on the missile in relation to the impulse proposed in the theoretical model.



INERIS

*maîtriser le risque
pour un développement durable*

Institut national de l'environnement industriel et des risques

Parc Technologique Alata
BP 2 - 60550 Verneuil-en-Halatte

Tél. : +33 (0)3 44 55 66 77 - Fax : +33 (0)3 44 55 66 99

E-mail : ineris@ineris.fr - **Internet :** <http://www.ineris.fr>